Plasmid DNA and Bacterial Artificial Chromosomes Processing for Gene Therapy and Vaccination: Studies on Membrane Sterile Filtration

Sim Yee Kong

A thesis submitted in partial fulfilment of the requirements of the degree of Doctor of Philosophy of the University of London

UNIVERSITY COLLEGE LONDON
DEPARTMENT OF BIOCHEMICAL ENGINEERING

December 2006

ProQuest LLC
789 East Eisenhower Parkway
P.O. Box 1346
Ann Arbor, MI 48106-1346

I. Abstract

Plasmids currently applied in clinical trials are generally ≤ 20 kb, but the interest in larger circular vectors is rising. However, due to their size and character, filterability and irreversible damage intensified by elongational shear are major concerns during a sterilising filtration procedure. Therefore, key parameters affecting the normal-flow membrane filtration performance of solutions containing purified plasmid DNA and bacterial artificial chromosomes were investigated in this study.

Two small scale filtration systems were designed to enable information on material properties to be obtained. Firstly, a pressure driven syringe system was used to conduct constant flux experiments. Data on transmission and degradation could be obtained rapidly and only required small sample volumes (≤ 1 mL). Secondly, a positive pressure filtration system which permitted operations at constant transmembrane pressure had been applied to determine the filter capacity, this information is useful to facilitate the scale-up of a membrane filtration process.

The results showed transmission of DNA vectors decreased linearly with molecular size (6–116 kb) and confocal microscopy images confirmed that a fraction of the DNA molecules were being retained by the membrane filters. Degradation increased with molecular weight, flux and number of filtration passes for vectors ≥ 20 kb. The filtration performance was affected by the membrane type used and could be improved by addition of NaCl in the formulation buffer.

For filtrations performed at constant pressure, permeate flow decayed with time. As predicted from controlled flux experiments, transmission decreased with increasing molecule size. Initial permeate flux was affected by vector size, DNA concentration and operating pressure. Increase in plasmid size and operating pressure led to reduced membrane capacities. The small scale membrane (filtration area = 1 cm^2) capacity was used successfully to predict the performance of a larger scale filtration (filtration area = 4 cm^2).

II. Acknowledgement

I am immensely grateful to both Dr Susana Levy and Professor Nigel Titchener-Hooker for not only their expert academic guidance, but also for their encouragement, patience and unfailing support. I am most thankful for Susana's ever helpful suggestions and intensive training.

I would like to thank members of the Gene Team for their interest and sharing of knowledge. I am especially indebted to Cassandra for her valuable advice and assistance in all the DNA analysis techniques. Special thanks to Supti and Andrew for help with the sample preparations for my formulation work. Also, I would like to extend my gratitude to Hu for performing the filtration simulations and Chau for providing the fluorescent dye and sharing of information on confocal microscopy.

The support and encouragement I received from my family have been invaluable in sustaining me throughout the duration of my project. My most special thanks and deepest gratitude is to James for being so understanding and supportive.

III. Table of Contents

IV. List of Figures

Figure 2.1: Schematic diagram of the small scale normal-flow filtration set-up using a pressure driven syringe unit which allowed controlled filtration flux.

Figure 2.2: Schematic diagram of the small scale normal-flow filtration set-up using a pressure reservoir unit which allowed constant pressure filtration.

Figure 2.3: Gel electrophoresis of purified pQR150 (20 kb) samples. Mass of DNA loaded into each well in the agarose gel was between 200-600 ng. Abbreviation: M is λ Hind III molecular weight marker, OC is open circular, SC is supercoiled, Chr DNA is chromosomal DNA. (B) Densitometry peak intensity using 200-600 ng/well of purified pQR150 (20 kb) samples. Error bars indicate 20% of variation associated with the gel densitometry technique and line represents linear regression.

Figure 2.4: Schematic outline of the modified PicoGreen assay. Fluorescence enhancement of PicoGreen at pH 12.4 ($F_{pH12.4}$) is normalised by its value at pH 8.0 ($F_{pH8.0}$) to give a relative fluorescence ratio (RF) that is proportional to the average backbone integrity of the DNA molecules in the sample (Rock et al., 2003).

Figure 2.5: Calibration of relative fluorescence for the determination of SC content. The results shown are average of two sets of tests and error bars indicate standard deviation and line represents linear regression.

Figure 2.6: Illustration of components and properties of the LID complex (Sarkar et al., 2003).

Figure 3.1: Atomic force microscopy image of a 2 kb plasmid (p1868) in water (Rippe et al., 1997).

Figure 3.2: The effect of vector DNA size on product transmission. Plasmids gWIZ (6 kb), pQR150 (20 kb), pMT103 (29 kb), p5179 (33 kb), p5180 (72 kb) and p5176 (116 kb) were filtered through 0.22 μm PVDF with feed concentrations of 30 ± 2 μg/mL. The results shown are average of two sets of experiments error bars indicate standard deviation and line represents linear regression.

Figure 3.3: The effect of operating flux on product recovery. Solutions containing pQR150 (20 kb) (—▲—), p5179 (33 kb) (—◆—), p5180 (72 kb) (—■—) and p5176 (116 kb) (—●—) were filtered through 0.22 μm PVDF membranes at operating fluxes of 0.1, 0.2, 0.8 and 2.3 mL/min.cm^2. The results shown are average of two or three sets of data, error bars indicate standard deviation and lines are linear regressions. Please note some error bars are smaller than the symbols.

Figure 3.4: The effect of operating flux and vector size on product recovery. Solutions containing the 6, 20, 33, 72 and 116 kb vectors were filtered

through 0.22 μm PVDF membranes at operating fluxes of 0.2 (—♦—) and 2.3 (·····■·····) mL/min.cm^2. The results shown are average of two or three sets of data, error bars indicate standard deviation and lines are linear regressions.

Figure 3.5: The effect of DNA concentration on product recovery. Solutions containing pQR150 (—▲—), p5179 (—♦—) and p5180 (—■—) with concentrations ranging from 25 to 100 μg/mL were filtered at a flux of 2.3 mL/min.cm^2. The results shown are average of two or three sets of spectrophotometry measurements, error bars indicate standard deviation and lines are linear regressions.

Figure 3.6: The effect of preparing and priming the membrane filter on product recovery. BAC p5176 (116 kb) was filtered using 0.22 μm PVDF membranes at a constant flux of 2.3 mL/min.cm^2. The results shown are average of two or three sets of data, error bars indicate standard deviation.

Figure 3.7: The effect of consecutive filtration passes on product transmission. Solutions containing plasmids gWIZ (6 kb), pQR150 (20 kb) and p5180 (72 kb) were subjected to five consecutive filtrations. The feed concentration was 30 μg/mL and filtration flux of 2.3 mL/min.cm^2 was applied. The results shown are average of two sets of experiments, error bars indicate standard deviation. Please note that the standard deviation of the last two points (2 and 5 passes) for the gWIZ samples were < 0.1%.

Figure 3.8: An example of a PCR trace. Fluorescence units are shown on the y-axis. The base line was first set in the figure. The black horizontal line is the threshold line. The cycle number at which the increase in fluorescence is logarithmic was measured and the CT values were obtained at which the fluorescence crosses the threshold. CT values correspond to DNA concentration.

Figure 3.9: Genomic DNA (*E. coli* DH5α) standard curve for the quantification of DNA concentration.

Figure 3.10: (A) Confocal microscope image of membrane filter surface used for filtration of plasmid pQR150 (20 kb). Membrane was stained with PicoGreen and bound DNA gives green fluorescence. The line across the membrane represents an example of the cross section scanned. (B) Intensity profile across the selected membrane cross section.

Figure 3.11: (A) Confocal microscope image of top surface of filtration membrane used for filtration of p5180 (72 kb) BAC vector. Membrane was stained with PicoGreen and bound DNA gives green fluorescence. The line across the membrane represents an example of the cross section scanned. (B) Intensity profile across the selected membrane cross section.

Figure 4.8: The effect of membrane type on DNA transmission. Solutions containing pQR150 (20 kb) (□) and p5180 (72 kb) (◇) were filtered through 0.22 μm PVDF (——) and 0.2 μm PES (- - - - -) membranes at a flux of 2.3 mL/min.cm^2 and were subjected to five consecutive filtrations. The feed concentration was 30 μg/mL and analysis was carried out by the modified PicoGreen assay. The results shown are average of two sets of data, error bars indicate standard deviation.

Figure 4.9: The effect of membrane type on relative integrity. Solutions containing gWIZ, pQR150 and p5180 were filtered through 0.22 μm PVDF (——) and 0.2 μm PES (- - - - -) membranes at a flux of 2.3 mL/min.cm^2 and were subjected to five consecutive filtrations, first pass (◆, ◇) and fifth pass (▲,△). The feed concentration was 30 μg/mL and analysis was carried out by the modified PicoGreen assay. The results shown are average of two sets of data, error bars indicate standard deviation and lines are linear regressions.

Figure 4.10: Effect of formulating buffer on product transmission. Solutions of p5180 (72 kb) and p5176 (116 kb) prepared in TE buffer plus 150 mM NaCl were filtered through 0.22 μm pore size PVDF membranes at a flux of 2.3 mL/min.cm^2. The feed concentration was 30 μg/mL.

Figure 4.11: The particle size measurement of the PEI/DNA complexes over a 60 minute period. Average particle diameter was determined to be around 140 ± 14 nm.

Figure 4.12: The particle size measurement of the LID complexes over a 60 minute period. Average particle diameter was determined to be 221 ± 22 nm.

Figure 4.13: Effect of formulating buffer on product transmission. Solutions of p5180 (72 kb) in the presence of 150 mM NaCl, complexed with PEI and LI filtered through 0.22 μm pore size PVDF membranes at a flux of 0.2 mL/min.cm^2. The feed concentration was 30 μg/mL. For formulations in TE and NaCl, results shown are the average of two experiments, error bars indicate standard deviation.

Figure 4.14: Stability of plasmid pQR150 (20 kb). All samples were subjected to degradation at 60°C for 0, 2, 4 and 24 hours. Analysis performed using gel densitometry scanning. (A) Percentage of SC pQR150 (20 kb) plasmid in non-filtered feed control and filtered samples through 0.22 μm PVDF membrane and 0.2 μm PES membrane. (B) Normalised data from (A) showing relative SC plasmid in non-filtered control (◆) and samples filtered with PVDF (■) and PES (▲).

Figure 5.1: (A) Viscosity data of plasmid DNA solutions between concentrations of 30 to 950 μg/ml. Plasmid pQR150 (20kb) was used. (B) Experimental data (◆) combined with viscosity of DNA solutions obtained from data presented by Copper et al (2003) (▪).

Figure 5.2: (A) The flow decay of solutions containing plasmid gWIZ (6 kb). (B) The flow decay of solutions containing plasmid pQR150 (20 kb). Feed concentrations were 15, 30 and 100 μg/mL. Pressure was kept constant at 30 ± 1 kPa. (C) The V_{max} analysis for filtrations of plasmid gWIZ (6 kb) at 100 μg/mL and pQR150 (20 kb) at 30 μg/mL.

Figure 5.3: The effect of DNA concentration on initial filtration flux. The 6 (◆) and 20 kb (■) plasmids were filtered using 0.22 PVDF membranes. Feed concentrations were 15, 30 and 100 μg/mL. Pressure was kept constant at 30 ± 1 kPa. The results shown are averages of calculated initial flux values based on filtration durations of 1, 4 and 6 minutes, error bars indicate standard deviation and lines are linear regressions.

Figure 5.4: The effect of DNA concentration on V_{max} per membrane area. The 6 (◇) and 20 kb (□) plasmids were filtered using 0.22 PVDF membranes. Feed concentrations were 15, 30 and 100 μg/mL. Pressure was kept constant at 30 ± 1 kPa. The results shown are averages of calculated V_{max} values based on filtration durations of 1, 4 and 6 minutes, error bars indicate standard deviation.

Figure 5.5: The effect of DNA concentration on membrane capacity. The 6 (◇) and 20 kb (□) plasmids were filtered using 0.22 PVDF membranes and filtration performed at 30 kPa. The results shown are averages of calculated V_{max} values based on filtration durations of 1, 4 and 6 minutes, error bars indicate standard deviation.

Figure 5.6: The flow decay of solutions containing gWIZ (6 kb), pQR150 (20 kb) and p5180 (72 kb). Feed concentration was 15 ± 2 μg/mL. Filtrations were performed at 30 ± 1 kPa.

Figure 5.7: The effect of vector size on initial flux. Solutions of gWIZ (6 kb), pQR150 (20 kb) and p5180 (72 kb) filtered at 30 ± 1 kPa. Feed concentration was 15 ± 2 μg/mL.

Figure 5.8: The effect of vector size on V_{max}. Solutions of gWIZ (6 kb), pQR150 (20 kb) and p5180 (72 kb) filtered at 30 ± 1 kPa. Feed concentration was 15 ± 2 μg/mL.

Figure 5.9: Transmission of gWIZ (6 kb), pQR150 (20 kb) and p5180 (72 kb) filtered at 30 ± 1 kPa. Feed concentration was 15 ± 2 μg/mL. The results shown are based on an average of two sets of spectrophotometry measurements, error bars indicate standard deviation and lines are linear regressions.

Figure 5.10: The effect of vector size on membrane capacity. Filtrations were performed at 30 ± 1 kPa. Feed concentrations were 15 ± 2 μg/mL. The results shown are based on an average of two sets of spectrophotometry measurements, error bars indicate standard deviation and lines are linear regressions.

centrifuges. Results shown are average of measurements based on 2–4 independent resuspensions, and error bars represent standard deviations.

Figure 7.4: Effect of continuous centrifugation on supercoiled plasmid pQR150 (20 kb) yield. Agarose gel electrophoresis of purified pQR150 samples derived from an equal mass of cells harvested using a solid-bowl centrifuge operated at 60 L/h (lane 1) and a disk-stack centrifuge operated at 50 L/h (lane 2). Lanes 1 and 2 were loaded with an equal mass of total DNA (250 ng).

Figure 7.5: Effect of continuous centrifugation on supercoiled plasmid gWIZ (6 kb) yield. Agarose gel electrophoresis of purified pQR150 samples derived from an equal mass of cells harvested using a solid-bowl centrifuge operated at 60 L/h (lane 1) and a disk-stack centrifuge operated at 90 L/h (lane 2). Lanes 1 and 2 were loaded with an equal mass of total DNA (200 ng).

Figure 7.6: Effect of cell resuspension holding temperature. *E. coli* cells harvested using a solid-bowl centrifuge were stored frozen which was subsequently thawed and resuspended at 13 °C for 0, 2 and 6 h. Cells were centrifuged briefly and supernatants analysed in triplicates using PicoGreen, dilution of supernatant was 1/5000 (analysis point a^1, Figure 7.1), results shown are averages, error bars represent standard deviations.

Figure 7.7: Effect of cell resuspension holding times on the yield of supercoiled plasmid pQR150 (20 kb).Agarose gel electrophoresis of purified pQR150 samples derived from cells harvested using a solid-bowl centrifuge. Lanes 0, 2 and 6 corresponded to holding times of 0, 2 and 6 h at 13 °C, and were loaded with equal volume of purified DNA solution to enhance visualisation of decreased total yield. Abbreviations: M, λ Hind III molecular weight marker; S2, control sample chemically degraded at 60°C for 48 hours.

Figure 7.8: Process flowsheet for clarified lysate. Sampling points for analysis are indicated (|a).

Figure 7.9: Agarose gel electrophoresis of isopropanol precipitated plasmid pQR150 (20 kb) samples collected from large-scale pumping studies using the Mono and Centrifugal pumps at fixed feed flow rates over a period of 60 minutes. Control sample S1 corresponds to purified plasmid pQR150 (20 kb) and S2 is S1 degraded at 60°C for 48 hours. Abbreviations: OC – open circular; SC – supercoiled.

Figure 7.10: Relative integrity of plasmid pQR150 (20 kb) based on the gel densitometry scan of isopropanol precipitated samples collected from large-scale pumping studies using the mono (◆) and centrifugal (■) pumps at fixed feed flow rates over a period of 60 minutes.

Figure 7.11: Agarose gel electrophoresis isopropanol precipitated plasmid pQR150 (20 kb) samples after passing through the centrifuge feed zone at flow rates of 50, 70 and 120 L/h. Control sample S1 corresponds to purified plasmid pQR150 (20 kb), S2 is S1 degraded at 60°C for 48 hours and S3 is single stranded S1 obtained by performing the alkaline lysis step in the presence of excessive NaOH. Abbreviations: M – λ HindIII molecular size marker; OC – open circular; SC – supercoiled.

V. List of Tables

VI. List of Publications

Kong S, Titchener-Hooker N, Levy MS. (2006). Plasmid DNA processing for gene therapy and vaccination: Studies on the membrane sterilisation filtration step. Journal of Membrane Science, 280, 824-831.

Hoare M, Levy MS, Bracewell DG, Doig SD, Kong S, Titchener-Hooker N, Ward JM, Dunnill P. (2005). Bioprocess Engineering Issues That Would Be Faced in Producing a DNA Vaccine at up to 100 m^3 Fermentation Scale for an Influenza Pandemic. Biotech Progress, 21, 1577-1592.

Kong S, Rock CF, Booth A, Willoughby N, O'Kennedy R, Relton J, Hoare M, Ward JM, Levy MS. Large-scale plasmid DNA processing: Evidence that cell harvesting and storage methods affect supercoiled plasmid yield. Biotechnology and Applied Biochemistry (submitted).

Zhang H, Kong S, Booth A, Boushaba R, Levy MS, Hoare M. Prediction of Shear Damage of Plasmid DNA in Pump Operations Using an Ultra Scale-Down Devise. Biotechnology Progress (in progress).

Kong S, Titchener-Hooker N, Levy MS. Plasmid DNA processing for gene therapy and vaccination: Studies on membrane filtration. Vaccine Technology, Engineering Conferences International, Puerto Vallarta, Mexico (25-30 June 2006).

Chapter 1 – Introduction

1.1 Project Overview

The number of plasmid DNA-based gene therapy and DNA vaccines clinical trials have soared to 206 in recent years (Gene Therapy Trials Worldwide, January 2006), and the interest in these treatments requires production of pharmaceuticals that meet stringent regulatory requirements. One such requirement is the sterility of the product. Membrane filtration is considered to be the most suitable option currently available for sterilisation of DNA as the molecules are susceptible to degradation and mutagenesis with the use of heat and radiation methods.

Sterile filtration through membranes with pore size of ≤ 0.2 or 0.22 μm is typically the last operation in the production of DNA-based drugs and nonetheless it is also often used at intermediate points during purification. During a filtration procedure, irreversible conformational changes intensified by elongational shear, retention of molecules by the membrane filter or a combination of both could contribute to product loss. Plasmid DNA presently produced for use in clinical trials applications is typically between 5 and 20 kb (Prazeres et al., 1999; Urthaler et al, 2004). However, there are strong indications of using higher molecular weight vectors which could provide greater effectiveness in therapeutic treatments through the

inclusion of regulatory regions and multiple genes (Kelly, 2003; Lindenbaum et al., 2004). Due to their size and character, processing these large DNA vectors is a challenge.

1.1.1 Aims and Objectives

In this work, key parameters affecting the normal-flow membrane filtration performance of solutions containing purified plasmid DNA and bacterial artificial chromosomes were investigated. Two small scale filtration systems were designed to enable information on material properties to be obtained. Firstly, constant flux experiments were conducted with a pressure driven syringe system which allowed data on transmission and degradation to be obtained rapidly using small sample volumes of $\leq$ 1 mL and commercially available sterilising grade 0.2 or 0.22 μm pore size hydrophilic membranes. The second system design was a positive pressure filtration setup which constant transmembrane pressure operations were applied to enable the estimation of membrane capacity.

Constant flux experiments were performed with the intention to determine if the prevailing mechanism for product loss was due to retention/sieving by the membrane filter or due to unspecific adsorption (as frequently observed in the filtration of proteins). Although helical properties would enable molecular stretching in the direction of the fluid flow to promote permeation through membrane pores, product transmission may be low given that regular size 6–20 kb (4×10^6 – 13×10^6 Da) plasmids used in therapies even have radii of gyration 4–13 times larger than the typical pore diameter of the sterilising membranes. Aside from being retained by the

membrane filter, high density of negative charges on the DNA backbone may contribute to unspecific adsorption further enhancing the membrane fouling. Various vector sizes, DNA concentrations and operating flux rates were tested.

Another purpose of the experiments was to test whether DNA vectors $\geq$ 20 kb could be filter sterilised without substantial loss of the desired supercoiled form. An advantage of the constant flux filtration setup was the ability to apply high fluxes to accentuate molecular backbone breakage. Since the generation of degraded plasmid forms would lead to reduced product efficacies, evaluation of product damage following filtration was essential. In further work, two membrane types were compared as it has been suggested that pore microstructure can influence transmission and degradation rates. Additionally, formulation buffer modification methods for improving the filtration performance by increasing molecular flexibility using sodium chloride (NaCl) and alteration of hydrodynamic size using condensing agents were investigated.

Lastly, filtrations at constant pressure were conducted to determine the capacity of the membrane filter with respect to vector size, DNA concentration and operating pressure. It is also important to find means of relating product transmission and filter capacity. As in any normal flow or dead-end filtration system, the build up of retained material can often increase resistance to filtration and lead to permeate flux decline over time. Since material deposition rather than adsorption was expected to be dominating the fouling phenomenon, the gradual pore constriction model was selected for estimation of the filter capacity which can later be used to predict the performance of larger scale filtrations.

1.1.2 Additional work

A number of people have died by infection an avian influenza virus from chickens and the World Health Organisation is concern of the virus mutating and being capable of human to human transfer. In view of the current situation, collaboration work with other researchers at the UCL Innovative Manufacturing Research Centre (IMRC) was conducted with aim to look into issues that would be faced in a large scale production of the DNA vaccine in case of a pandemic. A thesis chapter is dedicated to report and discuss the two studies that I was involved in. These studies were performed to:

- Assess the effect of *E. coli* cell harvest using centrifugation methods and cell handling in the initial stages of plasmid DNA processing.
- Evaluate the impact of passing *E. coli* clarified lysate through a centrifugal pump, a mono pump and a disk-stack centrifuge feed zone.

Bacterial cells and plasmid DNA exposed to these typical industrial operations are subjected to fluid stresses. Large quantities of contaminating species such as degraded plasmid isoforms, singe stranded DNA and fragmented genomic DNA could be generated. Processes further downstream are likely to be affected, and the overall product quality as well as yield could decrease considerably.

1.2 Background

1.2.1 Gene Therapy and DNA Vaccines

Gene therapy is a revolutionary approach aimed at treating or eliminating the causes of disease instead of treating the symptoms (Mountain, 2000). Gene therapy and DNA vaccination offer great potential for prevention of infectious diseases caused by bacterial, viral and parasitic organisms, and new treatment possibilities for many commonly inherited human diseases where conventional clinical procedures are less effective including monogenic disorders, such as cystic fibrosis, and more complex disorders, such as cardiovascular diseases, diseases of nervous system, autoimmune diseases, and cancer (Gardlik et al., 2005; Mountain, 2000). In the gene therapy approach, a corrective gene is transferred to specific cells or tissues in a patient to produce therapeutic biomolecules for the treatment of diseases (Mountain, 2000; Orkin, 1986). Gene therapy on somatic cells can either be *ex vivo* where cells are modified in an artificial environment outside the body before being transplanted back or *in vivo* where defective genes are changed in cells while still in the body (Gene Therapy, Human Genome Project Information, n.d.). The type of vectors commonly used in gene therapy trials are shown in Figure 1.1.

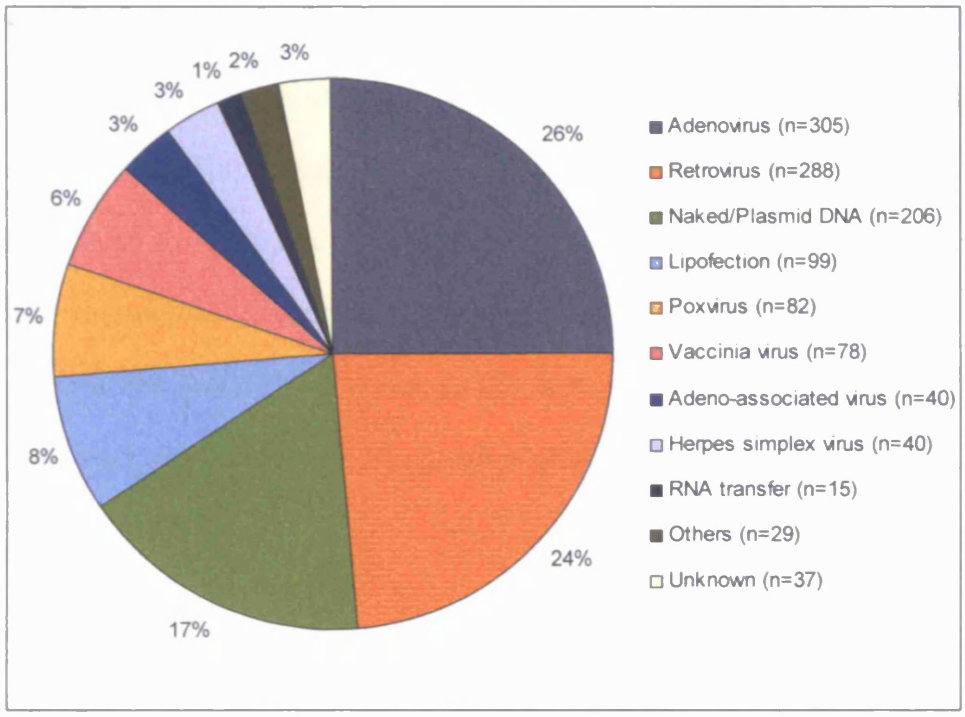

Figure 1.1: Vectors used in gene therapy trials (adapted from Gene Therapy Trials Worldwide, January 2006).

Both viral and non-viral delivery systems can be used in gene therapy and vaccination. In general, viruses attack their host cells and introduce their genetic material with high efficiency into the host as part of their replication cycle (Walter and Stein, 2000). Therefore it is possible to take advantage of this by introducing a foreign gene that encodes the desired effect into the virus and then using the properties of the virus to deliver this gene into the target cells (Gardlik et al., 2005). Viral vectors may be effective in transferring genes into specific cells and into cellular interior (Felgner et al., 1997) but viral vectors have shown adverse cellular reactions such as severe immunological reactions or development of leukaemia-like conditions in the treatment of severe combined immunodeficiency (SCID) recently (Voβ et al., 2003). Problems of viral gene therapy need to be overcome before widespread use is implemented.

Hence, there are increasing preferences towards non-viral delivery methods based on naked plasmid DNA or a complex of lipids or proteins with DNA because they are more economical (simpler large scale production), safer (low host immunogenicity) and not limited to insert-size (Shizuya et al., 1992). Previously, non-viral methods were not as desirable compared to viral vectors due to low levels of transfection and expression of the gene; however, recent advances have demonstrated that non-viral vector technology has yielded transfection efficiencies similar to that of viruses (Gardlik et al., 2005).

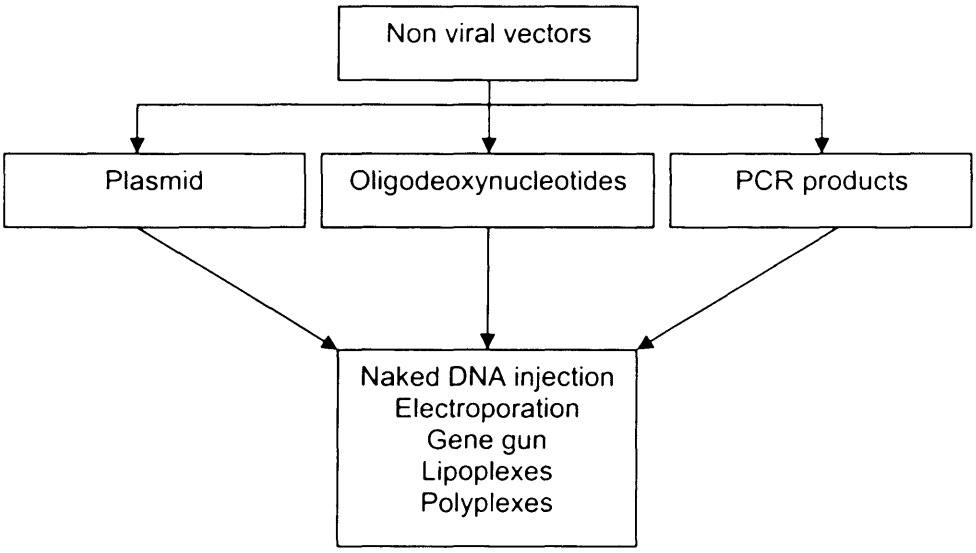

Figure 1.2: Non-viral vectors alongside various methods and techniques applied for the introduction of DNA vector into targeted cells in gene therapy (adapted from Gardlik et al., 2005).

A simple technique of non-viral gene transfer is the use of naked DNA introduced directly into target cells. Plasmid DNA or polymerase chain reaction (PCR) products that encode the desired gene are usually used. *In vitro* transfection by non-viral DNA has been more effective than *in vivo* (which is a more complex system) (Darquet et al., 1999). Nonetheless Wolff el al. (1990) demonstrated naked plasmid DNA injected *in vivo* showed activity especially in skeletal muscles. This had sparked off an intense interest in generating antiviral immune response by intramuscular injection of a plasmid encoding a viral antigen which led to the development of DNA vaccines (Li and Huang, 2000). Among techniques developed to improve transfection efficiency and expression level is the electroporation methodology where short electric pulses are applied to induce the membrane potential and transiently create pores on the target cell's membrane which would allow DNA penetration into the cell (Gehl, 2003). The "gene gun" approach involves coating DNA onto gold micro particles to accelerate the entry of the DNA vector into target cells using electrical currents (Kuriyama et al., 2000; Qiu et al., 1996).

In addition, complex molecular architecture involving different condensing agents and targeting domains and moieties containing one or a combination of charged polymers, dendrimers, lipids and liposomes to condense naked DNA vectors forming complexes such as lipoplexes (DNA-liposomes complexes) and polyplexes (DNA-polymers complexes) are currently applied to improve the stability of DNA and also facilitate the entry into the cell (Hart et al., 1997; Sarkar et al., 2003; Udeuehi, et al., 2001). Cationic lipids which could form complexes with the negatively charged DNA and moreover, allow interactions with the negatively charged cell membrane can be used to enhance delivery and penetration into the cell and thus improving

expression of DNA *in vitro* or *in vivo* (Subramanian et al., 2000; Zhdanov et al., 2002). Researchers like Hart et al. (1997) and White et al. (2003) have conducted studies based on the understanding of mechanisms of cellular barriers and transport of vectors using a synthetic peptide moiety that has high affinities for cell surface integrins and a polymer moiety for DNA binding aimed to improve transfection efficiency. Other researchers such as Godbey et al. (1999) have worked on the development of polyplexes and the optimisation of DNA vector complexation based on ionic interactions using the condensing polycation – polyethylenimine (PEI) for gene delivery.

Synthetic oligodeoxynucleotides may be used in gene therapy applications (Gardlik et al., 2005; Stein and Cohen, 1988). However, oligodeoxynucleotides do not encode any therapeutic gene, but instead they are involved in the inactivation of the targeted genomic genes concerned in the disease process by disrupting the transcription of the target gene using specific antisense fragments or cleaving the mRNA transcript sequence with ribosomes (Gardlik et al., 2005).

1.2.2 Production and Downstream Processing of Plasmid DNA

Plasmids in their supercoiled form are desirable for use in gene therapy and vaccination applications (Horn et al., 1995; Kelly, 2003; Levy et al., 2000b; Marquet et al., 1995). As illustrated in Figure 1.2 below, plasmids and artificial chromosomes can exist in various isoforms such as supercoiled circular (SC), open circular (OC) and linear forms. Based on FDA regulations, more than 90% of the plasmids are required to be in the SC form (Butler, 1996). Although a SC yield of 80–90% can be expected in small-scale preparations of DNA that are smaller than 20 kb in size, physical breakage and chemical degradation increases significantly during large scale processing and long-term storage (Horn et al., 1995; Middaugh et al., 1998). For large plasmids where not even small-scale preparations yield very high amounts of SC vectors, damage during large scale processing is expected to be even more drastic.

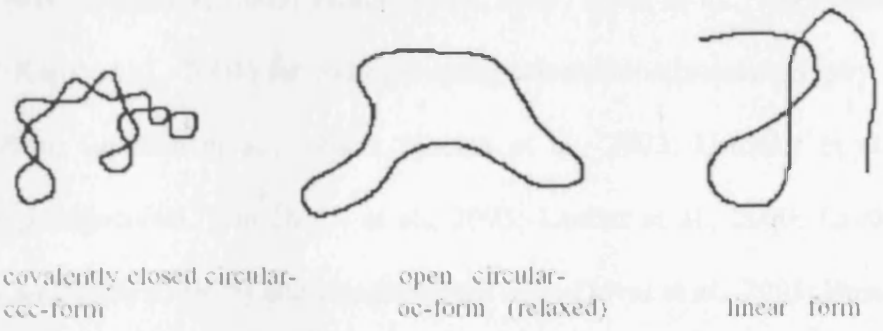

Figure 1.3: Illustration of different circular DNA isoforms (Voβ et al., 2003)

In a typical downstream process (Figure 1.4), plasmid DNA propagated in *E. coli* is to be isolated. In depth details of industrial plasmid DNA processes are well described for example in patents by Hitchcock (2005), Necina et al. (2003), Thatcher et al. (2003) and Urthaler et al. (2004). Bacterial cells are harvested at late log or stationary phase via centrifugation, resuspended in an appropriate buffer and chemically lysed to obtain the valuable intracellular plasmid DNA (Birnboim and Doly, 1979; Durland and Eastman, 1998; Ferreira et al., 2000; Levy et al., 2000a; O'Kennedy et al., 2003). Another method of cell lysis used in the production of plasmid DNA is by boiling the bacterial cells which was introduced by Holmes and Quigley (1981).

The next step is centrifugation or filtration to separate cell debris and lysis by-products; clarified lysate is transferred further downstream for purification to attain the high purity plasmids separated from *E. coli* genomic DNA, RNA, protein and endotoxin (Durland and Eastman, 1998; Ferreira et al., 2000; Ish-Horowitz and Burke, 1981; Hitchcock, 2005; Hoare et al., 2005; Horn et al., 1995; Levy et al., 2000a; Urthaler et al., 2004) for example using adsorption/chromatography (Levison et al., 1998a; Levison et al., 1998b, Necina et al., 2003; Urthaler et al., 2005), fractional precipitation (Eon-Duval et al., 2003; Lander et al., 2000; Lander et al., 2002; Lis and Schleif, 1975) and ultrafiltration (Eon-Duval et al., 2003; Bussey et al., 1998; Kahn et al., 2000) methods. In intermediate production steps, sterilising grade membrane filters may be applied to reduce the bioburden levels while the final filtration procedure of purified DNA prior to vialing and formulation is essential and necessary to ensure sterility (Jornitz et al., 2003).

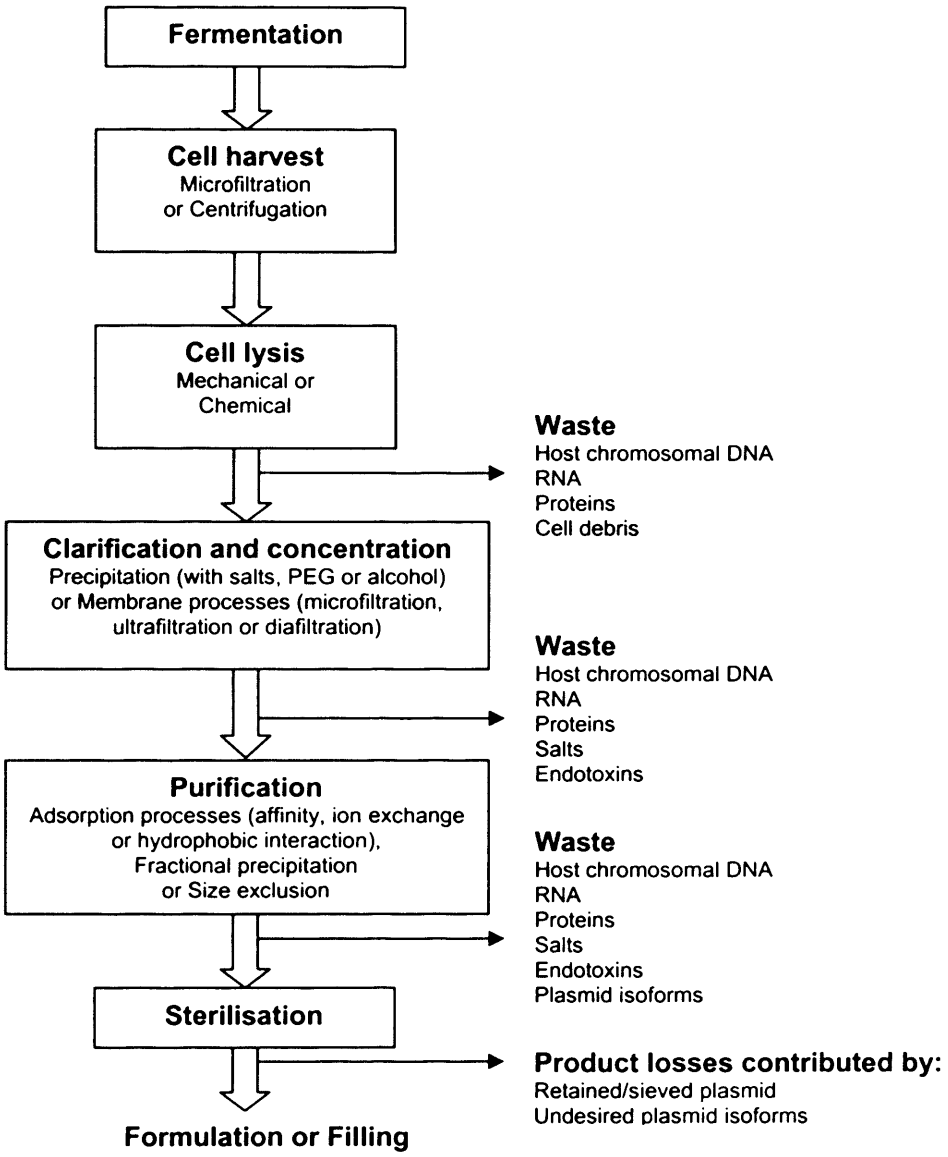

Figure 1.4: Process flow sheet for a large-scale production of supercoiled plasmid DNA (adapted from Ferreira et al. 2000).

Since QIAGEN® purification kits (which contain ion exchange chromatography columns) are widely available and are easy to use, they are frequently used in laboratory scale preparations of plasmid DNA. However, it is important to note that because these kits are designed for laboratory use only, purity of the product obtained may not achieve the industrial standards of pharmaceutical grade DNA as described in the patent by Thatcher et al. (2003).

1.2.3 Sterilisation of DNA Solutions

Sterilisation is a vital step in the manufacture of pharmaceuticals in order to minimise the risks of microbiological, particulate and pyrogen contamination (WHO Technical Report, 2002). There are numerous ways to achieve sterilisation. Some of the common sterilisation methods include the use of moist or dry heat, irradiation with ionising radiation (excluding ultraviolet radiation), ethylene oxide (or other suitable gaseous sterilising agents), and filtration devices with subsequent aseptic filling into sterile final containers (WHO Technical Report, 2002). Suitability of the technique is of great importance as any product losses could have a very substantial economic impact particularly in the late stages of downstream processing. The terminal sterilisation step prior to vialing or formulation is essential to assure sterility while the application of aseptic processing throughout the entire production series would not be economical or desired.

Depending on the suitability, the above-mentioned techniques may present advantages and disadvantages for sterilisation uses. Sterilisation by moist heat (autoclaving) is suitable for water-wettable materials and aqueous formulations while dry heat should only be used for non-aqueous liquids or dry powder products and radiation should be used for heat sensitive materials (WHO Technical Report, 2002). It is very important to note sterilisation options such as heat and radiation methods are not suitable for DNA as they would cause DNA degradation and mutagenesis affecting the product's biological activity and efficacy (e.g. Brannen, 1970; Francis and Regan, 1986). Gasses and fumigants such as ethylene oxide and hydrogen peroxide vapour can be used for sterilisation purposes as well. Once again, the use of

gasses is not advisable for DNA solutions due to the potential risk of physical damage on DNA molecules attributed to shear associated effects at the gas-liquid interface (Levy et al., 1999). Furthermore, degassing needs to be performed with extra care and has a risk of residual gas presence.

After taking into consideration the commonly used sterilisation options, the filtration technique is considered the best method for sterilising DNA solutions. In order to maintain a high standard in sterility, attention needs to be given to the type of sterilising filters used, in appropriate environment for aseptic filling into sterile containers, and finally handling by the right personnel (WHO Technical Report, 2002). The final sterile filtration involves only low level of impurity removal based on sieving effects through a porous membrane. Unwanted microorganisms and other contaminants are retained either on the surface or within the pore structures while the desired product, in this case, DNA molecules and solutes permeate through the pores. In accordance to the current Good Manufacturing Practices (cGMP), the filtration membrane should have a nominal pore size of 0.22 μm or less and the bulk of particulates similar in size to *Brevundimonas diminuta* should not be able to penetrate through the membrane filters (Jornitz, 2003; US FDA 21 Code of Federal Regulations-Parts 210 and 211, updated December 2005; WHO Technical Report, 2002).

Backbone breakage of DNA vectors in an elongational flow during the sterile filtration procedure is a serious concern since the integrity of DNA vectors plays such an essential role in assuring product efficacy. Flux of saline for commonly used polyethersulfone membranes are typically in the region of 0.1–0.4 mL/min.cm^2

(Dosmar, 2004). Shear rates are estimated using computational fluid dynamics simulations to be 10^2–10^3 s^{-1} for the respective filtration fluxes and can be expected to be significant at the entrance of the pore with reference to the flow characterisation work done using capillary devices (Zhang, H., Department of Biochemical Engineering, UCL, personal communication). The shear forces applied might induce irreversible molecular damage particularly for the larger plasmid DNA (> 10 kb).

In view of the increment of radius of gyration with molecular size, transmission levels may potentially be affected especially when considering the filtration of large plasmids. Besides, the possibility of unspecific chemical adsorption to the membrane filter cannot be ruled out either since the DNA backbone has a high density of negative charges. Permeation of concentrated and viscous DNA solutions is also difficult to achieve due to the high viscous force exerted on the membrane's surface which could then rupture the membrane itself or cause breakages of the filtration capsule or cartridge. Therefore, it is crucial to identify adequate processing strategies for the sterilisation particularly of higher molecular weight DNA vectors to ensure high yield and throughput.

1.2.4 DNA Molecules in a Flow Field

Shear sensitivity of DNA molecules had been demonstrated to increase with molecular weight (Bowman and Davidson, 1972; Larson et al., 2006; Lengsfeld and Anchodoquy, 2002; Levy et al., 1999; Reese and Zimm, 1990). DNA chains moving with the liquid flow are subjected to shear stress and tensile force being maximal near the centre of the molecular chains triggers mid-length strand breakage (Bowman and Davidson, 1972). In a flow field, DNA molecules will undergo bending motion and elongation deformation (Larson et al., 1997). Flow-induced deformation of molecular chains in solutions will be observable whenever hydrodynamic drag forces overcome the random Brownian forces which tend to keep the chain in a coiled state (Hunkeler et al., 1996).

During the course of filtration, DNA molecules will elongate by the shear stress and deform in the direction of the flow to permeate through the pores on the membrane (Hirasaki et al., 1995; Higuchi et al., 1996). The molecules' ability to respond elastically will help prevent strands fractures but as flow stresses increases, elastic response could diminish. Due to the fact that DNA molecules are macromolecular polymers with long chain of repeated units, molecular structure and dynamics will govern their polymeric properties such as supercoiling and stretching in solution. The following sections will provide a brief insight into the composition and structure of the DNA molecules.

1.2.4.1 DNA Composition

The backbone of the nucleic acid chain consists of repeating sugar units connected by phosphate residues and perpetuated by phosphate-hydroxyl links (Mandelkern, 1983). A heterocylic base is attached to the hydroxyl group on the carbon-1 position of each sugar unit (Stryer, 1981). Overall, the components of the DNA are the five-membered ring sugar 2'-deoxyribose, phosphate residues, and four heterocyclic bases: two purines (adenine and guanine) and two pyrimidines (thymine and cytosine) (Stryer, 1981).

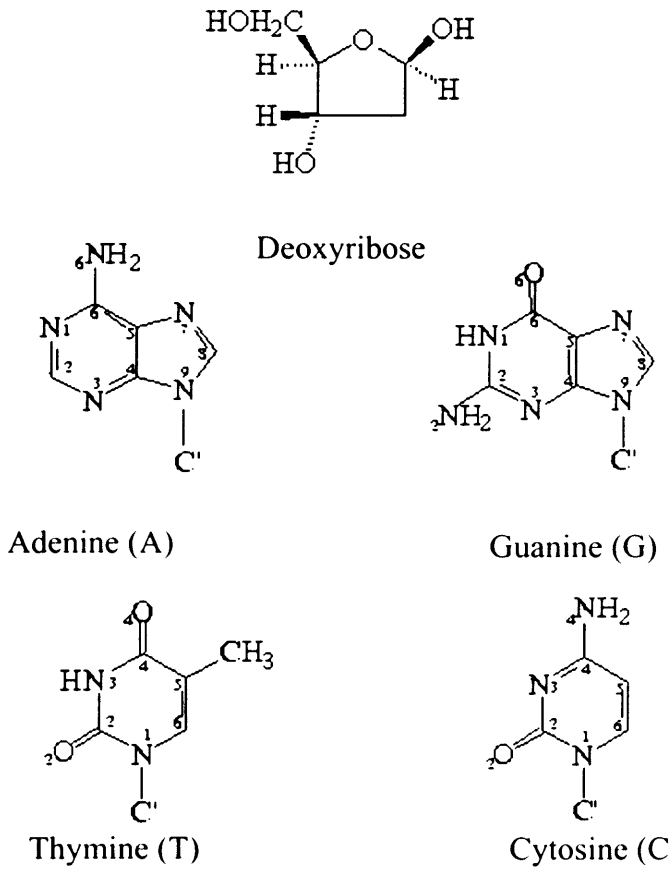

Figure 1.5: Structural formulas of the components of DNA: the deoxyribose sugar and the four heterocyclic bases – adenine, guanine, thymine and cytosine (Stryer, 1981).

In the native state, the two antiparallel chains of alternating deoxyribose and phosphate intertwined into a double helix to form the helical backbone structure in which hydrogen bonding between the purine bases (A is paired with T by two hydrogen bonds) and the pyrimidine bases (C is paired with G by three hydrogen bonds) secures the strands together (Stryer, 1981). Due to the geometry of the double helix, a purine base always pair complementarily with a pyrimidine as a consequence of the size, shape and chemical composition of the bases (Stryer, 1981). When the two sugar-phosphate chains twist around each other, the planar base pairs stack on top of each other and the overall stability of the double helix is further strengthened by Van der Waals and hydrophobic interactions between stacked adjacent pairs (Stryer, 1981).

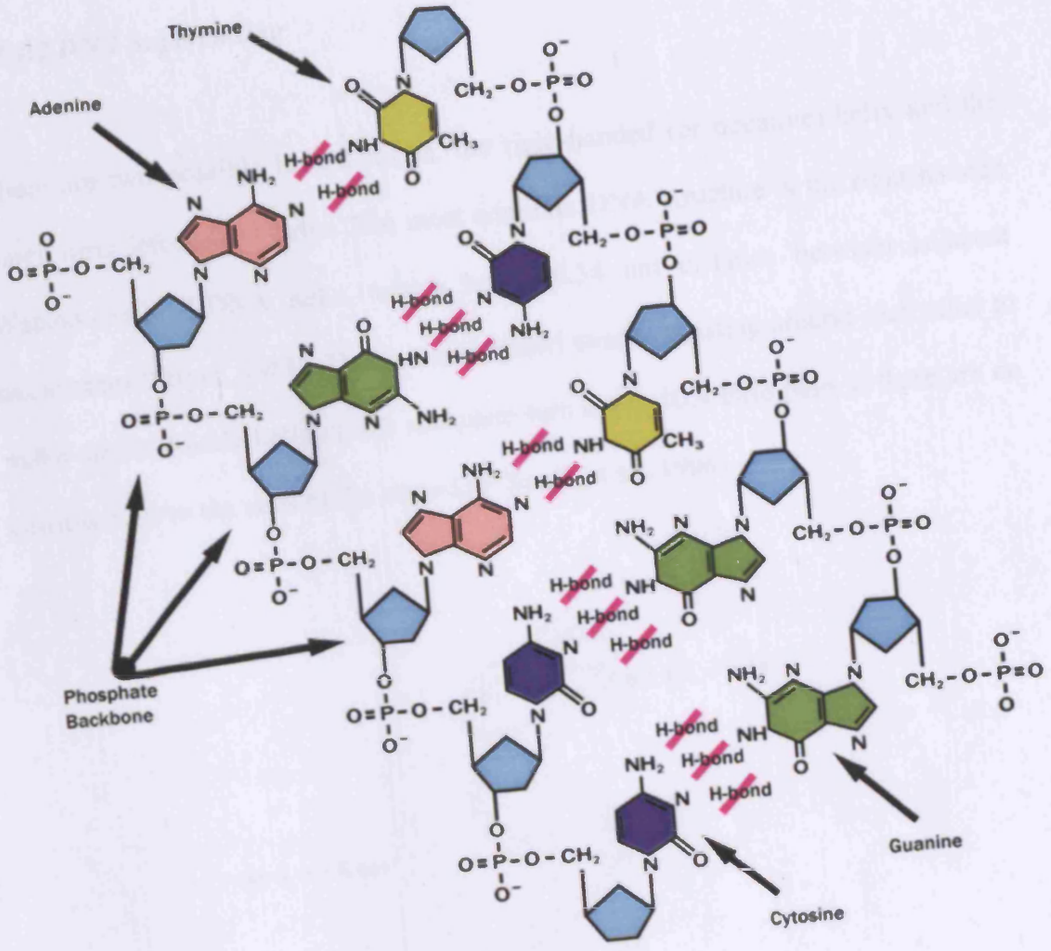

Figure 1.6: Skeletal structure of the DNA backbone (DNA-labels, 2006).

1.2.4.2 DNA Supercoiling

There are two possible helical forms: the right-handed (or negative) helix and the much rarer left-handed helix. The most common DNA structure is the right-handed Watson-Crick B-DNA helix, which has a 0.34 nm distance between adjacent nucleotides (Stryer, 1981). The two antiparallel strands twisting around each other to make up the double helix makes complete turn every 10.4 base pairs if there are no constrictions to the ends of the molecule (Strick et al., 1998).

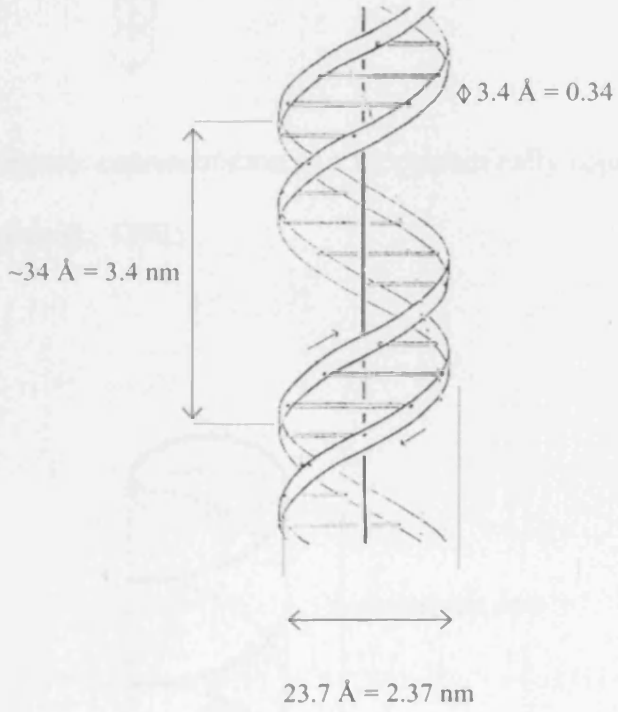

Figure 1.7: Dimensions of a right-handed Watson-Crick B-DNA (Watson and Crick, 1953).

When the two double helix strands of sugar-phosphate backbone are torsionally constrained for example in the case of a circular plasmid, DNA molecules will

further twist into interwound supercoiled structures or branched plectonemic form as a mean to release torsional stress (Strick et al., 1998). When stretching force is applied, the highly coiled DNA (like a telephone cord) will lessen its writhe, and then revert back to its plectonemes form when the stretching force is absent (Strick et al., 1996).

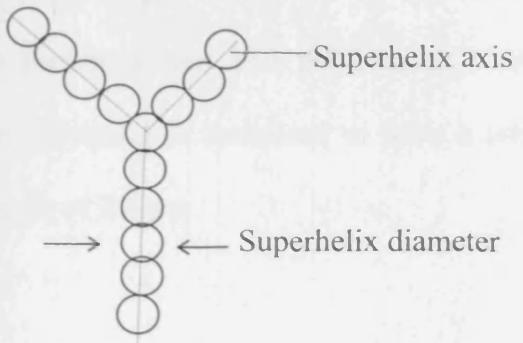

Figure 1.8: Schematic representation of a plectonemically supercoiled DNA (adapted from Vologoskii et al., 1992).

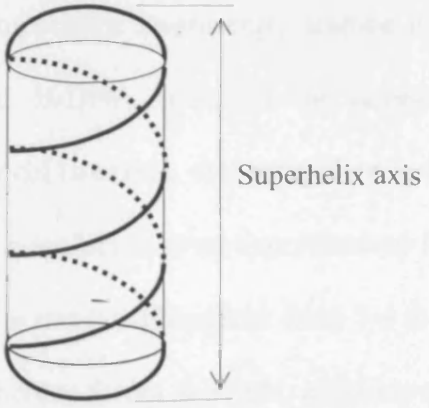

Figure 1.9: Simplified model of a plectonemic supercoiled DNA (with no branch). The number of supercoil is equivalent to the number of helical turns around the cylinder (adapted from Boles et al., 1990).

From electron microscopy and topological methods, it was found that the superhelix radius decreases hyperbolically as supercoiling increases and the average length for a negatively supercoiled DNA axis was deduced to be around 41% of the DNA contour length (Boles et al., 1990). The contour length or end-to-end distance of the DNA molecule is proportional to its molecular weight. For example, a 20 kb plasmid having a molecular weight of 13×10^6 Da (calculated by summing the molecular weight of the backbone unit and the base unit minus one for removal of one hydrogen from the base) is estimated to have a contour length of 6.8 μm and a supercoiled length of 2.8 μm.

1.2.4.3 DNA Stretching

Experiments conducted by Bustamante et al. (1994) have shown that single DNA molecules would respond to applied forces as elastic bodies. Soon after, it was discovered through fluorescence microscopy studies involving the stretching of a single double stranded B-DNA molecule in aqueous solution tethered to a microsphere held by optical tweezers, that an applied longitudinal stress $\geq$ 65 pN can dramatically lengthen the molecule to an overstretched form of 1.7 times its contour length (corresponded to a rise per phosphate from 3.4 to 5.8 Å) (Smith et al., 1996; Larson et al., 1997). Whereas forces $\leq$ 50 pN, a double-stranded DNA molecule can rapidly and reversibly contract to its normal contour length the moment the stress was relaxed (Smith et al., 1996).

Fluctuations of DNA chain conformations undergoing strong elongational flow in solutions have been demonstrated in some recent experimental studies (e.g. Larson et al., 1997; Perkins et al., 1994; Perkins et al., 1995; Perkins et al., 1997). Distinct stretched conformation shapes with differing dynamics are possible in an elongational flow and the different shapes gave rise to stretching rate variations at high strain rates (Hu and Perkins, 1999; Perkins et al., 1997). Observed conformations include 'dumbbell', 'half-dumbbell', 'kinked', 'folded', 'uniform', 'extended', and 'coil'; in general, molecule chains with dumbbell shapes stretched more rapidly than folded ones (Perkins et al., 1997).

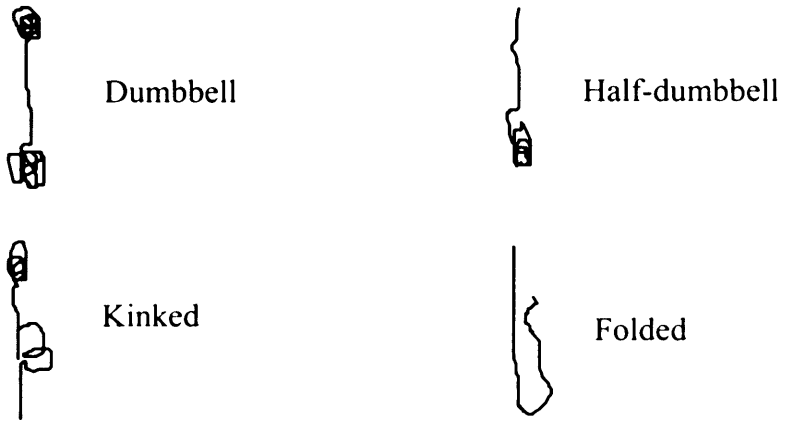

Figure 1.10: Classification model of conformation-dependant rate of stretching of supercoiled DNA at high strain rates (adapted from Perkins et al., 1997).

1.2.4.4 The Effect of Ionic Strength on DNA in Solution

Shear effects on supercoiled plasmids of 13, 20 and 29 kb in solution were evaluated in earlier studies, and the results showed that strand breakage was dependent on molecule size and ionic strength of solution (Levy et al., 2000a). Due to the double helix structure, the effective diameter of a DNA molecule can be affected by the ionic strength of the solution. Referring to a right-handed Watson-Crick double helix DNA, base pairs are stacked within the helix while the anionic groups have their electrostatic repulsion minimised on the outside the sugar phosphate backbone (Barton et al., 1980). Permeation of DNA in solution is governed by its flexibility (Hirasaki et al., 1995; Higuchi et al., 1997). Negatively charged DNA in close proximity could be very rigid due to the intermolecular electrostatic repulsion; consequently inhibiting molecular elongation in the flow direction during the filtration process.

The binding of counter ions to the nucleotides will affect the overall stability of the structure and the outcome can be either the formation of a compact highly coiled structure or an extended flexible conformation (Bloomfield, 1991). Ions or ionic groups can bind to a number of places along the polynucleotide. Common sites are the phosphates, the oxygen and nitrogen atoms on the bases, and the hydroxyl groups on the sugars (Marzilli et al., 1980).

The presence of counter ions will neutralise electrostatic repulsion causing a change in the helical diameter. But when there are no counter ions around, repulsive forces between the neighbouring phosphate anions will promote helical unwinding.

Therefore, the addition of mono- or divalent cations can directly affect the stiffness of the molecule (Bloomfield, 1991). Generally, at low metal ion: DNA-phosphate ratios, the cations bind exclusively to the phosphate anions while at high ratios, binding of counter ions to the bases increases (Barton et al., 1980). Reductions in viscosity due to increased molecular stability and flexibility have been observed in DNA solutions in the presence of the phosphate binding Cu^{2+}, Ag^{+} and Hg^{2+} ions (Barton et al., 1980).

The helical structure can also be stabilised by counter ions that link the bases in a similar intercalative manner as the aromatic dyes such as ethidium bromide, proflavin or acridine (Barton et al., 1980). But this non-specific stacking interaction will stiffen the double helix structure (Barton et al., 1980). For example, the presence of a platinum reagent due to the formation of a platinum complex will help the double helix to unwind, lengthen and stiffen (Barton et al., 1980). For a closed circular DNA, the platinum-intercalating reagent will cause a decrease in duplex turns and increase in superhelical turns while a nicked relaxed circular DNA will wind into a superhelix in its presence (Barton et al., 1980). Covalent binding to the bases on DNA molecules becomes more significant than phosphate binding as one move across and down the periodic table (Barton et al., 1980).

With the knowledge that by increasing the ionic strength (in particular the addition of phosphate binding ions) can improve the flexibility of the DNA molecules, readily available salts such as NaCl or $MgCl_2$ can be added to the DNA solutions. The manipulation of salt quantity added to DNA solutions during processing may significantly reduce degradation rates and improve yield. However, the selection of

ions used needs to be carefully screened to ensure suitability for use in a pharmaceutical formulation. For instance, Co^{2+} ions can disrupt a DNA double helix conformation as a result of hydrogen bond formation between the oxygens on the phosphate residues and the nitrogens on the bases is an undesirable final product (Marzilli et al., 1980).

Typical buffers for IV injections are phosphate buffered saline (PBS) or saline and according to the patents by Volkin et al. (2002, 2004), the type of buffer, salt concentration, and pH are some of the important parameters used to optimise DNA stability in a DNA vaccine formulation. The formulation that have provided the highest stability for a DNA vaccine includes a salt (either NaCl, KCl or LiCl) in the range of 100–200 mM, a demetalated solution containing a phosphate or bicarbonate buffer within the pH range of 7–8, a metal ion chelator (such as succinate, malate, inositol hexaphosphate, tripolyphosphate or polyphosphoric acid), and a non-reducing free radical scavenger (such as ethanol, glycerol, methionine or dimethyl sulfoxide) (Volkin et al., 2002). Thus, easily obtainable salt such as NaCl or KCl that could increase the conformational stability of plasmid DNA can be considered for use.

1.2.5 Flow of DNA Molecules through Membrane Pores in a Normal Filtration System

DNA molecules are in random Brownian motion when contained in a stationary phase liquid solution (Larson and Hu, 1999). Due to the helical properties of DNA, plasmids will orientate and elongate in the direction of the flow (Haber et al., 2004; Hirasaki et al., 1995). Entropic elasticity involves small deviations of the molecular chain due to thermal fluctuations but intrinsic elasticity relates to the elongation of the molecule contour length; therefore, intrinsic elasticity predominates in a flow field at ambient temperature (Smith et al., 1996). Overstretched DNA will have highly tilted base pairs and a reduced double helix diameter (Marko, 1998). The elasticity of DNA molecules has been well described by Porod and Kratky's worm-like chain model over a wide range of forces in a number of publications (e.g. Bustamante et al., 1994; Smith et al., 1996; Hu and Larson, 1999).

DNA molecules elongated by shear stresses in the direction of the flow while permeating a filtration membrane with mean pore sizes of 15 and 35 nm have been visualised by electron microscopy (Hirasaki et al., 1995). Stretching of tethered DNA molecules in the direction of the flow has also been visualised with fluorescence microscopy (Perkins et al., 1995; Perkins et al., 1997; Larson et al., 1997). Plasmid DNA with hydrodynamic diameters greater than the filter pore size will not permeate through the membrane unless there is sufficient elongation at the molecular level. As it has been demonstrated that the degree of DNA molecular extension in an elongational flow is proportional to velocity (Haber et al., 2004; Perkins et al., 1995, 1997; Larson et al., 1997), the velocity of flow during normal flow filtration might be

expected to be an important parameter in governing the elongation of DNA molecules during filtration, whilst operation at high velocities could also result in irreversible molecular changes.

1.2.6 Normal flow or Dead-end Filtration

Normal flow filtration can be applied at different production stages, from clarification of crude fermentation cells to final sterile filtration of purified solutions (Laska et al., 2005). Small membrane discs and syringe filters can be scaled up to larger capsules, and ultimately, large filtration installations with minimal process variation. For constant pressure filtration, membrane fouling caused by deposition of retained materials and adsorption causes flux decline over time and the analysis of this experimental data will lead to understanding and prediction of fouling in larger systems (Roorda et al., 2000). Various linearised membrane fouling models based on Darcy's Law such as the pore blockage, gradual pore constriction, intermediate pore blockage and cake filtration can be applied (e.g. Bowen et al., 1995; Hermia, 1982; Ho and Zydney, 2000; Laska et al., 2005).

The prevailing fouling mechanism will depend on the properties of the fluid and foulant, the specific filter membrane and fluid flow through the membrane (Laska et al., 2005). In the event when the classical models cannot predict well, combined models have been applied alternatively by some researchers as demonstrated by Ho and Zydney (2000) for the filtration of proteins using a combined pore blockage and cake filtration model. This combination explicitly accounts for the inhomogeneity in

the cake layer thickness over different regions of the membrane arising from the time-dependent blockage of the pore surface (Ho and Zydney, 2000).

In a normal flow or dead-end filtration system, fluid velocity increases as liquid flow becomes abruptly constricted by the pores of the membrane similar to an orifice or nozzle system. Although both shear and elongation effects are present, elongational forces will be dominant with negligible shear effects when the pressure across the orifice is sufficient to generate a velocity gradient (Marko, 1997). Elongational flows are much more effective than shear flows in stretching macromolecular chains (Termonia, 2000) and the elongational effects may generate degraded plasmid isoforms such as open-circular and linear during filtration.

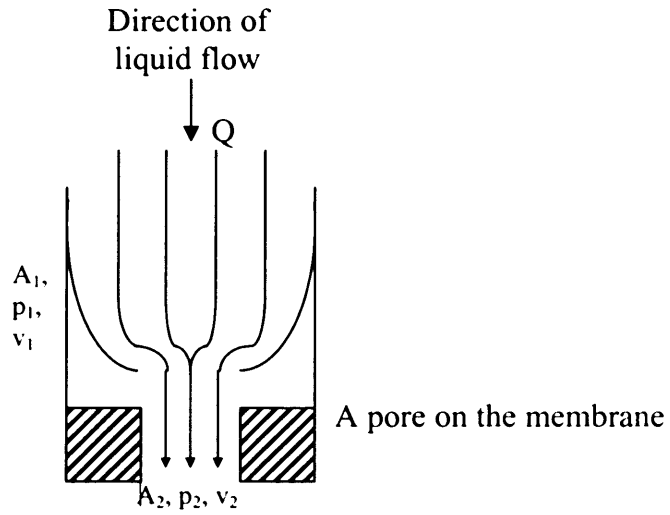

Figure 1.11: A schematic diagram of a pore of the filtration membrane with converging flow where p_1, v_1, and z_1 corresponds to the pressure, velocity and height of the upper section and p_2, v_2, and z_2 the corresponding values of the lower/outlet region.

1.2.6.1 Types of Sterile Filtration Membranes

There are numerous microporous membranes available in the market today and some of the very familiar major membrane filters producers are manufacturers such as Millipore, Whatman and Pall. In accordance to the cGMP requirements, sterilising filters should be product compatible and made-up of non-fibre-releasing materials of maximum mean 0.22 μm porosity (US FDA 21 Code of Federal Regulations-Parts 210 and 211, updated December 2005). Sterilising grade membrane filters are not only applied in final sterilising stages prior to filling liquid drug products but also widely used in intermediate production steps to reduce the bioburden level (Jornitz et al., 2003).

The selection of appropriate membrane filter media involves consideration of feed stream properties, compatibility with product and desired product quality (Laska et al., 2005). In this case, suitable membranes for use with DNA solutions should possess low charged surfaces or adsorption properties. A hydrophilic membrane is to be used for water-based fluids as the filter will be wetted without the need of a wetting agent (Cardona and Blosse, 2005). Besides, an appropriate membrane should provide high flow rate and throughput with minimal differential pressure gradient. Optimal total throughputs and flow rates can significantly reduce costs per litre and processing times.

Filter membranes intended for sterilisation applications are required to appropriately retain unwanted particles or contaminants for instance bacterial or fragmented cells either on the surface or within the functional pore structures. The design and

construction of sterilising grade membrane filters need to meet stringent requirements of regulatory authorities and the biopharmaceutical industry. Using single use capsule filters which do not require cleaning and cleaning validation may beneficial. Commercial-grade sterilisation membrane filter constructions should generally be steam resistant up to 134°C, gamma irradiation resistance, having minimal amount of extractable substances, mechanically stable up to 5000 pulsations at 5 bar differential pressure and passed integrity testing of common non-destructive tests, such as diffusive flow, pressure decay, water intrusion or bubble point (Jornitz et al., 2003).

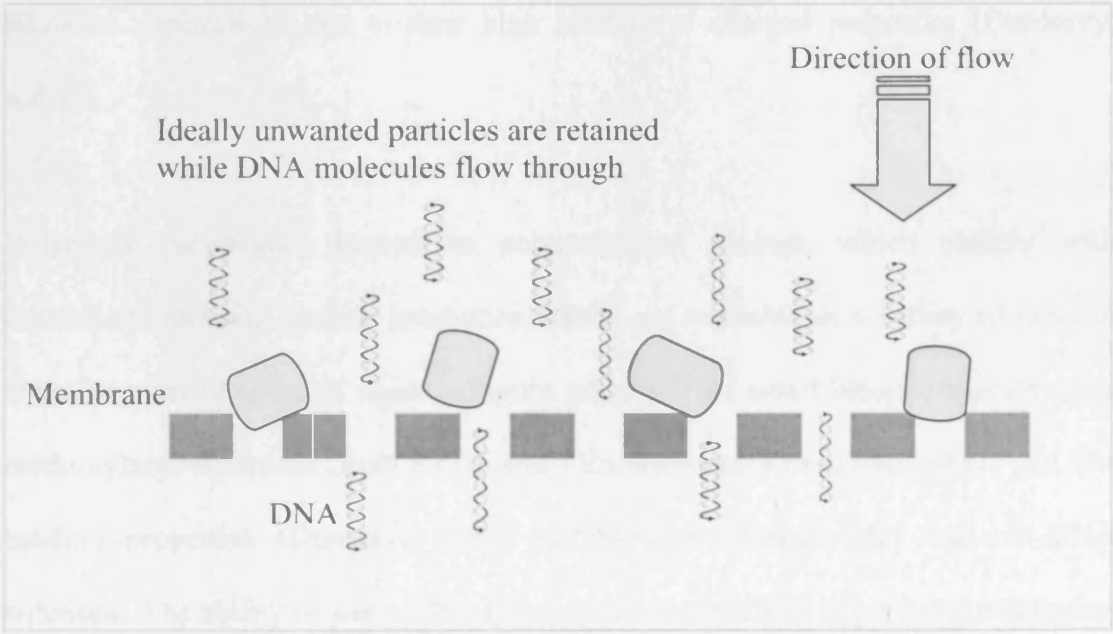

Figure 1.12: Schematic representation of a normal flow filtration through a membrane.

Membranes made from cellulosic materials such as cellulose nitrate, cellulose acetate, and mixed cellulose esters were among the first to be used in filtration applications (Dunleavy, n.d.; Jornitz et al., 2003). However, these membrane

materials have drawbacks in terms of resulting low flow rates, low throughput, and high protein binding properties (Dunleavy, n.d.). Possessing charged properties, these cellulosic materials are more suited for use as depth filters which capture particles within the interior of the membrane by adsorption (Baker, 2000). Screen filters which separate by retention or sieving effects are adequate for sterilisation purposes according to current guidelines (US FDA 21 Code of Federal Regulations- Parts 210 and 211, updated December 2005). Commonly available synthetic polymeric membrane materials are polyvinylidene difluoride (PVDF) and polyethersulfone (PES). Hydrophilic nylon and poly(tetrafluoroethylene) (PTFE) membranes are widely available, however they are not suitable for use in DNA filtration applications due to their high binding or charged properties (Dunleavy, n.d.).

Polymeric membranes housed in polypropylene casings, which comply with regulations and also gamma irradiation stable, are available in a variety of sizes to cater for a broad range of liquid volumes ranging from small laboratory-scale up to medium/large filtrations. Both PVDF and PES membranes have hydrophilic and low binding properties (Dunleavy, n.d.), suitable characteristics for use on DNA solutions. The ability to wet a filter membrane completely is important for filtration because if a membrane is not wet properly, the filtration flow rate can be impaired by non-full utilisation of the filtration area (Cardona and Blosse, 2005). Hydrophilic PVDF and PES membranes which do not require pre-wetting are available.

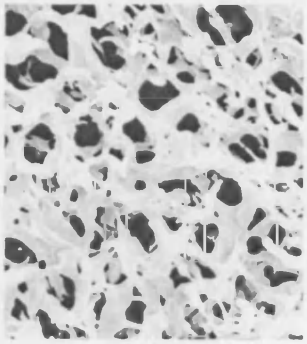

(A)

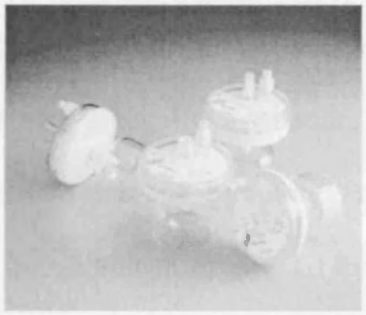

(B)

Figure 1.13: (A) Scanning electron microscopy (SEM) image of polyvinylidene difluoride (PVDF) membrane surface with pore diameter of 0.22 μm. (B) Single use sterile syringe filter capsules from Millipore Corporation.

As seen in the SEM image above (Figure 1.13), the microscopic morphology of PVDF membranes is diverse and irregular. The 'lacy' morphology of the semicrystalline PVDF polymer results a highly permeable fibrous network which is very desirable for microfiltration purposes (Zeman and Zydney, 1996). Due to the complexity, diversity and irregularity of these intersecting pore networks, creating mathematic models that describe these structures have been difficult and simplifications or approximations of geometries such as the 'cylindrical pore model' have been used by some researchers instead (Zeman and Zydney, 1996). However, this mathematical model is most applicable to specially made membranes like the track-etched Nuclepore® polycarbonate membrane with parallel, non-intersecting and cylindrical capillaries (Zeman and Zydney, 1996). For simplification, the PVDF membrane is described as having uniform symmetrical pore diameters throughout its whole thickness (Microporous Membrane Structures, n.d.).

Differing from PVDF, the PES membrane has a structure which is more open at the top ("open" side flow inlet where filtration starts), than at the bottom "tight" side; resulting in axially asymmetrical pore passages with gradually descending mean pore sizes from "open" to "tight" side (Microporous Membrane Structures, n.d.). SEM cross-sections of PVDF and PES membranes are shown in Figure 1.14 below. The asymmetrical membrane wider inlet architecture is expected to promote greater flow rate where the wider side acts as a built-in pre-filter trapping larger particles before they have a chance to clog the bacterially retentive tight side (Dunleavy, n.d.). Since filtration speed, throughput, and price are important criteria for decision making, both the PVDF and PES membranes' performance on DNA solutions should be investigated.

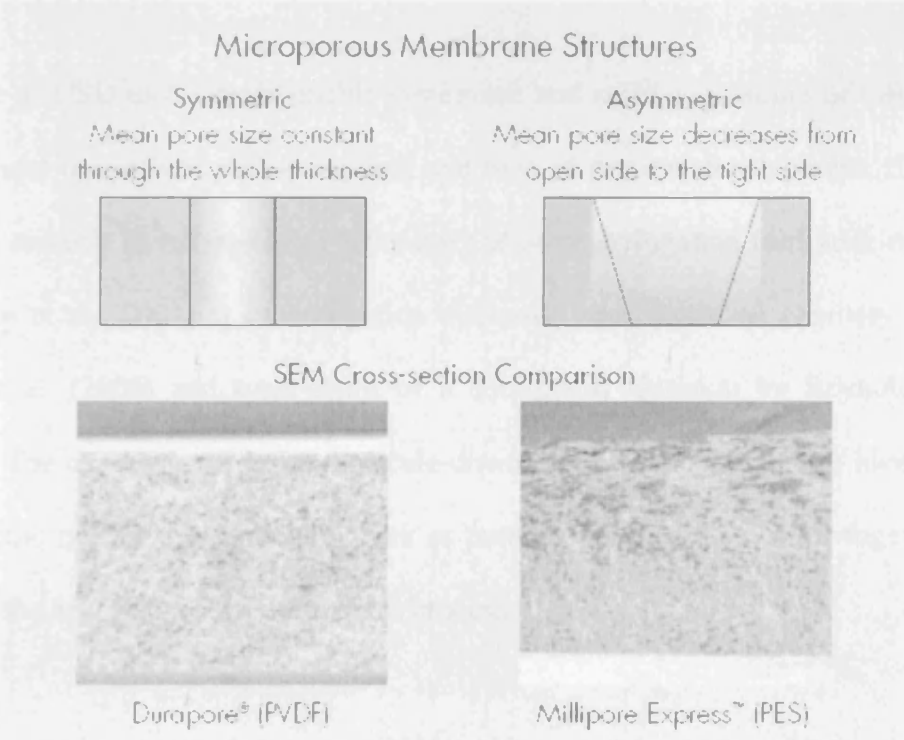

Figure 1.14: SEM cross-sectional comparison of symmetrical and asymmetrical pore membranes (Microporous Membrane Structures, n.d.).

1.2.7 Concepts of High Throughput Process Data Collection

The UCL Innovative Manufacturing Research Centre (IMRC) is dedicated to creating and designing new ways of proceeding faster from discovery to manufacture by developing ultra scale-down (USD) tools to mimic the engineering environments of large or pilot-scale industrial processes and high throughput technologies that allows parallel evaluation using small quantities of materials at benchtop laboratory level. As not all new medicines successfully meet the criteria of clinical trials, it is not sensible to manufacture large quantities of the product in the early development stage or delay developing and running large scale manufacturing trials until very late in the development stage. Thus, approaches that enable effective scale up early in process development would be very advantageous.

The use of USD tools would enable systematic and rapid acquisition of information on material properties minimising cost and time of process development. Examples of tools recently developed are a laboratory scale centrifugation feed zone mimic by Boychyn et al. (2001), a centrifugation discharge zone based on capillary flow by Chan et al. (2006) and scale-down of a continuous filtration by Reynolds et al. (2003). The challenge of designing scale-down mimics is being able to identify and specify the type of unit operation such as pumps, valves, filters, centrifuges and so forth in the sequence of the production process.

The microwell based platform is a very useful tool for high throughput parallel evaluation of the impact of process conditions and allows rapid process characterisation. Recent development include establishments such as an automated

high throughput microscale technique for the quantitative and parallel analysis of microfiltration operations by Jackson et al. (2005), a high throughput measurement of protein stability in microtitre plates by Aucamp et al. (2005) and microlitre scale prediction methods from microbial and mammalian cell cultures by Micheletti et al. (2006).

Since only a small amount of material is required using these tools, comprehensive experimental data can be produced for detailed understanding of the mechanisms involved to identify the key parameters for scaling purposes and efficient design of processing strategies. Simultaneously, critical process issues and operating windows can be identified early in the development stage. This would reduce a significant amount of capital cost.

Chapter 2 – Methods and Materials

2.1 Experimental Setup

2.1.1 Constant Flux Filtration

Normal-flow filtration of purified DNA solutions was performed at room temperature using sterilising grade 13-mm Millex™/0.22 μm Durapore® polyvinylidene fluoride (PVDF) capsules (Millipore Corporation, MA, USA) or 13-mm Acrodisc®/0.2 μm Supor® polyethersulfone (PES) capsules (Pall Corporation, MI, USA) affixed to the end of standard 1-ml BD Plastipak™ disposable plastic syringes (Becton Dickinson, NJ, USA). Each filter capsule contained a hydrophilic membrane disc. DNA solutions were passed through the membrane capsules at calibrated flow rates of 0.1–3 mL/min corresponding to constant fluxes of 0.1–2.3 mL/min.cm^2 respectively. A Harvard PHD2000 Syringe Pump (Harvard Apparatus, MA, USA) was used and most of the filtration experiments were set up to run in duplicates. Routinely, membranes were used dry as recommended by manufacturers. It was noted that prewetting the membranes with buffer or DNA solutions did not affect transmission.

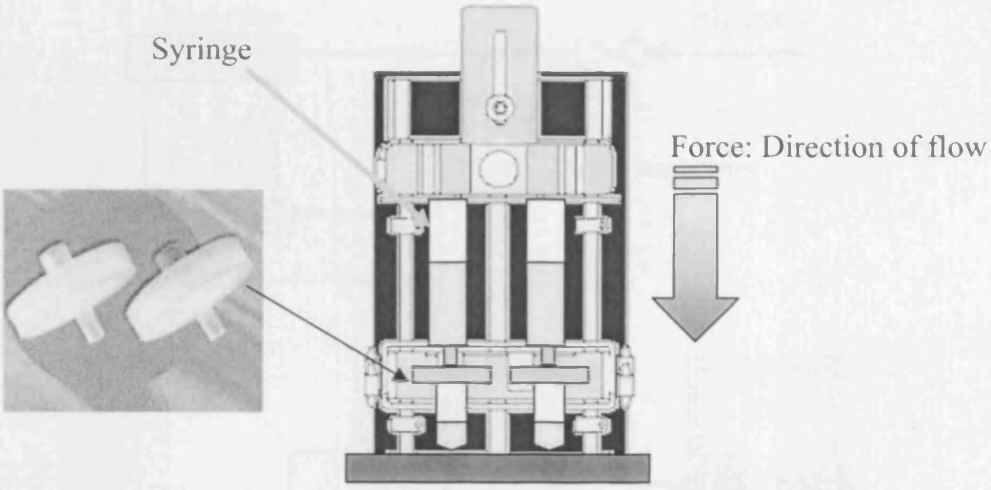

Figure 2.1: Schematic diagram of the small scale normal-flow filtration set-up using a pressure driven syringe unit which allowed controlled filtration flux.

2.1.2 Constant Pressure Filtration

Filtrations of the purified DNA vectors were performed at room temperature using sterilising grade 13-mm Millex™/0.22 μm Durapore® PVDF capsules (Millipore Corporation, MA, USA) and the positive pressure operation setup is as shown in Figure 2.2. The system was pressurised using nitrogen gas controlled by a regulator valve. The operating pressure was kept constant at 30, 50 or 65 kPa throughout each filtration. Permeate mass was logged on a computer for the monitoring of flow decay. The gradual pore plugging model and V_{max} analysis method were applied for the estimation of membrane area or membrane capacity for each condition tested.

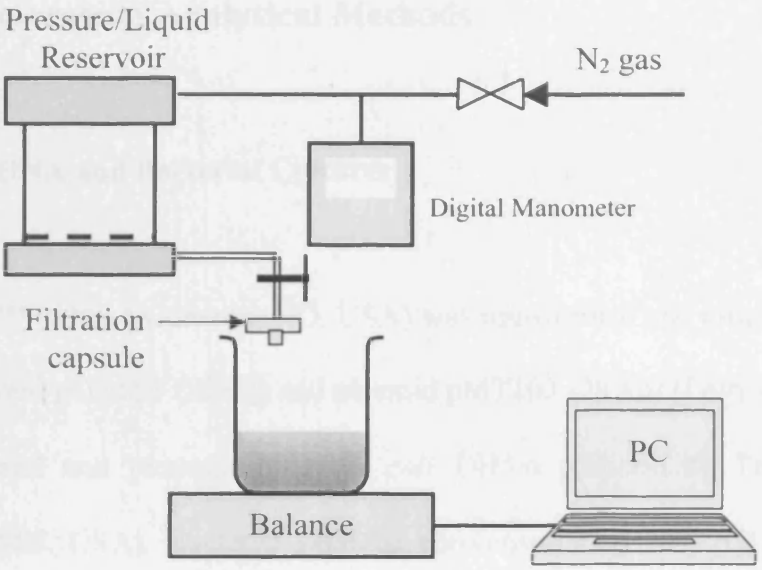

Figure 2.2: Schematic diagram of the small scale normal-flow filtration set-up using a pressure reservoir unit which allowed constant pressure filtration.

2.2 DNA Vectors and Analytical Methods

2.2.1 Plasmid DNA and Bacterial Cultures

Plasmid gWIZ™ (6 kb) (Aldevron, ND, USA) was transformed and propagated in *E. coli* DH1. Plasmid pQR150 (20 kb) and plasmid pMT103 (29 kb) (Levy et al., 1999) were transformed and propagated in *E. coli* DH5 α (Gibco-Life Technologies, Gaithersburg, MD, USA). Bacterial artificial chromosomes (BAC) p5179 (33 kb), p5180 (72 kb) and p5176 (116 kb) (Wellcome Trust Centre for Human Genetics, University of Oxford, Oxford, UK) were transformed and propagated in *E. coli* DH10β (Wade-Martins et al., 1999). The recombinant bacteria stocks were stored in 20%v/v glycerol at -70°C.

Cultures of *E. coli* DH1 gWIZ and DH5α pQR150 were grown in Luria-Bertani (LB) medium supplemented with 50 μg/mL kanamycin while DHα pMT103 were grown in LB medium supplemented with 100 μg/mL ampicillin. *E. coli* DH10β p5179, DH10β p5180 and DH10β p5176 were grown in Terrific broth media (1.2%w/v tryptone, 2.4%w/v yeast extract, 0.4%v/v glycerol, 0.2%w/v potassium dihydrogen phosphate, 1.3%w/v dipotassium monohydrogen phosphate) supplemented with 12.5 μg/mL chloramphenicol on agar plates and 5 μg/mL in shake flask cultures. Trypton and yeast extract were obtained from Oxoid (Basingstoke, Hamphire, UK), and sodium chloride and phosphate salts were obtained from Sigma-Aldrich (Poole, Dorset, UK). Please refer to Appendix B for full details of the recipes used.

2.2.2 Plasmid DNA Purification

Purified solutions of gWIZ, pQR150, pMT103, p5179, p5180 and p5176 were obtained using Qiagen Mega, Qiagen Maxi or Qiaprep Spin Miniprep kits with purification protocols for high and low copy number vectors (Qiagen Ltd, West Sussex, UK). Tris-EDTA (TE) buffer (10 mM Tris-HCl, 1 mM EDTA), adjusted to pH 8.0, was used in all DNA dilutions unless specified. Tris-HCl and EDTA were obtained from Sigma-Aldrich (Poole, Dorset, UK). Please refer to Appendix B for full details of recipes used.

2.2.3 UV Spectrophotometry

DNA concentrations from purified solutions were determined using the quick and reproducible UV spectrophotometry methodology at 260 nm. The nitrogenous bases in nucleotides have an absorption maximum at around 260 nm. The concentration of base pairs are the same for the various supercoiled (SC), open circular (OC) and linear plasmid DNA isoforms. The difference in isoforms is not expected to affect the absorbance readings since they are still double stranded. The absorbance at 260 nm (A_{260}) of a 50 μg/mL solution of double stranded DNA is equal to 1 and the equation for calculation is as shown below.

$$DNA\ concentration\ (\mu g/ml) = A_{260} \times (dilution\ factor) \times \left(\frac{50 \mu g/ml}{1\ A_{260}\ unit} \right) \qquad [2.1]$$

In contrast to nucleic acids, proteins absorb maximally at a wavelength of 280 nm due to the presence of tryptophan residues (Blaber, 2004). Measuring the absorbance of the sample at 280 nm gives an estimate of the protein contamination and the ratio of the absorbance at 260 nm to absorbance at 280 nm (A_{260}/A_{280}) gives an estimation of sample purity. All samples used had an initial A_{260}/A_{280} ratio between 1.6–1.9 and this is considered of high purity (Sambrook et al., 1989).

For the determination of product recovery, DNA concentration of the feed and filtered samples was determined spectrophotometrically. The permeate concentration was expressed as a percentage of the initial DNA concentration and the percentage of transmission was determined as follows.

$$\%DNA\ retained = \frac{[DNA]_{Filtered} - [DNA]_{Feed}}{[DNA]_{Feed}} \times 100\%$$

$$\Rightarrow \%Transmission = 100\% - \%DNA\ retained \qquad [2.2]$$

2.2.4 Gel Electrophoresis and Densitometry Scanning

The integrity and change in the proportion of isoforms of plasmid DNA was assessed by gel electrophoresis. A stock solution of 10× Tris-borate electrophoresis buffer (0.89 M Tris base, 0.89 M boric acid, 0.02 M EDTA), pH 8.3 was obtained from Sigma-Aldrich (Poole, Dorset, UK) and running solutions were prepared to the required dilution prior to use. Plasmids gWIZ, pQR150 and pMT103 were loaded onto 0.8%w/v agarose containing 0.05 μg/mL ethidium bromide and electrophoresed

at 40 V for 2-9 hours in 1× Tris-borate electrophoresis buffer. BAC p5179, p5180 and p5176 samples were loaded onto 0.8%w/v agarose containing 0.05 μg/mL ethidium bromide and electrophoresed at 4.5 V/cm for 16-24 hours in 2× Tris-borate electrophoresis buffer. For pulsed field gel electrophoresis (PFGE), BAC p5179, p5180 and p5176 samples were loaded onto 1.0%w/v agarose and electrophoresed at 6 V/cm on the Chef-DR® II Pulsed-field Electrophoresis System (Bio-Rad, Hercules, CA, USA). The PFGE gels were stained for 1 hour after electrophoresis with ethidium bromide (0.05 μg/ml in 1× Tris-borate buffer) before visualisation and analysis.

The supercoiled (SC), open circular (OC) and linear DNA bands were analysed with densitometric scanning methods. All the gels were scanned and analysed using the Gel Doc™ EQ Gel Documentation System and Quantity One™ analysis software (Bio-Rad Laboratories Inc, CA, USA). In order to ensure that the density of the individual bands was within the linear range of the densitometry scan, a calibration curve was prepared by loading 200–600 ng of DNA into each well in the agarose gel. The plasmid used was pQR150 (20 kb) and the scanned gel image is shown in Figure 2.3(A). The peak intensities along with band widths were measured by the Quantity One™ software and a plot following analysis is shown in Figure 2.3(B).

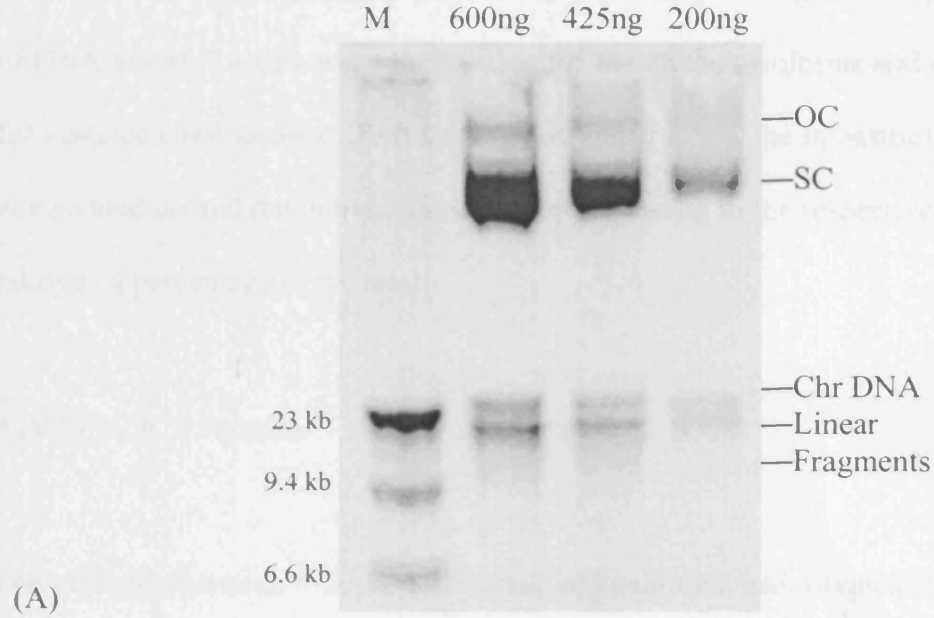

(A)

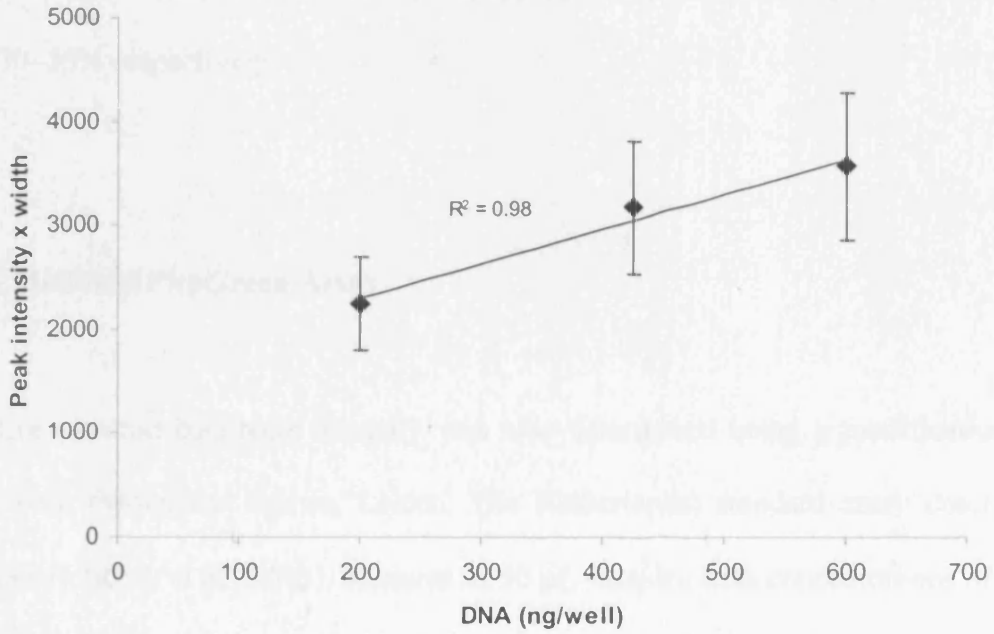

(B)

Figure 2.3: (A) Gel electrophoresis of purified pQR150 (20 kb) samples. Mass of DNA loaded into each well in the agarose gel was between 200–600 ng. Abbreviation: M is λ Hind III molecular weight marker, OC is open circular, SC is supercoiled, Chr DNA is chromosomal DNA. (B) Densitometry peak intensity using 200–600 ng/well of purified pQR150 (20 kb) samples. Error bars indicate 20% of variation associated with the gel densitometry technique and line represents linear regression.

A good linear fit was obtained (R^2 = 0.98) from the plot (Figure 2.3B) for the mass of DNA tested. To determine the content for the various isoforms and other species, for instance chromosomal DNA or single stranded DNA, the intensities on each lane were added up and the individual bands corresponding to the respective species were taken as a percentage of the total.

$$\%SC + \%OC + \%Linear + \%Other\ species = 100\% \qquad [2.3]$$

For plasmids between 6-20 kb unfiltered feed solutions had a typical SC content of 80–95%. For vectors between 29–72 kb, the SC content of unfiltered feed solutions was 70–50% respectively.

2.2.5 Modified PicoGreen Assay

Relative plasmid backbone integrity was also determined using a modification of PicoGreen (Molecular Probes, Leiden, The Netherlands) standard assay described previously (Rock et al., 2003). Aliquots of 50 μL samples with concentrations of 300 ng/mL were mixed with 50 μL PicoGreen (1 in 200 working concentration) in a microwell plate. After an incubation of 5 minutes, the fluorescence of samples was recorded using a Packard Fluorocount Microplate Fluorometer (Packard Instrument Company, Meriden, CT, USA) at an excitation wavelength of 480 nm and emission of 520 nm. This was followed by addition of 100 μL of NaOH at pH 12.6 (ultrapure water was added to 0.1M NaOH until pH 12.6 was achieved) to attain a final pH 12.4

in the sample mixtures. Following a further incubation of 5 minutes, fluorescence of samples was recorded.

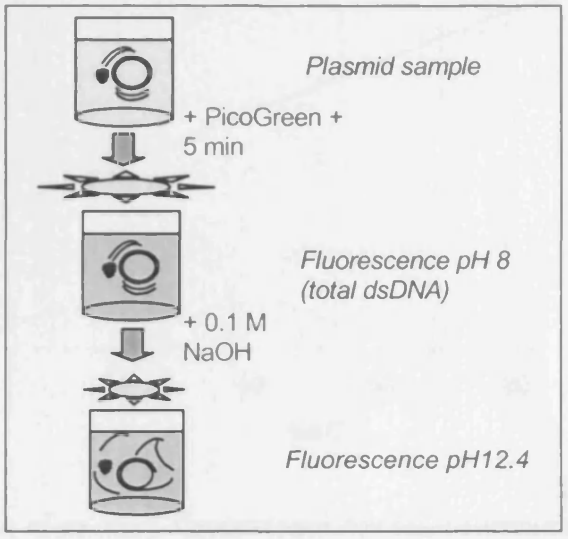

Figure 2.4: Schematic outline of the modified PicoGreen assay. Fluorescence enhancement of PicoGreen at pH 12.4 ($F_{pH12.4}$) is normalised by its value at pH 8.0 ($F_{pH8.0}$) to give a relative fluorescence ratio (RF) that is proportional to the average backbone integrity of the DNA molecules in the sample (Rock et al., 2003).

The samples were corrected for background fluorescence values using blanks of TE buffer and PicoGreen. Tests were performed in duplicates or triplicates. For the determination of SC content in a sample, the percentage of SC can be read off from the calibration curve prepared with known SC quantities as shown below (Figure 2.5). The SC quantity was validated using the gel densitometry method. For each run, known SC quantities were loaded onto the same microwell plate to ensure consistency in readings.

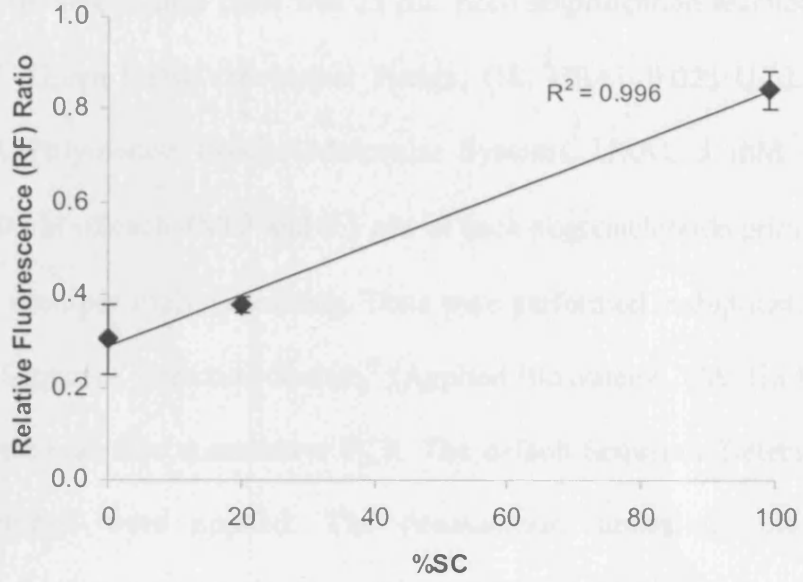

Figure 2.5: Calibration of relative fluorescence for the determination of SC content. The results shown are average of two sets of tests and error bars indicate standard deviation and line represents linear regression.

2.2.6 Quantitative Polymerase Chain Reaction (qPCR)

Chromosomal DNA contamination was measured via qPCR of an *E. coli* gene. Oligonucleotide primers (Qiagen Ltd., West Sussex, UK) 23S-sense (5' GAA AGG CGC GCG ATA CAG 3') and 23S-antisense (5' GTC CCG CCC TAC TCA TCG A 3') were used to amplify a 70-bp fragment of the 23S ribosomal RNA gene present in the *E. coli* genome as reported in Vilalta et al. (2002).

To prepare for amplification reactions, all DNA samples were diluted using ultrapure water and were denatured at 95°C for 15 minutes then cooled on ice for 5 minutes. This procedure was repeated prior to use. The total volume in each well of the

MicroAmp® 96-well optical plate was 25 μL. Each amplification reaction contained 0.5× SYBR® Green I Dye (Molecular Probes, OR, USA), 0.025 U/μL AmpliTaq Gold® DNA Polymerase (Roche Molecular Systems, USA), 3 mM magnesium chloride, 200 μM of each dNTP and 0.3 μM of each oligonucleotide primer. 10 ng of plasmid was used per analysis reaction. Tests were performed in duplicates. The ABI Prism 7700 Sequence Detection System® (Applied Biosystems, CA, USA) was used for running the real-time quantitative PCR. The default Sequence Detection System software settings were applied. The denaturation, annealing and extension temperatures were set to 94°C for 30 s, 56°C for 30 s and 76°C for 30 s respectively and the number of cycles was 45. *E. coli* DH5α genomic DNA was used to generate standard curves from 1 pg to 5 ng.

2.2.7 Confocal Scanning Laser Microscopy

PicoGreen, a fluorescent dye (Molecular Probes, Leiden, The Netherlands) was used to label plasmid DNA deposition on the membrane during filtration. Microfiltration experiments using the 20 and 72 kb vectors were carried out as described in section 2.1.1. Then solutions of PicoGreen (1 in 400 dilution) were circulated through the membrane twice slowly over a period of 20 minutes. Lastly, the membranes were washed with TE buffer to remove any access unbound PicoGreen dye.

The fluorescence labelled membranes were removed from their casing carefully to be placed on glass slides and covered with glass slips (sealed to prevent drying) for analysis using the Leica TCS SP confocal laser scanning microscope (Leica,

Heidelberg, Germany). The fouled membranes were scanned using the fluorescence mode with the laser wavelength of 525 nm. The resolution of the images was set to 1024×1024 pixels, corresponding to an area of 215×215 μm^2 (about 0.2 μm/pixel). Evaluation of the images was performed using the Lite Leica Confocal Software.

2.3 DNA Formulation

2.3.1 PEI/DNA Complexes

Polyethylenimine (PEI) has been frequently used for gene delivery and showed high transfection efficiency (Godbey et al., 1999). The sizes of the PEI/DNA complexes are influenced by the molar ratio of the PEI nitrogen atoms to DNA phosphate atoms (N/P), usually adjusted to between +6 and +10 in order to create strong positive surface charged particles to induce repulsion interactions among individual particles and this prevents aggregation (Boussif et al., 1995; Clamme et al., 2003).

Non-labelled 25 kDa branched PEI (Sigma-Aldrich, Dorset, UK) and 30 μg/mL plasmid p5180 (72 kb) prepared in 20 mM HEPES and 75 mM NaCl solution at pH 7 were mixed directly by pipetting into disposable cuvettes. The concentration of the components used produced a corresponding nitrogen/phosphate (N/P) charge ratio of +10.

2.3.2 LID Complexes

The lipid-integrin binding peptide-DNA (LID) complexes were made by the addition of lipofectin (L) (Invitrogen, Paisley, UK) and integrin-targeting peptide (I) (Zinsser Analytic, Maidenhead, UK) to plasmid DNA (D) at a weight ratio of 0.75:4:1 as previously described in Sarkar et al. (2003). These individual LID components combine together through electrostatic interactions. Lipofectin is a cationic lipid composed of DOTMA (*N*-[1-(2,3-dioleyloxy)propyl]-*N*,*N*,*N*trimethylammonium chloride) and the co-lipid DOPE (dioleoyl phosphatidylethanolamine). The peptide contained a 16-lysine-chain and a head group that targets specific integrins on the surface of restricted range of cell types expressing the target integrin (Sarkar et al, 2003). White et al. (2003) had shown promising transfection results using LID vectors containing BAC-based plasmids ranging in size from 12 to 242 kb.

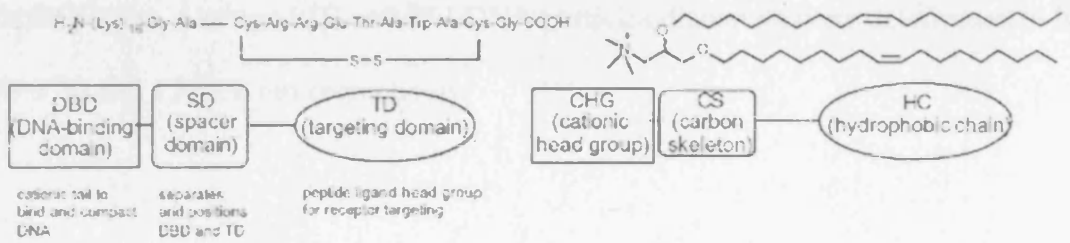

Figure 2.6: Illustration of components and properties of the LID complex (Sarkar et al., 2003).

The concentration of the components used produced a corresponding nitrogen atoms to phosphate atoms (N/P) charge ratio of +10. The charge ratio is calculated as follows:

$$Charge\ ratio\ of\ particle = \frac{\left(\frac{Mass\ of\ lipid \times Lipid\ charge}{Lipid\ molecular\ weight}\right) + \left(\frac{Mass\ of\ peptide \times Peptide\ charge}{Peptide\ molecular\ weight}\right)}{\left(\frac{Mass\ of\ DNA \times nucleotide\ charge}{Nucleotide\ molecular\ weight}\right)} \quad [2.4]$$

2.3.3 Particle Size Distribution

The particle size distributions of the PEI/DNA and LID complexes were measured using a Malvern Zetasizer, Model 3000 (Malvern Instruments Ltd., Worcs., UK) as previously described in Sarkar et al. (2003). Before each measurement, the calibration of the instrument was checked against standard mono-sized latex particles (Duke Scientific Corporation, CA, USA). All measurements were conducted at 25°C. The particle size measurement of the LID and PEI/DNA complexes over a 50-60 minute period. Average LID and PEI/DNA particles diameters were determined to be 199 ± 10 and 131 ± 8 nm respectively.

2.4 Viscometry and Solution Concentration

Preliminary experiments were carried out to examine the viscosity of plasmid DNA solutions of increasing concentration and to determine a suitable working concentration. A purified plasmid DNA solution containing plasmid pQR150 was diluted serially from 950 to 30 μg/mL. Viscosity of the solutions was measured at room temperature using a Wells-Brookfield cone/plate viscometer (Brookfield Engineering Laboratories Inc., MA, USA).

The solutions' viscosity increased in a logarithmic manner reaching a plateau approximately 3 mPa.s. The viscosity values obtained were in agreement with those reported by Cooper et al. (2002). A concentration of 30 μg/mL was chosen for all studies unless otherwise stated as more concentrated solutions with viscosities greater than 2.5 mPa.s caused filter capsules to collapse at fluxes $\geq$ 0.8 mL/min.cm^2.

Chapter 3 – Filtration and Recovery of DNA vectors

3.1 Introduction

The problems associated with the processing of plasmid DNA are mainly related to the structure of the molecule – high molecular weight, highly negative charged and flexible, which are not common to recombinant-proteins (Prazeres et al., 1999). Proteins, polysaccharides and/or polyphenols can cause extensive fouling despite being smaller in size than the membrane pore diameter (Ferrando et al., 2002). The plasmids used for gene therapy are very large molecules comparatively to proteins for they contain human or non-human genes and these macromolecules can easily possess radii of gyration greater than the pore diameter of the sterilising grade membrane filters frequently applied in the intermediate steps or as a final sterilisation procedure in the downstream processing of biopharmaceuticals.

The structure of supercoiled DNA has been visualised using electron microscopy (Boles et al., 1990) and atomic/scanning force microscopy techniques (Lyubchenko and Shlyakhtenko, 1997; Rippe et al., 1997; Thundat et al., 1992). Langowski et al. (1999) have reported that the superhelix diameter (average distance between opposing DNA double strands in the interwound regions) of a plasmid in TE buffer to be around 16 nm using light scattering methods. A very useful estimation of the

superhelix axis or supercoiled length of plasmids was deduced by Boles et al. (1990) – the length of the superhelix axis is constant at 41% of the DNA contour length.

Based on the estimation described by Boles et al. (1990), supercoiled lengths of the circular DNA vectors used in this study are calculated and shown in Table 3.1. For comparison to actual imaging sizes, an example of an atomic force microscopy image of a 3 kb plasmid (extracted from Rippe et al., 1997) which is about half the size of the smallest plasmid used in this study is shown in Figure 3.1. The measured superhelical lengths of the 3 kb plasmids are generally around 0.3 μm agreeing with a predicted value of 0.3 μm.

Table 3.1: Estimated supercoiled length of circular DNA vectors used in this study.

DNA vector	Size		Contour length[α] (μm)	Estimated supercoiled length (μm)[β]
	(Da)×10^6	(kb)		
gWIZ	4	6	1.9	0.8
pQR150	13	20	6.8	2.8
pMT103	19	29	9.9	4.0
p5179	21	33	11.2	4.6
p5180	47	72	24.5	10.0
p5176	75	116	39.4	16.2

[α] The contour length of the plasmid DNA molecule is proportional to its molecular weight. Molecular weight is calculated by the summing the molecular weight of the backbone unit and the base unit minus one for removal of one hydrogen from the base.

[β] The plasmid supercoiled length is 41% of contour length based on Boles et al. (1990).

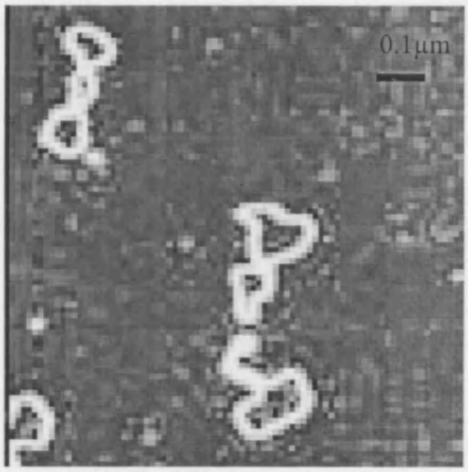

Figure 3.1: Atomic force microscopy image of a 2 kb plasmid (p1868) in water (Rippe et al., 1997).

The supercoiled lengths of DNA vectors will increase proportionally to their molecular weights and cannot readily permeate the membrane filter without any elongating deformation at the molecular level. DNA molecules are flexible due to their helical structures and can stretch out by the shear stress of the flow when velocity is adequate (Haber et al., 2004; Hirasaki et al., 1995). Stretched out small supercoiled plasmids (3–5 kb) orientated in the flow direction have been visualised in narrow pore channels using transmission electron microscopy techniques by Hirasaki et al. (1995).

In this work, filtration of a wide range of purified circular DNA vectors (6–116 kb) in solution through 0.22 µm sterilising grade PVDF membrane filters were performed with the aim to define the magnitude of product loss and then determine if the predominant mechanism for product loss was due to retention/sieving by the membrane filter or due to unspecific adsorption in view of the high density of negative charges on the DNA backbone. The filtration setup consisted of a small scale normal-flow pressure driven syringe unit through which constant filtration flux

operations and small samples volumes (≤ 1 mL) could be applied. Details of the setup can be found in Chapter 2 – Methods and Materials (section 2.2.1).

3.2 Effect of Vector Size

Based on the estimation of supercoiled lengths shown in Table 3.1, the 6–116 kb (4×10^6 – 75×10^6 Da) circular DNA vectors are 4–74 times larger than the nominal 0.22 μm pore diameter of the sterilising membranes. The flexible helical DNA molecules are expected to stretch out under the influence of fluid flow (Haber et al., 2004; Hirasaki et al., 1995) and high recovery rates have already been observed during the sterile filtration of small 6 kb plasmids (Bos et al., 2000). It was unknown whether larger DNA vectors could elongate sufficiently to permeate through the sterilising membrane filters. Therefore in this study, the transmission of purified DNA vectors with a wide range of sizes was measured to determine the effect of molecular weight on a normal-flow sterile filtration performance.

Purified DNA vector solutions containing gWIZ (6 kb), pQR150 (20 kb), pMT103 (29 kb), p5179 (33 kb), p5180 (72 kb) and p5176 (116 kb) were prepared and adjusted to a DNA concentration of 30 ± 2 μg/mL. The filtrations were performed at a constant flux of 0.2 mL/min.cm^2 and 0.22 μm pore size hydrophilic PVDF membrane filters were applied. In order to determine the transmission of DNA vectors, the average DNA concentration after filtration was recorded for each plasmid and expressed as a percentage of the initial concentration based on UV spectrophotometry measurements.

The UV spectrophotometry method is based on the principle of the ability of the bases in a DNA molecule to absorb UV light maximally at a wavelength of 260 nm. Since the concentration of base pairs are the same in different double stranded plasmid DNA isoforms (SC, OC and linear), the difference in isoforms are not expected to affect the absorbance readings. For this study, the concentration of DNA in solution was taken for comparison as it can be measured quickly using the UV spectrophotometry methodology although the number of molecules for each vector size per mass will vary. Table 3.2 shows an estimation of number of molecules per mass and volume.

Table 3.2: Estimated number of molecules of circular DNA vectors per mass and per volume used in this study.

DNA vector	Size		Number of molecules per mass $(g^{-1})\times10^{15}$	Number of molecules per volume $^{\chi}$ (mL^{-1}) $\times10^{11}$
	$(Da)\times10^{6}$	(kb)		
gWIZ	4	6	150	46
pQR150	13	20	46	14
pMT103	19	29	32	10
p5179	21	33	28	8
p5180	47	72	13	4
p5176	75	116	8	2

$^{\chi}$ Based on a DNA concentration of 30 μg/mL.

The experiment results showed a linear relationship between vector size and DNA transmission (Figure 3.2). High transmission levels of 98–89% were observed for plasmids ranging from 6–20 kb. In a non-flow environment DNA molecules are constantly undergoing conformation changes in Brownian fluctuations and deformations will become more significant when influenced by fluid stresses (Larson and Hu, 1999). The results observed here indicated elongation of molecules which led to the transmission of DNA vectors. Particularly for the smaller 6–20 kb constructs tested, despite being 4–13 times larger than the nominal pore diameter of the membrane filters recovery rates were high. This is in agreement with observations by Seeley (Millipore Corp, n.d.) where high transmission rates of $\geq$ 99% for the filtration of small plasmids (< 10 kb) using a variety of 0.2 μm pore size commercial hydrophilic membrane filters were observed and Bos et al. (2000) who reported that during the sterile filtration of a 6 kb plasmid the mass of plasmid retained by the cellulose acetate membrane filter was low and the DNA recovery was found to be around 91%.

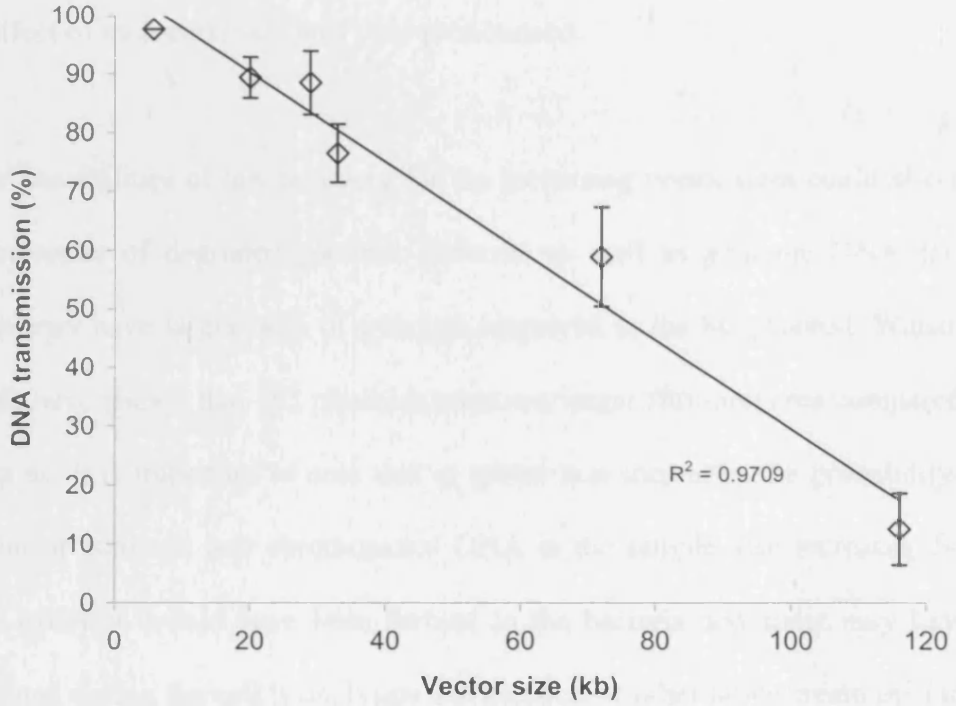

Figure 3.2: The effect of vector DNA size on product transmission. Plasmids gWIZ (6 kb), pQR150 (20 kb), pMT103 (29 kb), p5179 (33 kb), p5180 (72 kb) and p5176 (116 kb) were filtered through 0.22 μm PVDF with feed concentrations of 30 ± 2 μg/mL. The results shown are average of two sets of experiments error bars indicate standard deviation and line represents linear regression.

For the larger constructs tested in this study, the transmission levels fell to 77 ± 5%, 59 ± 8% and 13 ± 6% for the filtration of the 33, 72 and 116 kb vectors respectively. Insufficient elongation or molecular entanglement may have contributed to the low transmission levels or high number of molecules being retained. The data obtained shows that 45×10^{11} of the 6 kb plasmid molecules permeated through the 0.22 μm pores as oppose to only 0.3×10^{11} of the 116 kb BAC molecules. This indicated that

in terms of number of molecules that can be passed through a given filtration area, the effect of molecular size was very pronounced.

Other possibilities of low recovery for the increasing vector sizes could also include the presence of degraded plasmid isoforms as well as genomic DNA fragments which may have larger radii of gyration compared to the SC plasmid. Watson et al. (2006) have shown that OC plasmids require a larger filtration area compared to SC plasmids. It is important to note that as vector size increases, the probability of OC and linear isoforms and chromosomal DNA in the sample also increases. Some of these isoforms would have been formed in the bacteria and some may have been generated during the cell lysis, lysate clarification or other downstream operations in large quantities which the purification process could not efficiently remove. Further studies on the integrity of plasmid DNA following filtration will be discussed in Chapter 4. Unspecific adsorption could also play a role in the low recovery rates since the density of negative charges per molecule inherently increases with increasing vector size.

3.3 Effect of Operating Flux

As a DNA molecule is negatively charged due to the phosphate anions in its backbone, it is important to determine whether adsorption to unspecific membrane sites could be contributing to the obstruction of pores and the low DNA transmission levels. A common problem with the filtration of therapeutic proteins is membrane fouling due to adsorption of protein molecules which eventually plug the pores (Ho and Zydney, 1998; Maa et al., 1998). It was hypothesised that if charged adsorption was the prevailing mechanism affecting the filtration performance, higher transmission of DNA would be observed when the filtration flux increases as a consequent of shorter residence time in contact with the membrane.

In this study, solutions containing purified DNA vectors pQR150 (20 kb), p5179 (33 kb), p5180 (72 kb) and p5176 (116 kb) at a concentration of 30 ± 2 μg/mL were filtered at fixed fluxes of 0.1, 0.2, 0.8 and 2.3 mL/min.cm^2 to examine the effect of varying residence time. Hydrophilic PVDF membranes (0.22 μm pore size) were used in this study as the aqueous based DNA solutions can wet the membrane without requiring any wetting agent. Although PVDF is naturally hydrophobic, it can be modified to render the membrane hydrophilic and suitable for aqueous applications without the need of pre-wetting (Cardona and Blosse, 2005; Zeman and Zydney, 1996).

For the vectors tested, the results did not show significant higher transmissions for the increasing filtration fluxes. This suggests product transmission was not significantly affected by the operating flux (Figure 3.3). Figure 3.4 shows

transmission as a function of DNA vector size, comparing two fluxes (0.2 and 2.3 mL/min.cm^2) with a magnitude difference of 10-fold. Once again, substantial differences in transmission levels were not observed between the two flux rates.

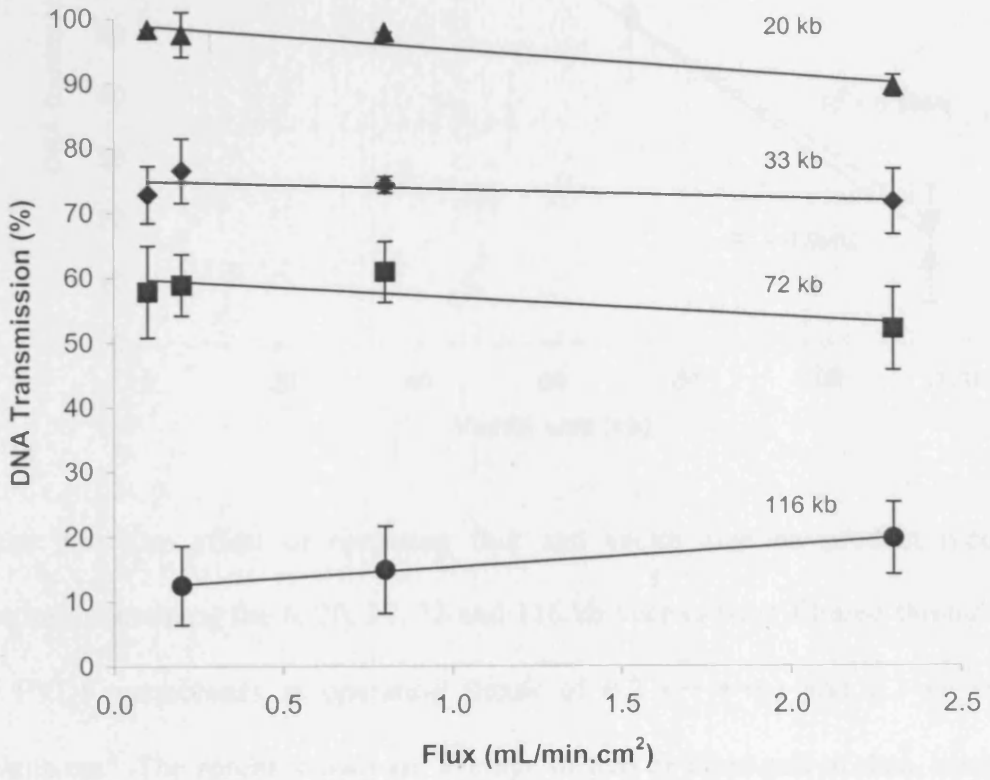

Figure 3.3: The effect of operating flux on product recovery. Solutions containing pQR150 (20 kb) (—▲—), p5179 (33 kb) (—◆—), p5180 (72 kb) (—■—) and p5176 (116 kb) (—●—) were filtered through 0.22 μm PVDF membranes at operating fluxes of 0.1, 0.2, 0.8 and 2.3 mL/min.cm^2. The results shown are average of two or three sets of data, error bars indicate standard deviation and lines are linear regressions. Please note some error bars are smaller than the symbols.

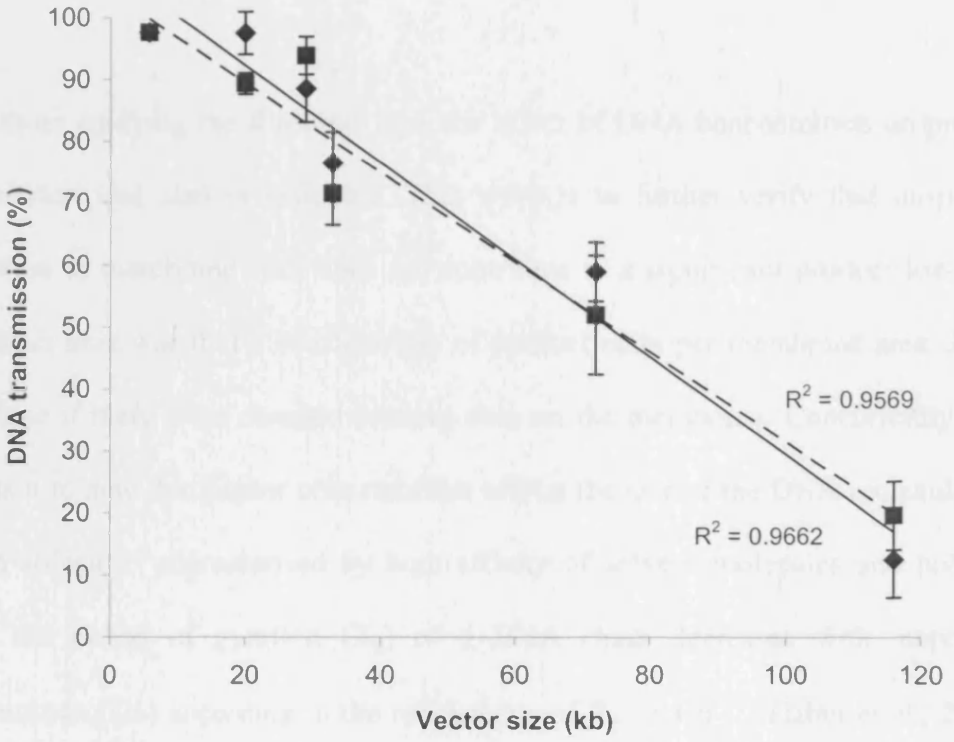

Figure 3.4: The effect of operating flux and vector size on product recovery. Solutions containing the 6, 20, 33, 72 and 116 kb vectors were filtered through 0.22 μm PVDF membranes at operating fluxes of 0.2 (— ◆ —) and 2.3 (····· ■ ·····) mL/min.cm^2. The results shown are average of two or three sets of data, error bars indicate standard deviation and lines are linear regressions.

From the operating flux experiment results, unspecific chemical adsorption of the negatively charged plasmids on the membrane was not prominent. Further experiments to evaluate the effect of DNA concentration and pre-wetting of membranes would be required to further validate this observation.

3.4 Effect of DNA Concentration

Aside from studying the filtration flux, the effect of DNA concentration on product transmission was also investigated. This work is to further verify that unspecific adsorption to membrane sites does not contribute to a significant product loss. The hypothesis here was that a constant loss of product mass per membrane area should take place if there were charged binding sites on the membrane. Concurrently, it is important to note that higher concentration affects the size of the DNA molecules. In a good solvent – characterised by high affinity of solvent molecules and polymer chain, the radius of gyration (R_g) of a DNA chain decreases with increasing concentration (Cn) according to the relationship of $R_g^2 \propto Cn^{-1/4}$ (Haber et al., 2004). The second hypothesis was that having smaller radius of gyration may improve transmission. But on the contrary, closer proximity of the phosphate anions on the DNA backbone in higher concentration would inherently increase the repulsion between molecules and may consequently cause the more rigid molecules to be retained by the membrane.

In this study, solutions containing DNA vectors pQR150 (20 kb), p5179 (33 kb) and p5180 (72 kb) with concentrations ranging from 25–100 μg/mL were filtered at a constant flux of 0.2 mL/min.cm^2. It is important to note that the DNA concentrations commonly found in large scale industrial processes may be of higher concentrations of around 2–6 mg/mL (Sagar, S., Merck Research Laboratories, personal communication). However, obtaining DNA solutions of such high concentrations were not possible due to the low product yield particularly of the larger DNA vectors (≥ 20 kb) in laboratory scale preparations. Further steps to concentrate the purified

DNA solution would risk loosing more of the valuable material. Figure 3.5 shows transmissions of 89–92%, 72–73% and 57–59% for the 20, 33 and 72 kb vectors respectively. As stated, the percentage of loss was consistent with the increasing DNA concentration. In this case, a constant loss in mass had not been achieved. Therefore, for a given plasmid size, the transmission levels were independent of the feed stream DNA concentration. This suggests the hypotheses of unspecific adsorption and increase in molecule rigidity were not mechanisms contributing to product loss.

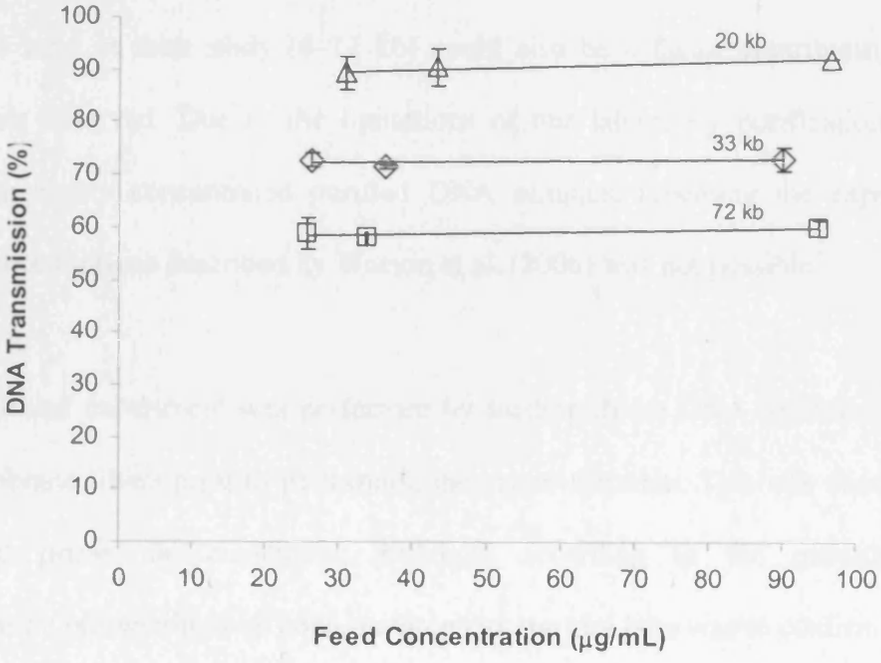

Figure 3.5: The effect of DNA concentration on product recovery. Solutions containing pQR150 (20 kb) (—△—), p5179 (33 kb) (—◇—) and p5180 (72 kb) (—□—) with concentrations ranging from 25–100 μg/mL in prepared in TE buffer were filtered at a flux of 2.3 mL/min.cm^2. The results shown are average of two or three sets of spectrophotometry measurements, error bars indicate standard deviation and lines are linear regressions.

A slight increase in the percentage of DNA transmission with increasing concentrations was observed, however, considering the error associated with the spectrophotometry measurements, this increase is difficult to be justified and be considered significant. Watson et al. (2006) reported that membrane area required for filtration decreases with increasing DNA concentration (2–6 mg/mL) and the reason being lowered plugging of pores due to the reduced plasmid cross sectional area as concentration increases. The concentration applied by Watson et al. was 60–80 times greater than the ones used in the present study and this could explain why this phenomenon was not clearly observed in this study. Besides, the much smaller plasmids used in their study (6–11 kb) could also be a factor contributing to the difference observed. Due to the limitations of our laboratory purification kits in obtaining highly concentrated purified DNA samples, repeating the experiments using concentrations described by Watson et al. (2006) was not possible.

An additional experiment was performed by loading dilute DNA solutions through the membrane filters prior to performing the actual filtration. This was done to pre-wet and prime the membrane. Although according to the manufacturer's specification pre-wetting was not a requirement, the aim here was to confirm that the wettability of the membrane did not influence product loss. At the same time, useful information can be extracted to confirm the presence of charged binding sites if any existed.

For this experiment, the largest construct (116 kb) available in our laboratory was tested so that changes could be detected more readily. A dilute solution containing 3 μg/mL of p5176 BAC vector was initially filtered through 0.22 μm pore size PVDF

membranes then followed by the actual 30 µg/mL solution. Filtrations were performed a constant flux of 2.3 mL/min.cm^2. From Figure 3.6, the results showed that the transmission was 18 ± 5% for the primed sample compared to 20 ± 4% for the control sample (in which no dilute samples were applied to pre-wet/prime the membrane). There was no significant difference between the two filtrations performed and pre-wetting did not reduce product loss.

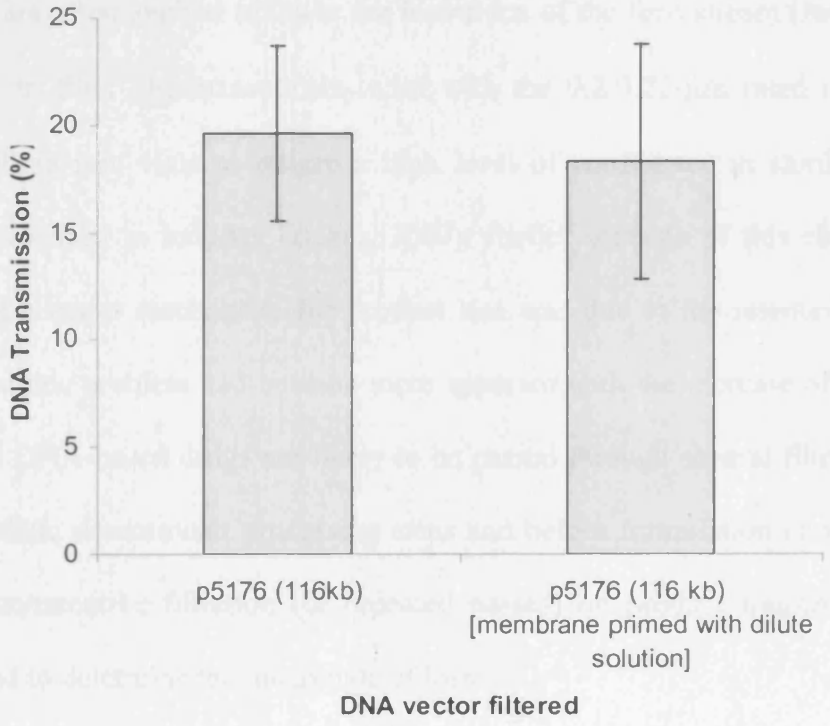

Figure 3.6: The effect of preparing and priming the membrane filter on product recovery. BAC p5176 (116 kb) was filtered using 0.22 µm PVDF membranes at a constant flux of 2.3 mL/min.cm^2. The results shown are average of two or three sets of data, error bars indicate standard deviation.

The result confirmed that pre-wetting the membrane was not necessary and the adsorption mechanisms did not seem to be playing a role in affecting the performance of the sterile filtration operation. The apparent mechanism of product loss was associated to the retention of DNA vectors due to their size. The DNA

solutions were only filtered once through, retention of molecules could be even more considerable in processes involving multiple filtration passes.

3.5 Effect of consecutive filtration on DNA transmission

Pre-filters are often applied to lower the bioburden of the feed stream (Jornitz et al., 2003) and to filter pharmaceuticals twice with the 0.2/0.22-μm rated membranes prior to filling into vials to ensure a high level of confidence in sterility is also regularly practised in industry (Baker, 2000). Earlier sections of this chapter have shown that a major mechanism for product loss was due to the retention of DNA vectors and this problem had become more apparent with the increase of molecular size. Since DNA-based drugs are likely to be passed through several filtration steps in intermediate downstream processing steps and before formulation or vialing, the effect of consecutive filtration (or repeated passes) on product transmission was investigated to determine the magnitude of loss.

Three different DNA vectors to cover a broad range of sizes were applied in this experiment. The DNA vectors were gWIZ (6 kb), pQR150 (20 kb) and p5180 (72 kb). Filtrations were conducted at a constant flux of 2.3 mL/min.cm^2. For the consecutive filtration passes, the initial DNA feed solutions were adjusted to 30 ± 2 μg/mL. Once filtered, the permeate solutions collected were then filled into new syringes and passed through new membrane filters for the second time. This step was repeated up to five consecutive times. After each filtration pass a small aliquot of permeate was collected for analysis.

DNA transmission was observed to increase with the number of filtration passes for the plasmids tested (Figure 3.7). Notably, for the larger vector tested (72 kb), transmission levels changed from 56 ± 9% to 94 ± 4% for the first and second pass respectively. Contaminating species such as large DNA fragments, bacteria cells and debris or other particulates may have been removed after the first filtration pass and therefore higher transmission levels were observed in the subsequent filtration passes. Analysis of contaminating chromosomal DNA will be discussed in the following sections in this chapter.

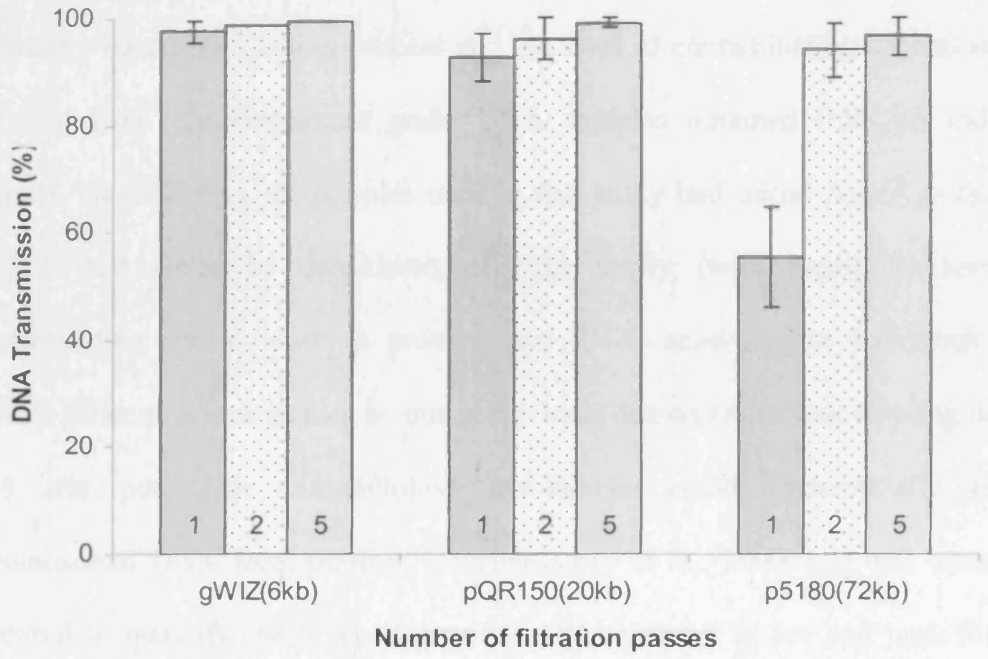

Figure 3.7: The effect of consecutive filtration passes on product transmission. Solutions containing plasmids gWIZ (6 kb), pQR150 (20 kb) and p5180 (72 kb) were subjected to five consecutive filtrations. The feed concentration was 30 μg/mL and filtration flux of 2.3 mL/min.cm^2 was applied. The results shown are average of two sets of experiments, error bars indicate standard deviation. Please note that the standard deviation of the last two points (2 and 5 passes) for the gWIZ samples were < 0.1%.

3.6 Analysis of contaminating chromosomal DNA

As mentioned in the previous section, the probability of chromosomal DNA in the sample tends to increase with the increase of plasmid size. Although all samples used had been ion exchange purified prior to filtration, remaining host derived high molecular weight chromosomal DNA present in the samples could contribute to the membrane's retention or sieving effects. However, it is important to note that the contaminants profile of purified plasmid DNA in solution may differ between various purification processes. For this study, DNA solutions were obtained via a laboratory based purification process and the level of contaminating species may be different from pharmaceutical grade DNA samples obtained from an industrial process. Nevertheless, all samples used in this study had initial A_{260}/A_{280} ratios of 1.7–1.9 and could be considered of high purity (with negligible levels of contaminating species such as proteins and RNA) according to Sambrook et al. (1989). Since previous studies by our group have demonstrated that filtering through 0.45 μm pore size nitrocellulose membranes could preferentially remove chromosomal DNA from plasmid samples (Levy et al., 2000c), it was considered essential to quantify the level of genomic DNA present in pre and post filtration samples containing the larger BAC constructs p5179 (33 kb), p5180 (72 kb) and p5176 (116 kb).

The amount of *E. coli* genomic DNA in the samples can be determined using the Quantitative Polymerase Chain Reaction (qPCR) technique. This is a highly precise technique to determine whether a genetic sequence is present by replicating DNA samples. If the sequence is present, the number of copies in the sample can be

detected and quantified. DNA is expected to be single stranded at 95°C. A single stranded DNA sample may be replicated using a DNA polymerase enzyme based, thermally activated cycle and the amount of DNA present following each thermal cycle is expected to double and this leads to logarithmic amplification. For this study, a 70-bp fragment of the ribosomal RNA gene present in the *E. coli* genome (as reported in Vilalta et al., 2002) was amplified using oligonucleotide primers. The SYBR Green fluorescence level increases as the dye binds to the increasing amount of double stranded DNA in each sample and this was detected using the ABI Prism 7700 Sequence Detection System®. An example of a PCR trace is shown in Figure 3.8. A calibration curve was prepared with 1 pg to 5 ng of *E. coli* genomic DNA (Figure 3.9) and certain samples were spiked with known amounts of chromosomal DNA for validation of the analysis.

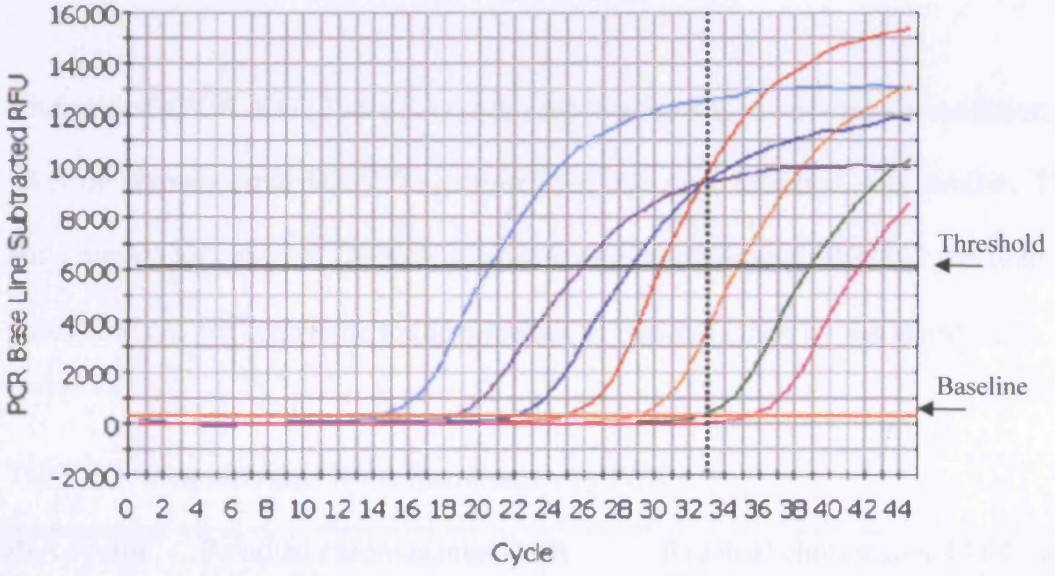

Figure 3.8: An example of a PCR trace. Fluorescence units are shown on the y-axis. The base line was first set in the figure. The black horizontal line is the threshold line. The cycle number at which the increase in fluorescence is logarithmic was measured and the CT values were obtained at which the fluorescence crosses the threshold. CT values correspond to DNA concentration.

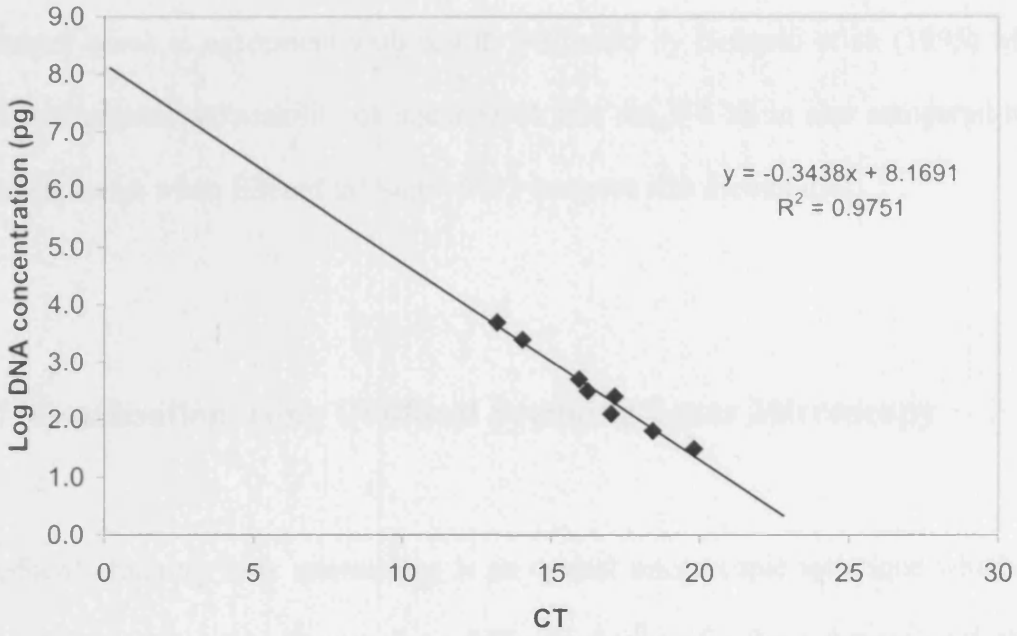

Figure 3.9: Genomic DNA (*E. coli* DH5α) standard curve for the quantification of DNA concentration.

Analysis of qPCR data (Table 3.3) indicated that for a given plasmid preparation, the level of chromosomal DNA for samples pre and post filtration was similar. Thus, most remaining genomic DNA was capable of passing through the 0.22 μm diameter pores, and did not contribute to the retention of plasmid DNA by the membranes.

Table 3.3: Chromosomal DNA quantitation by PCR.

DNA vector	Residual chromosomal DNA before filtration			Residual chromosomal DNA after filtration		
	CT	(ng)	(%)[α]	CT	(ng)	(%)[α]
p5179	14.89	1.59	16 ± 1	14.74	1.45	15 ± 1
p5180	14.91	1.26	13 ± 1	15.14	0.92	9 ± 1
p5176	14.57	1.10	11 ± 1	14.45	1.12	11 ± 1

[α] Error indicate 15% of coefficient of variation associated with the technique.

The results also suggest that linear DNA was able of passing through the 0.22 μm diameter pores in agreement with results published by Hirasaki et al. (1995) which reported greater permeability of linear DNA that are 3–5 kb in size compared to its circular forms when filtered through 15–35 nm pore size membranes.

3.7 Visualisation using Confocal Scanning Laser Microscopy

Confocal scanning laser microscopy is an optical microscopic technique which can provide high resolution images from different depths of a three dimensional object (Ferrando et al., 2005). This is a useful method to visualise adsorptive protein and DNA chromatography if use in combination with fluorescent labelling (Reichert et al., 2002). Additionally, this method can be applied to characterise membrane fouling and to obtain quantitative data (Ferrando et al., 2005). In the earlier observations of this work, transmission of the DNA vectors was found to decrease with increasing molecular weight and therefore confocal microscopy was applied to view the membrane surfaces in order to confirm that the DNA lost was indeed retained on the membrane and not lost due to other causes for example adsorption to the membrane housing or contacting surfaces. Fouled membranes used in filtration experiments were stained using the green fluorescence reagent, PicoGreen which binds to DNA molecules. Therefore, if there was DNA on the membrane, fluorescence would be detected.

Solutions containing 30 μg/mL of pQR150 (20 kb) and p5180 (72 kb) vectors were prepared. Filtrations were performed at a constant flux of 2.3 mL/min.cm^2. Diluted

PicoGreen solution (1 in 400 dilution) was then filtered slowly through the fouled membrane at a flux of 0.05 mL/min.cm^2. The PicoGreen solution was re-circulated through the membrane for the second time. Then TE buffer was passed through the fouled and PicoGreen stained membrane to remove any access unbound fluorescent dye. The membranes were removed from their housings carefully and placed on glass sides in preparation of visualisation in the confocal microscope. For quantification, confocal images can be translated into intensity profiles using the Leica software provided.

Figures 3.10 and 3.11 show the surface views of the two membranes used for the filtration of the DNA vectors pQR150 (20 kb) and p5180 (72 kb) respectively. The green fluorescence spots seen in the images below clearly indicate deposition of DNA on the membrane filters. When comparing the two images, the fluorescence intensity was less on the membrane containing the smaller 20 kb plasmid. Based on the fluorescence intensity profile generated by the Leica confocal software, for the membrane containing the 20 kb plasmid the average total intensity for the scanned membrane area was found to be $(4.2 \pm 0.8)\times10^6$ fluorescence signal units compared to $(17.8 \pm 2.1)\times10^6$ fluorescence units for the 72 kb vector. Please note that to obtain the fluorescence intensity profiles, two horizontal and two vertical lines across each membrane image were selected (to cover different areas) within the software and average fluorescence signal values were then calculated.

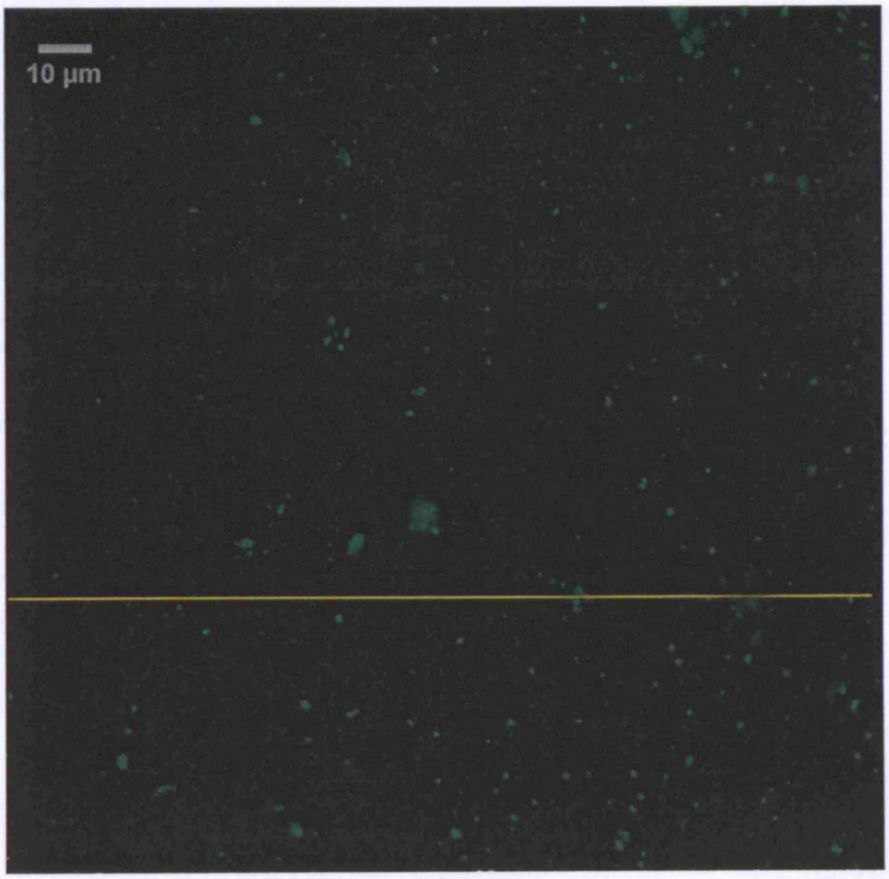

(A)

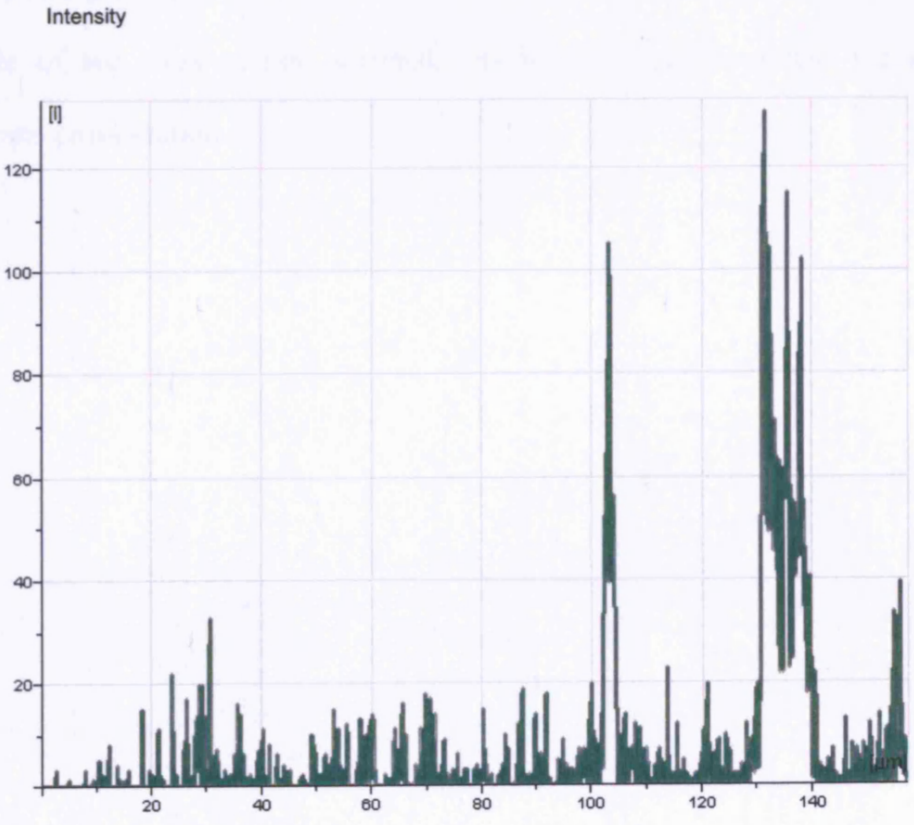

Channel 1

Length	157.18 µm
# Pixel	5070.00
Mean Amplitude	6.44
Max. Amplitude	133.00
Min. Amplitude	0.00
Average Deviation	8.73
Standard Deviation	16.52
Variance	272.76

Figure 3.10: (A) Confocal microscope image of membrane filter surface used for filtration of plasmid pQR150 (20 kb). Membrane was stained with PicoGreen and bound DNA gives green fluorescence. The line across the membrane represents an example of the cross section scanned. (B) Intensity profile across the selected membrane cross section.

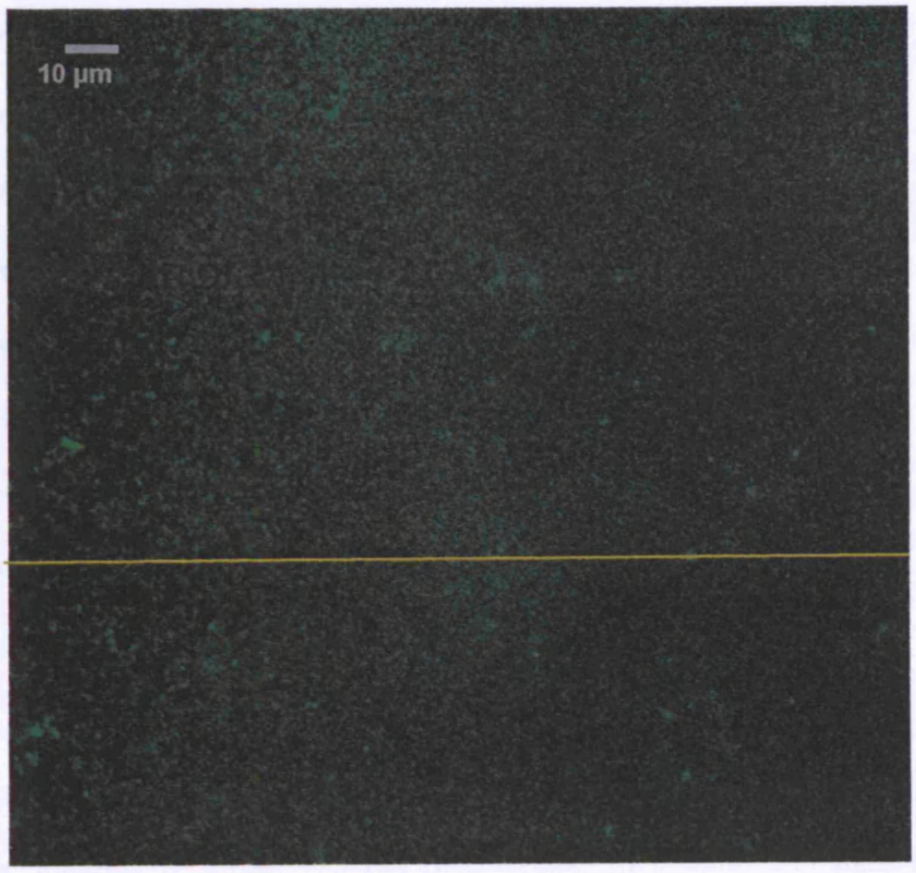

(A)

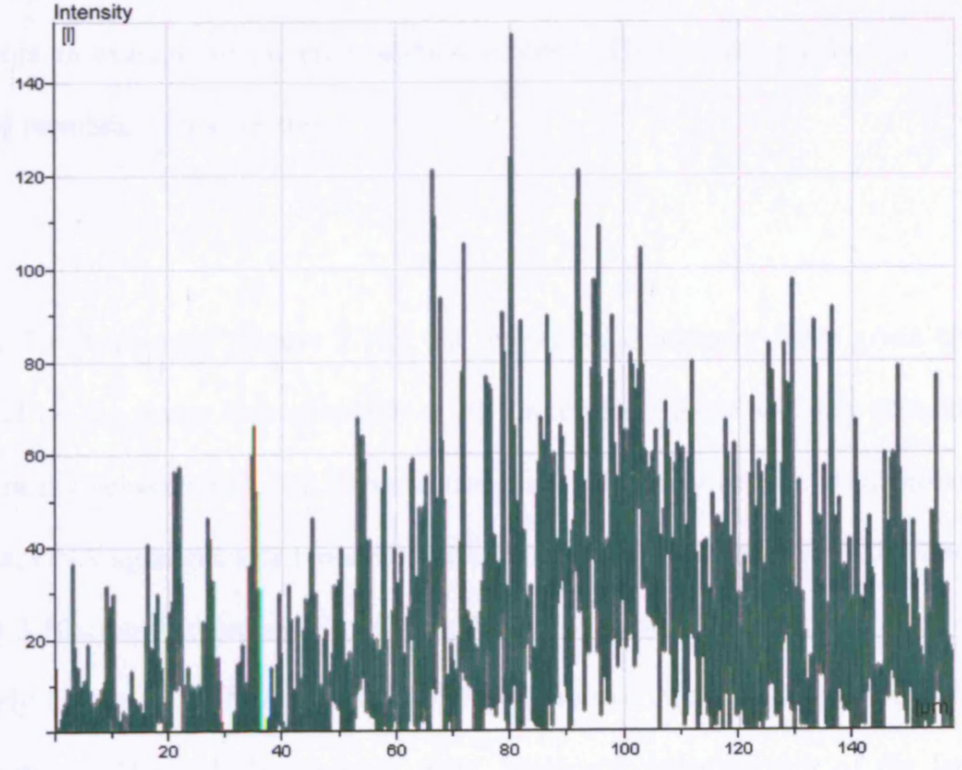

(B)

Channel 1

Length	157.59 µm
# Pixel	5083.00
Mean Amplitude	19.85
Max. Amplitude	153.00
Min. Amplitude	0.00
Average Deviation	16.29
Standard Deviation	20.68
Variance	427.56

Figure 3.11: (A) Confocal microscope image of top surface of filtration membrane used for filtration of p5180 (72 kb) BAC vector. Membrane was stained with PicoGreen and bound DNA gives green fluorescence. The line across the membrane represents an example of the cross section scanned. (B) Intensity profile across the selected membrane cross section.

For the 20 kb plasmid (Figure 3.10), the fluorescence intensity for a given cross sectional on the image was generally $\leq$ 20 fluorescence units with the occasional strong peaks between 133–255 fluorescence units. This may be due to retention of bacteria, DNA aggregates or blocked pore channels. Whereas for the 72 kb plasmid (Figure 3.10), the fluorescence signal distributed throughout the membrane area was relatively higher ($\leq$ 80 fluorescence units) and the maximum intensities picked up were between 155–255 fluorescence units. Molecular entanglement of the larger vector could be more significant, resulting in greater deposition and retention rates

which contributed to the large fluorescing area seen across the second membrane image.

Figures 3.12 (A and B) corresponds to the z-axis projection of ten images stacked along the axis perpendicular to the image plane for a three-dimension reconstruction, therefore, showing the inside of the membrane. No focal plane was found in a depth > 11 μm. As expected, the fluorescence intensity gradually decreased from 2.5×10^6 to 0.6×10^6 fluorescence units as the distance from the membrane surface increases (Figure 3.11C). Similarly, Ferrando et al. (2002) also reported the fluorescence intensity profile of proteins significantly decrease as the distance of from the membrane surface increases. Taken together, these results indicate that more molecules tend to be retained on the membrane's surface than below.

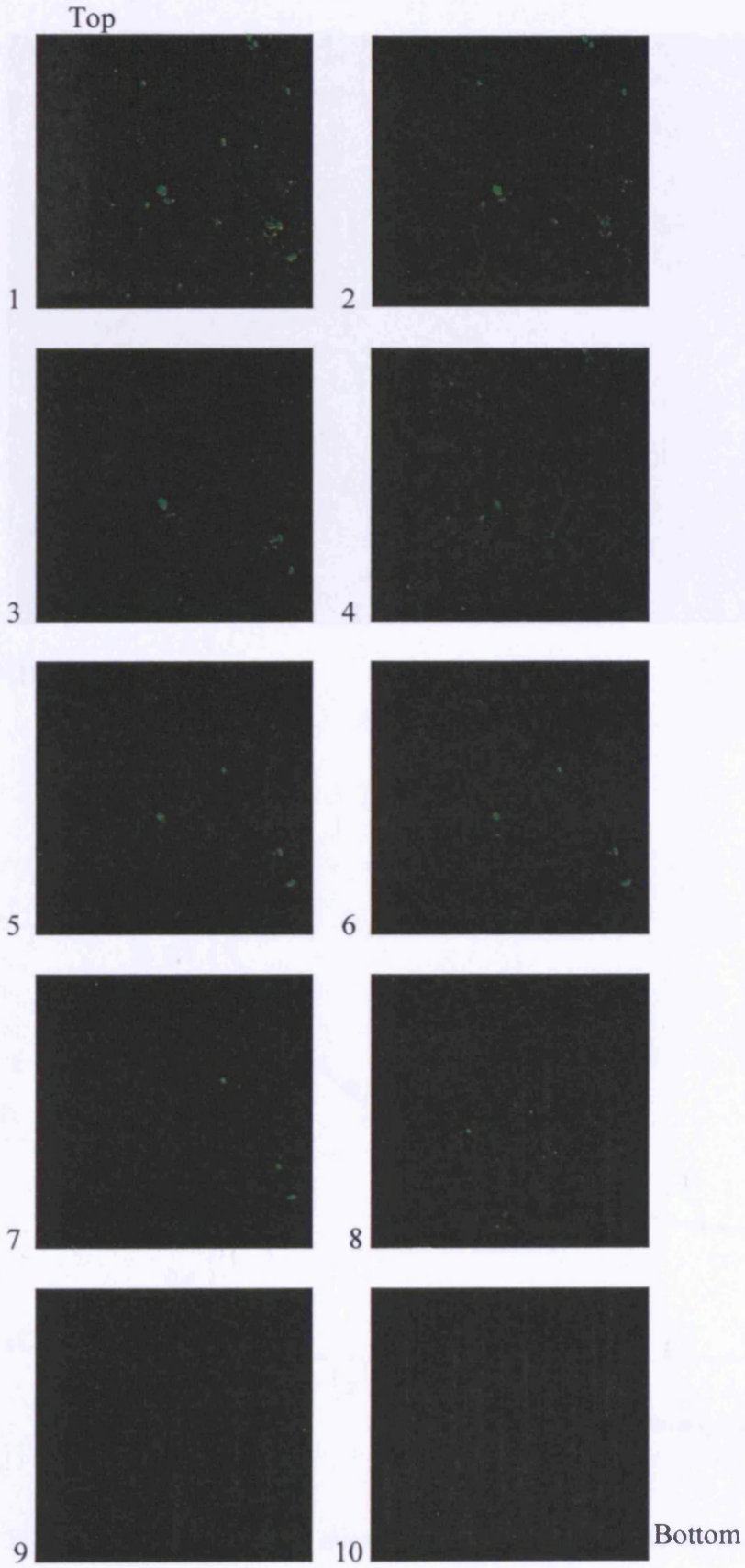

(A)

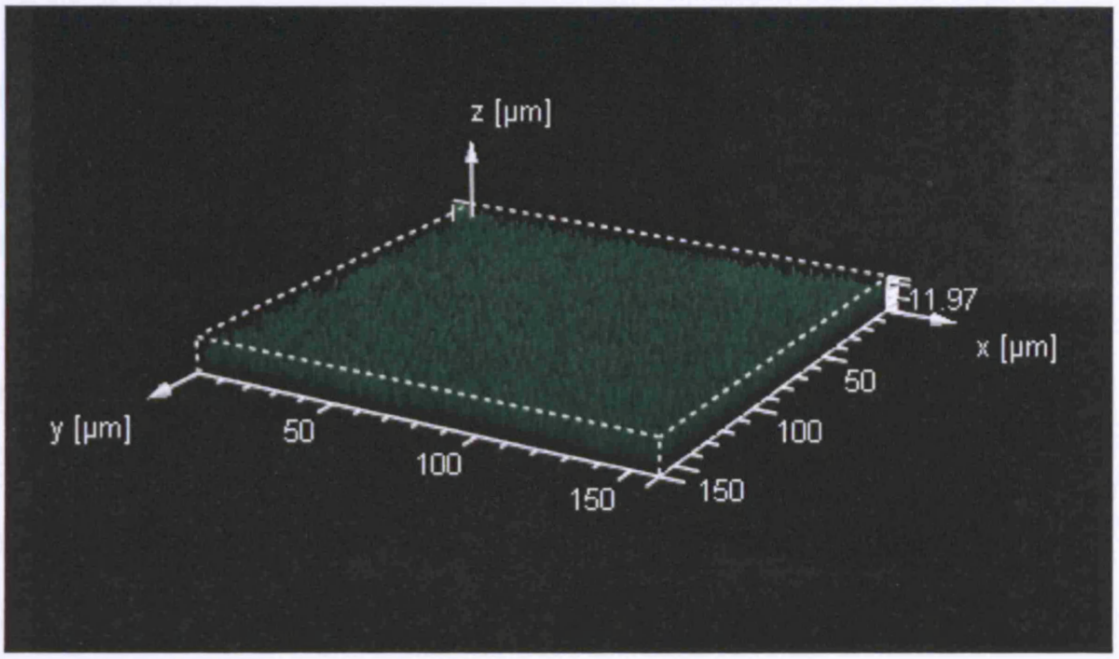

(B)

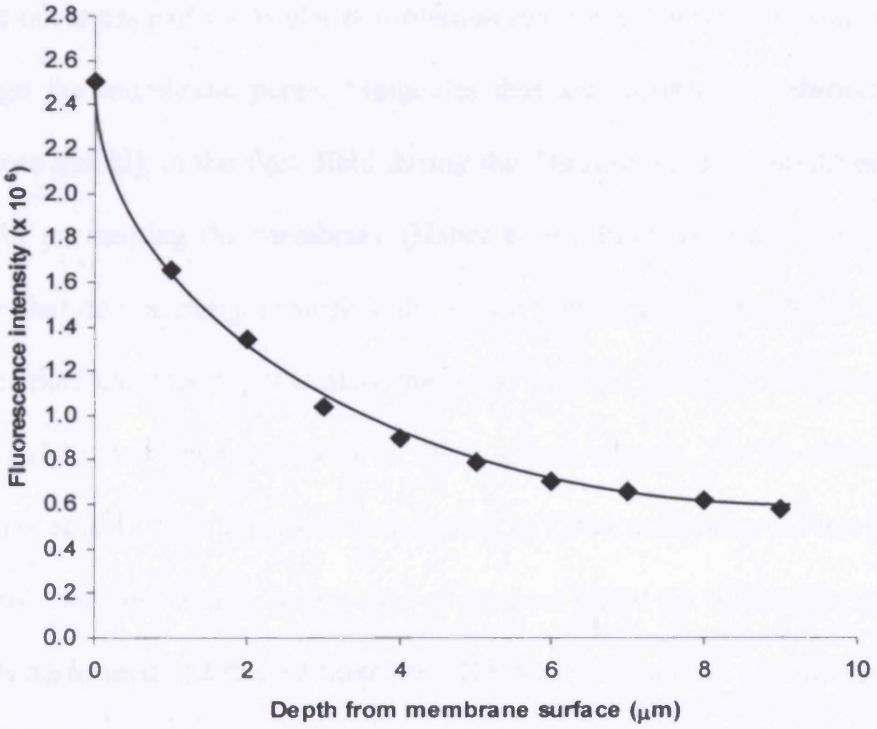

(C)

Figure 3.12: (A) Confocal microscope images up to a depth of 11.97 µm from the top surface of the filtration membrane used for filtration of pQR150 (20 kb) plasmid. (B) Three-dimension reconstruction using the z-axis projection of ten images from (A)

stack along the axis perpendicular to the image plane. Membrane was stained with PicoGreen and bound DNA gives green fluorescence. The image shows that some plasmid DNA was trapped within the pores of the membrane. (C) Fluorescence intensity with respect to the distance from the membrane surface.

3.8 Conclusion

The results shown in this chapter clearly indicate that the performance of the membrane sterilisation operation can be significantly affected by the circular vector molecular size. The high recovery rates for the smaller constructs tested seems to indicate the occurrence of molecular deformation into long thin structures in order to pass through the membrane pores. Molecules that are capable of deforming and aligning more quickly in the flow field during the filtration process would have the advantage of permeating the membrane (Haber et al., 2004; Hirasaki et al., 1995) while those that do not elongate sufficiently in the flow direction would be retained by the membrane and this might explain the linear trend of retention with increasing molecular weight described and seen in the confocal images. Unlike filtration of proteins (Maa et al., 1998), unspecific adsorption of DNA molecules did not play an important role in contributing to the loss of product based on observations of the experiments performed at different fluxes and DNA concentrations. Quantification of genomic DNA via qPCR techniques indicated that linear DNA permeates the membrane pores more sufficiently than circular DNA vectors as observed by Higuchi et al. (1996) and Hirasaki et al. (1995). The confocal images have shown deposition of DNA molecules on the membrane surfaces and within the pores. As filtration

proceeds, the resistance to flow can increases due to fouling. Fouling can increase the pressure for constant flow filtration or it can cause decay in flow for constant pressure operations. The extent of DNA damage due to the increase of pressure (in constant flux filtrations) caused by the plugging of pores is reported in Chapter 4 while the characterisation of fouling will be discussed in Chapter 5.

Chapter 4 – Backbone Breakage of DNA Vectors and Protection Methods

4.1 Introduction

For the duration of a normal flow filtration, each pore on the membrane filter acts like an orifice and coiled DNA molecules are expected to elongate in the direction of the flow (Hirasaki et al., 1995). Shear-induced damage of the DNA sugar-phosphate backbone will occur when molecular elasticity limits have been exceeded under the influence of high fluid stresses and midpoint breakages of double stranded DNA (dsDNA) molecules can occur due to elongational effects caused by an abrupt constriction (Bowman and Davidson, 1972). Single strand and double strands nicks will create open circular (OC) and linear plasmid forms respectively. These degraded isoforms are not desired as they do not transfect as efficiently as supercoiled (SC) plasmids into eukaryotic cells (Herman, 1996; Middaugh et al., 1997). Confocal images in the previous chapter have shown deposition of DNA molecules on the membrane surfaces and within the pores; this would eventually increase fouling and leads to an increase in transmembrane pressure (for constant flow filtration operations) which could further intensify the elongational shear and enhance irreversible molecular damage.

The elongation of DNA molecules has been widely studied by a number of researchers. Smith et al. (1996) have previously performed high resolution experiments to measure the elasticity of tethered single double stranded DNA molecules. It was found that a dsDNA behaves like a spring (due to its helical properties), and can be extended from its relaxed random coil configuration in response to applied external forces stretching linearly to 1.7 times its contour length (Smith et al., 1996). Other researchers such as Perkins et al. (1995) and Larson et al. (1997) have studied elongation of DNA molecules in a hydrodynamic flow field using fluorescence microscopy techniques. In addition, electron microscopy images of DNA molecules elongated by shear stresses in the flow direction while permeating a membrane filter were shown by Hirasaki et al. (1995).

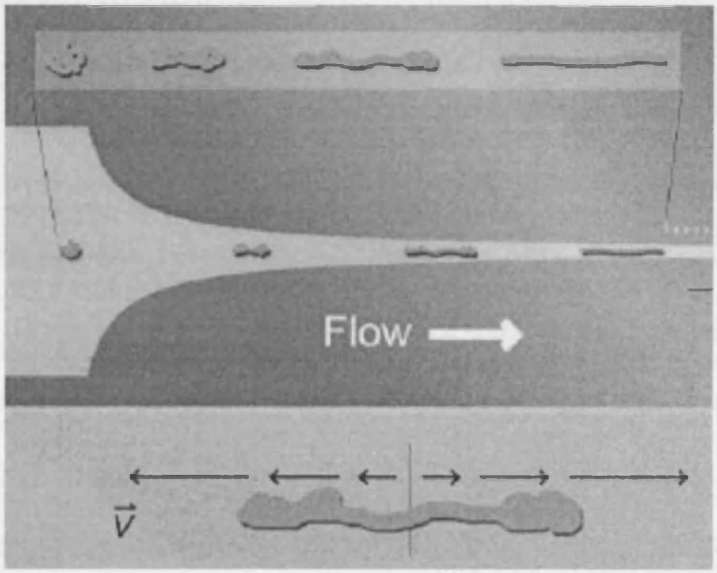

Figure 4.1: Illustration of single DNA molecule stretching in sudden mixed shear and elongational flow (Larson et al., 2006).

It has been demonstrated that the degree of DNA molecular extension in an elongational flow is proportional to velocity (Haber et al., 2004; Perkins et al., 1995; Perkins et al., 1997; Larson et al., 1997). Hence, the velocity of flow during normal flow filtration is expected to be an important parameter in governing the deformation of DNA molecules during filtration. On the contrary to the essential molecular elongation required for membrane permeation, operation at high velocities could result in irreversible molecular changes. Although Bos et al. (2000) reported that shear forces generated during sterile filtration did not affect the topology of small plasmids (6 kb), sensitivity to backbone strand breakage is likely to increase with molecular weight. In addition, the negative charges on the DNA backbone can cause its structure to be very rigid particularly in an unfavourable ionic environment. Therefore, the ease of deformation also plays an important factor in influencing molecular integrity and permeability (Hirasaki et al., 1995; Higuchi et al., 1996).

In this study, the effect of flux, consecutive filtration passes and membrane pore structure was investigated. The aim here was to determine the extent of irreversible damage of circular DNA vectors during the sterile filtration operation. A pressure driven syringe system which allowed the use of very small volumes ($\leq$ 1 mL) of sample and enabled controlled constant filtration flux was used. In certain experiments, high fluxes were applied with deliberation to accentuate molecular backbone breakage via elongational forces. The DNA isoform profile was analysed after each filtration procedure. For determination of the level of protection against irreversible damages, the effect of membrane type and formulating buffer was examined. Molecular stability of filtered DNA vectors was also investigated. Please note that a considerable amount of time had been dedicated to the characterisation of

the DNA vectors used in the study. This was due to the large sizes of the DNA vectors used. As it was essential to be able to differentiate SC molecules from OC ones in filtration samples before any level of damage can be determined, conditions used in the analytical techniques (gel electrophoresis and modified PicoGreen assay) had to be manipulated/modified till satisfactory results were obtained.

4.2 Effect of Flux on DNA Integrity

Due to the reason that membrane sterilisation is one of the last operations in the process sequence, preservation of the DNA backbone integrity is critical since there are no further steps to remove the undesired degraded plasmid isoforms such as OC and linear forms. As fluid to be filtered during the sterile filtration procedure is expected to have limited amount of solid particulates, filtration in the fastest time possible is always desired in industry but high velocity or flux could enhance molecular damage. Hence, the effect of filtration flux on DNA integrity was investigated to determine if the imposed flux rates of 0.1–2.3 mL/min.cm^2 affected the molecular backbone integrity.

A series of experiments were carried out of using the pQR150 (20 kb), pMT103 (29 kb), p5179 (33 kb) and p5180 (72 kb) DNA vectors. The purified DNA vector solutions were adjusted to a DNA concentration of 30 ± 2 μg/mL. The filtrations were performed using 0.22 μm pore size hydrophilic PVDF membrane filters. The change in SC conformation was derived from either gel electrophoresis or pulsed field gel electrophoresis images via densitometric scanning analysis of the gel. Due

to the wide size range involved, there was no single technique that could be used for all the DNA vectors. For the 29 kb plasmid and larger, the normal and pulsed field gel electrophoresis were applied. The different plasmid isoforms expected to be in a typical sample are SC, OC, linear and other smaller DNA fragments. For the establishment of a deliberately degraded sample to compare results, a non-filtered control sample was either subjected to a shear rate of 6×10^{4} s^{-1} or to chemical degradation by incubation at 60°C.

In the analysis, the relative conformational change refers to the ratio of %SC after filtration with respect to %SC in the feed stream (for each lane on a gel image, individual bands corresponding to SC, OC, linear and fragments adds up to a total of 100%). For illustration, an example of a gel image containing control and filtered samples of the 72 kb vector is shown in Figure 4.2.

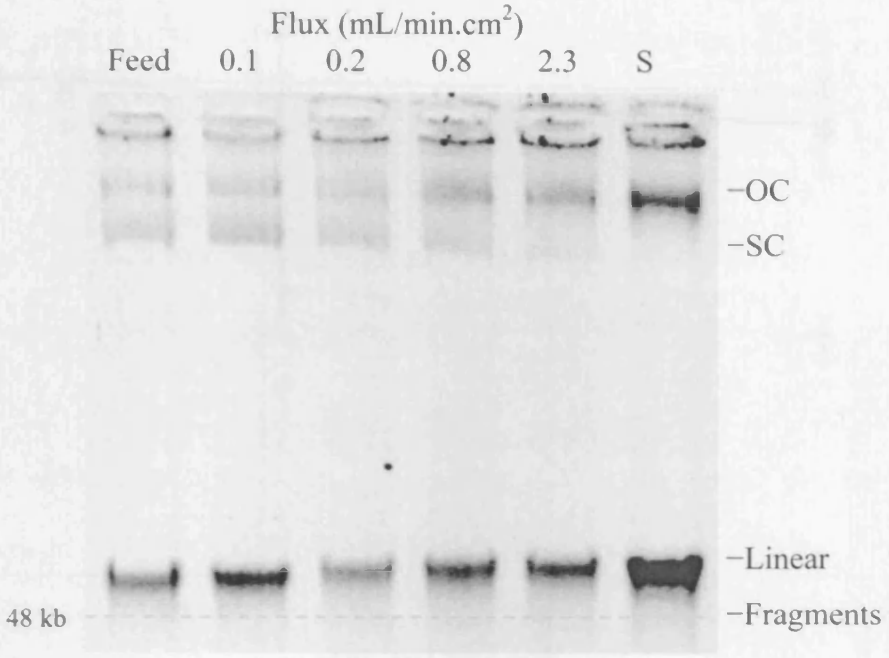

Figure 4.2: Gel electrophoresis of control and filtered p5180 (72 kb) samples. Feed, non-filtered control sample; 0.1, 0.2, 0.8 and 2.3, samples filtered at 0.1, 0.2, 0.8 and 2.3 mL/min.cm^2 through 0.22 μm pore size PVDF membranes; S, non-filtered control samples mechanically degraded at a shear rate of 6×10^4 s^{-1}. All the DNA solutions had starting concentrations of 30 ± 2 μg/mL. λ ladder marker was used.

For the 20, 29 and 33 kb plasmids filtered at constant fluxes of 0.2, 0.8 and 2.3 mL/min.cm^2, the change in the proportion of SC was ≤ 10% (Figure 4.3). As for the 72 kb vector, the backbone breakage was also ≤ 10% when filtered at fluxes of 0.1–0.2 mL/min.cm^2 but this increased to around 40-50% when filtered at higher fluxes of 0.8 and 2.3 mL/min.cm^2 (Figures 4.2 and 4.3).

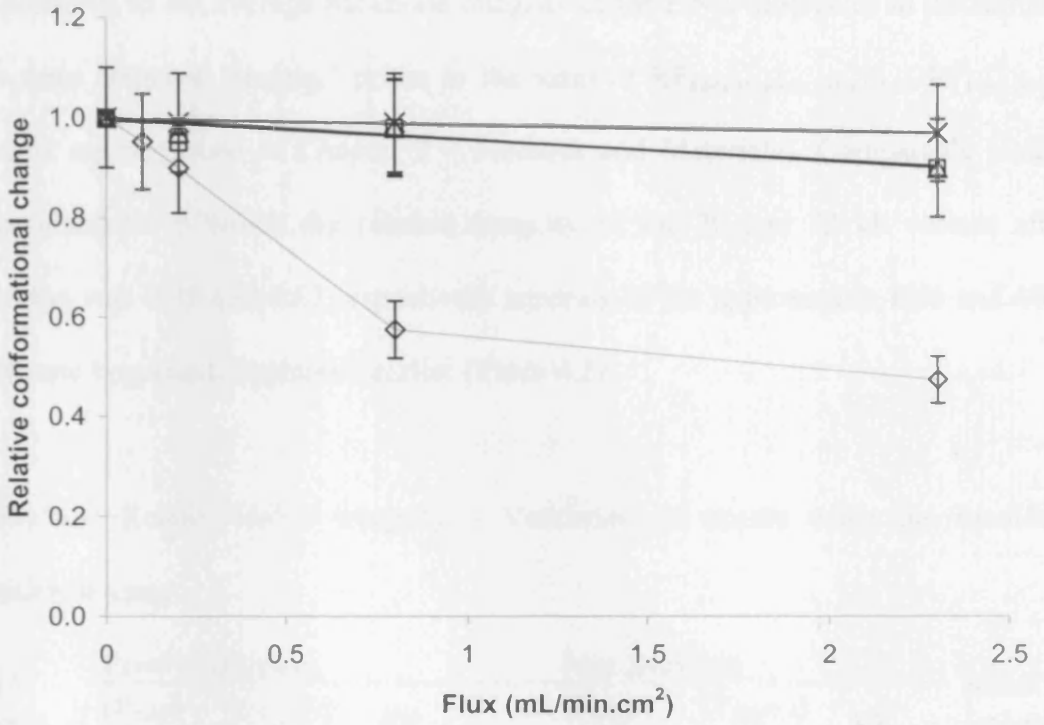

Figure 4.3: Effect of flux on DNA integrity. Relative conformational change of non-filtered control and filtered DNA vectors based on gel densitometry analysis. Solutions containing pQR150 (20 kb) (—x—), pMT103 (29 kb) (—□—), p5179 (33 kb) (—△—) and p5180 (72 kb) (—◇—) were filtered through 0.22 μm PVDF membranes at operating fluxes of 0.1, 0.2, 0.8 and 2.3 mL/min.cm^2. The results shown are average of two sets of densitometric scanning data, error bars indicate standard deviation.

To validate the gel densitometry results, two samples – the 20 and 72 kb vectors that had been subjected to the high filtration flux of 2.3 mL.min.cm^2 were further analysed using the modified PicoGreen technique which is sensitive in detecting plasmid structural changes. In the context of modified PicoGreen assay analysis, fluorescence enhancement of PicoGreen at pH 12.4 ($F_{pH12.4}$) was normalised by its value at pH 8 (F_{pH8}) to give a relative fluorescence ratio ($RF = F_{pH12.4} / F_{pH8}$) that is

proportional to the average backbone integrity of the DNA molecules in the sample. The term 'relative integrity' refers to the ratio of $RF_{sample\ after\ filtration}$ / $RF_{feed\ stream}$ (details are described in Chapter 2 – Methods and Materials). Comparable results were obtained in which the relative integrity of the 20 and 72 kb vectors after filtration was 0.95 and 0.62 respectively agreeing to the approximate 10% and 40% backbone breakage determined earlier (Table 4.1).

Table 4.1: Relative DNA integrity – Validation of results using the modified PicoGreen assay.

DNA Vector	Prior to filtration			Post filtration			Relative Integrity[α]
	(F_{pH8}) $\times 10^3$	$(F_{pH12.4})$ $\times 10^3$	RF	(F_{pH8}) $\times 10^3$	$(F_{pH12.4})$ $\times 10^3$	RF	
pQR150 (20 kb)	11.3	9.8	0.85	9.3	7.7	0.82	0.95 ± 0.07
p5180 (72 kb)	11.1	5.9	0.54	8.3	3.5	0.42	0.62 ± 0.15

[α]The results shown are average of three sets of fluorescence enhancement data ± coefficient of variation.

It is important to note that fluxes commonly used in a membrane sterilisation are typically in the region of 0.1–0.2 mL/min.cm^2. The rationale for using higher fluxes was to accentuate the DNA sugar-phosphate backbone breakage so that filtration data under more extreme conditions can be collected and be compared to the usual operating conditions. High flow rate filtrations can also be conducted in smaller scale processes and in this case, information gathered here would be useful. The overall results in this study suggest that circular DNA vectors of up to 33 kb can be filtered

through the 0.22 μm pore size sterilising membrane filters without substantial molecular damage.

Simulated fluid flow through the membrane pores using the computational fluid dynamics CFX software were kindly performed by Dr Hu Zhang (Table 4.1). Shear rates corresponding to the filtration fluxes of 0.1–2.3 mL/min.cm^2 were obtained. It is necessary to note that fouling of membranes with straight through cylindrical pores (occurred by pore blockage caused by deposition of large particulates on the membrane surface) are more rapid when compared to membranes with interconnected pores (which fouled more slowly since the fluid could flow around the blocked pores through the interconnected pore structure) (Ho and Zydney, 1998) but for the ease of calculation and simulation, pores on the PVDF membrane were assumed to be cylindrical, consistent in size and evenly distributed. Therefore, shear rates calculated can only be rough estimations.

Based on the simulation, shear rate increases proportionally to flux. This could explain the increase of degradation with respect to increasing filtration flux observed for the 72 kb vector. The highest shear rate was found to be near to the entrance of the pores. This suggests DNA backbone damage was mainly occurring at the pore entrances due to elongational forces. Figure 4.4 shows a plot of the percentage of DNA degradation in relation to the estimated shear rate.

Table 4.2: Approximate shear rate at the 0.22 μm size pore entrance during filtration.

Flux (mL/min.cm^2)	Estimated shear rate (s^{-1})
0.1	8.3×10^2
0.2	1.7×10^3
0.8	6.5×10^3
2.3	1.9×10^4

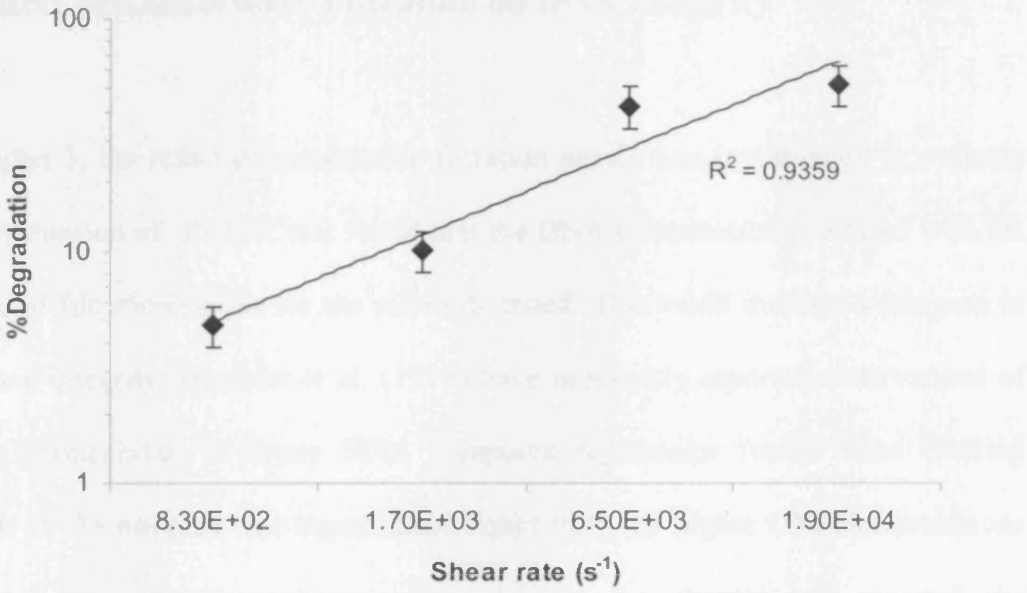

Figure 4.4: Percentage degradation of p5180 (72 kb) with respect to increasing shear rate. Degradation of DNA vector based on gel densitometry analysis. The results shown are average of two sets of densitometric scanning data, error bars indicate standard deviation.

For the smaller 20–33 kb vectors, irreversible damage was not substantial in all the flux rates or shear rates tested. Observations by Levy et al. (1999) where shear studies using a rotating disk showed plasmids ≤ 29 kb were sensitive to shear rates ≥ 10^5 s^{-1}. Whereas for the very large 72 kb vector, considerable backbone breakage

occurred when shear rate exceeds 1.7×10^3 s^{-1} (or flux of 0.2 mL/min.cm^2). In this study, DNA vectors were subjected to one filtration pass through the sterilising grade membranes. The number of filtration passes may have a detrimental effect on molecular backbone breakage.

4.3 Effect of Consecutive Filtration on DNA Integrity

In Chapter 3, the effect of consecutive filtration passes was investigated to evaluate the transmission of DNA. It was found that the DNA transmission increased with the number of filtration passes for the plasmids tested. This could indicate a decrease in backbone integrity. Hirasaki et al. (1995) have previously reported observations of greater permeability of linear DNA compared to circular forms when filtering through 15–35 nm pore size membranes. Apart from the higher DNA transmissions observed, the previous section (section 4.2) of the chapter had reported the occurrence of considerable backbone breakage of the larger 72 kb vector at higher fluxes/shear rates. The effect of consecutive filtration passes was examined to determine if multiple filtration passes would enhance the backbone breakage of DNA vectors.

DNA vectors used in this experiment were gWIZ (6 kb), pQR150 (20 kb) and p5180 (72 kb). The DNA concentration in the feed stream was adjusted to 30 ± 2 μg/mL and filtrations were performed at a constant flux of 2.3 mL/min.cm^2. Similar to the previous chapter, for the consecutive filtration passes, the initial DNA feed solutions were filtered and the permeate solutions were collected. Then the permeated DNA

solutions were filled into new syringes and pass through new membrane filters for the second filtration. This step was repeated up to five consecutive times. After each filtration pass a small aliquot of permeate was collected for analysis. Since the modified PicoGreen assay has demonstrated to be highly sensitive in detecting structural changes and gave complementary results to the gel electrophoresis technique in the earlier experiment, the backbone integrity analysis was performed using this fluorescence based method. An advantage of this method is that less sample mass is required for analysis and data can be obtained rapidly within 10 minutes. Furthermore, this technique generally shows inter-assay and intra-assay variation of $\leq$ 10% coefficient of variation (Rock et al., 2003). Gel electrophoresis was conducted for product quality visualisation and validation.

Based on the modified PicoGreen assay analysis, there was no significant change in the backbone breakage for the 6 kb plasmid tested (Figure 4.5). But for the larger vectors, the irreversible backbone damage increased with the increasing number of filtration passes (Figure 4.5). Agarose gel electrophoresis analysis confirmed results obtained with the modified PicoGreen assay. For illustration, gel images of the 20 and 72 kb vectors are shown in Figures 4.6 (A) and (B). The quantity of linear DNA increase proportionally to the number of filtration passes. This would explain the increase in DNA transmission with the number of filtration passes observed in the previous chapter. Linear DNA has better permeability than circular DNA and these results are in agreement with observations published by Hirasaki et al. (1995).

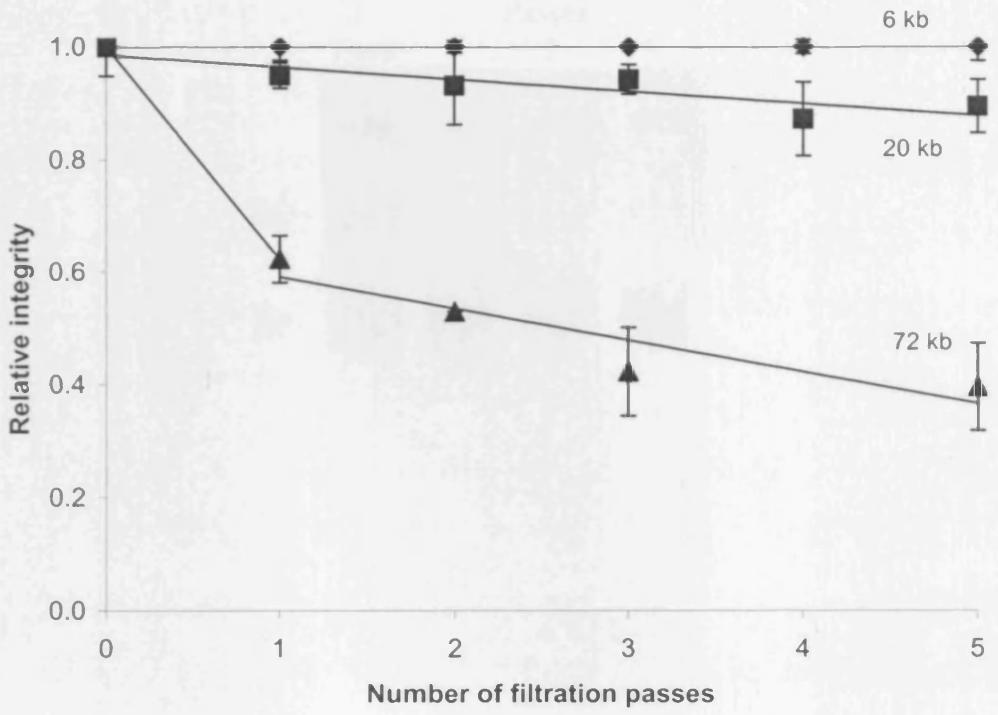

Figure 4.5: The effect of consecutive filtration on relative integrity of the 6 kb (◆), 20 kb (■) and 72 kb (▲) vectors. Relative integrity based on modified PicoGreen assay. The results shown are average of 3 independent experiments, error bars indicate coefficient of variation.

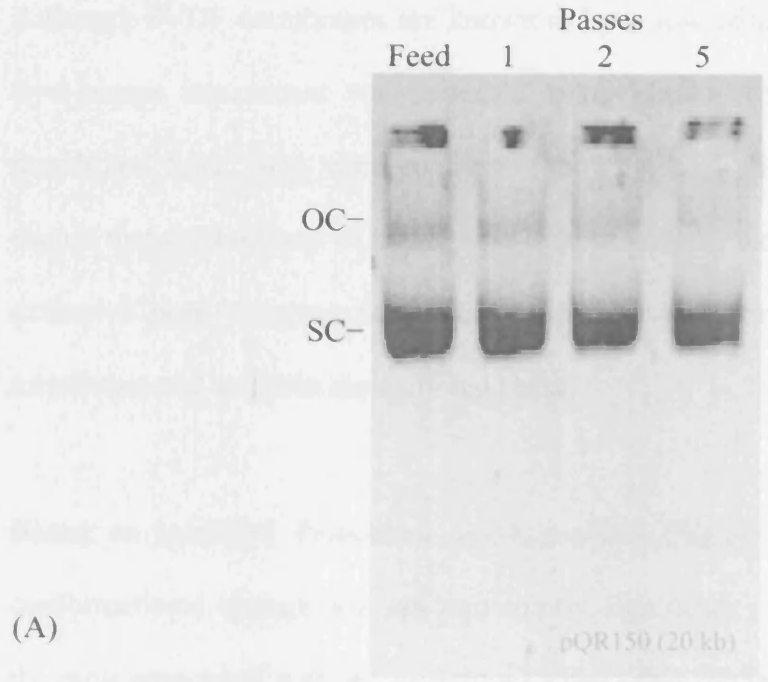

(A)

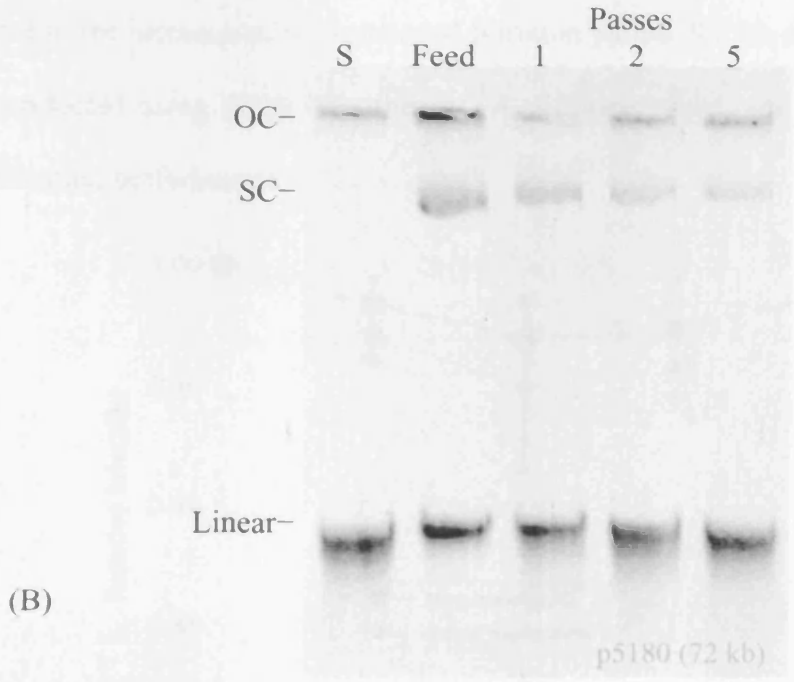

(B)

Figure 4.6: (A) Gel electrophoresis of control and filtered pQR150 (20 kb). (B) Gel electrophoresis of control and filtered p5180 (72 kb). Feed, non-filtered control sample; 1, 2 and 5, samples filtered 1, 2, and 5 times through 0.22 μm PVDF membranes; S, control sample mechanically degraded at a shear rate of 6×10^4 s^{-1}.

Although PVDF membranes are known to have low adsorption properties, a similar five passes experiment was repeated using similar conditions but new unused membrane filter units were replaced following each filtration pass. This was to ensure that the build-up of entangled DNA strands on the membrane did not caused extensive pore clogging that could increase the differential pressure across the membrane and heighten elongational shear.

Based on modified PicoGreen assay analysis (Figure 4.7), difference in DNA conformational change was not particularly significant (taken into consideration of the error associated with the technique) when fresh filtration capsules were replaced after each filtration pass. This confirms that the decrease of backbone integrity was due to the increase in the number of filtration passes. So far, all the experiments were conducted using PVDF membranes. A different membrane type may improve the filtration performance.

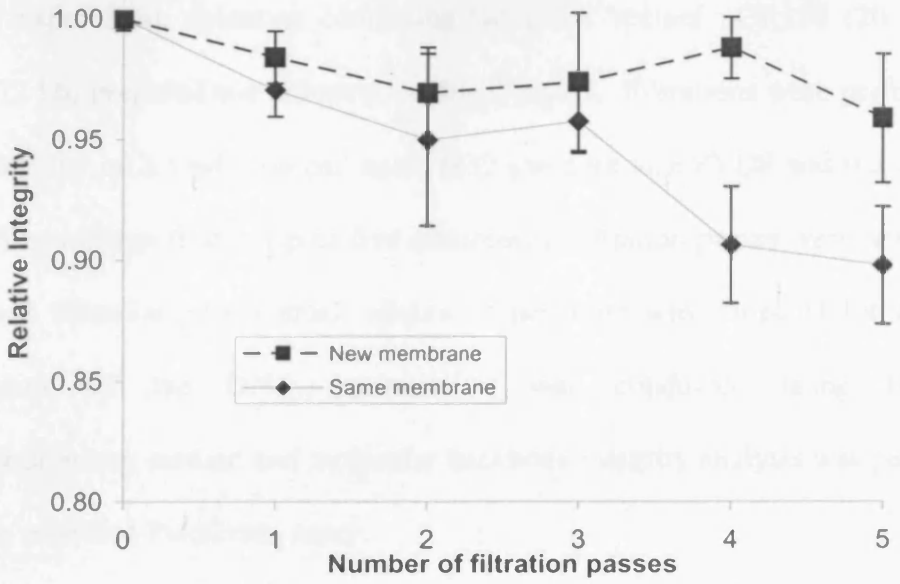

Figure 4.7: Relative integrity of pQR150 (20 kb) based on modified PicoGreen analysis. The results shown are average of 3 independent experiments, error bars indicate coefficient of variation.

4.4 Effect of Membrane Type

A series of experiments were performed to determine if the membrane type and structure could have an impact on the performance of the operation. In the first experiment, two hydrophilic synthetic polymeric membrane materials were compared. One of the two membranes used for comparison was the PVDF membrane (which has been applied throughout the earlier experiments). The semicrystalline PVDF polymer has a 'lacy' morphology and this gives it a highly permeable fibrous network which is very desirable for microfiltration purposes (Zeman and Zydney, 1996). PES was the other membrane tested. When viewed under the SEM, the PES membrane has a nodular morphology (formed by isolated nodules or spherical granules). The nodule size increases in the direction away from the skin/top surface layer giving it a very porous character (Zeman and Zydney, 1996).

For this experiment, solutions containing the DNA vectors pQR150 (20 kb) and p5180 (72 kb) prepared and adjusted to 30 ± 2 μg/mL. Filtrations were performed at a constant flux of 2.3 mL/min.cm^2 using 0.22 μm pore size PVDF and 0.2 μm pore size PES membrane filters. Up to five consecutive filtration passes were performed. After each filtration pass a small aliquot of permeate was collected for analysis. Quantitation of the DNA transmission was conducted using the UV spectrophotometry method and molecular backbone integrity analysis was performed using the modified PicoGreen assay.

The results obtained indicated that when the 0.2 μm pore size PES membrane was applied, transmissions improved by approximately 9% for the 20 kb and 30% for the

72 kb DNA vector respectively (Figure 4.8). Preservation of the backbone integrity also increased by 5% and 41% for the 20 and 72 kb vectors respectively when compared to consecutive filtration experiments performed with PVDF membranes (Figure 4.9).

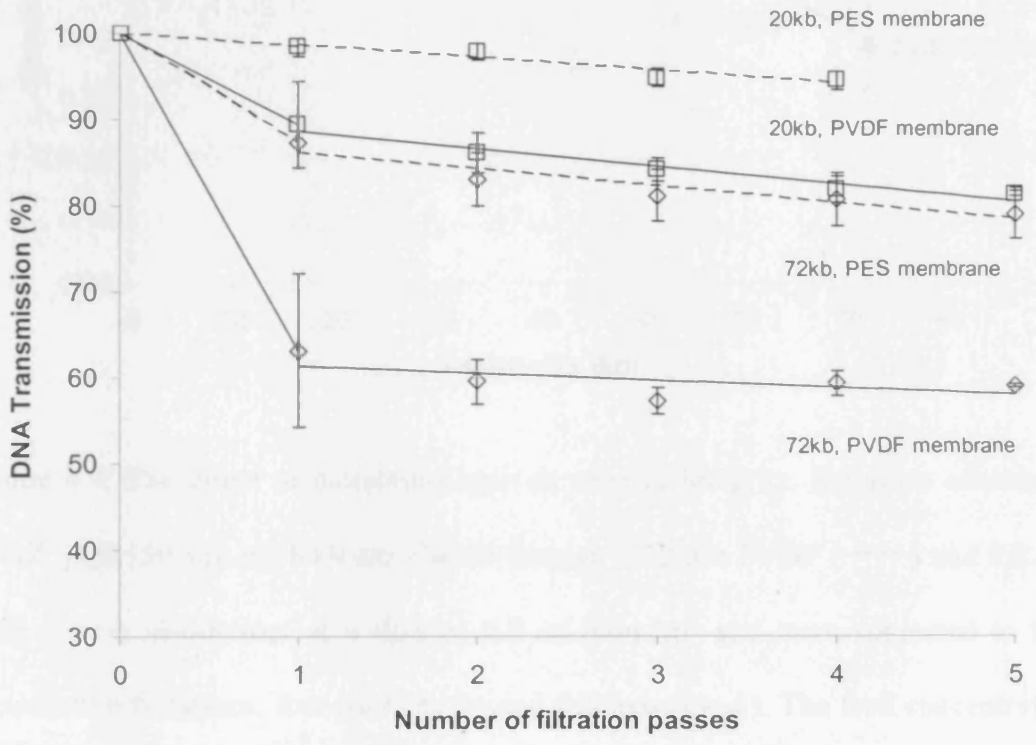

Figure 4.8: The effect of membrane type on DNA transmission. Solutions containing pQR150 (20 kb) (□) and p5180 (72 kb) (◇) were filtered through 0.22 μm PVDF (——) and 0.2 μm PES (- - - - -) membranes at a flux of 2.3 mL/min.cm^2 and were subjected to five consecutive filtrations. The feed concentration was 30 μg/mL and analysis was carried out by the modified PicoGreen assay. The results shown are average of two sets of data, error bars indicate standard deviation.

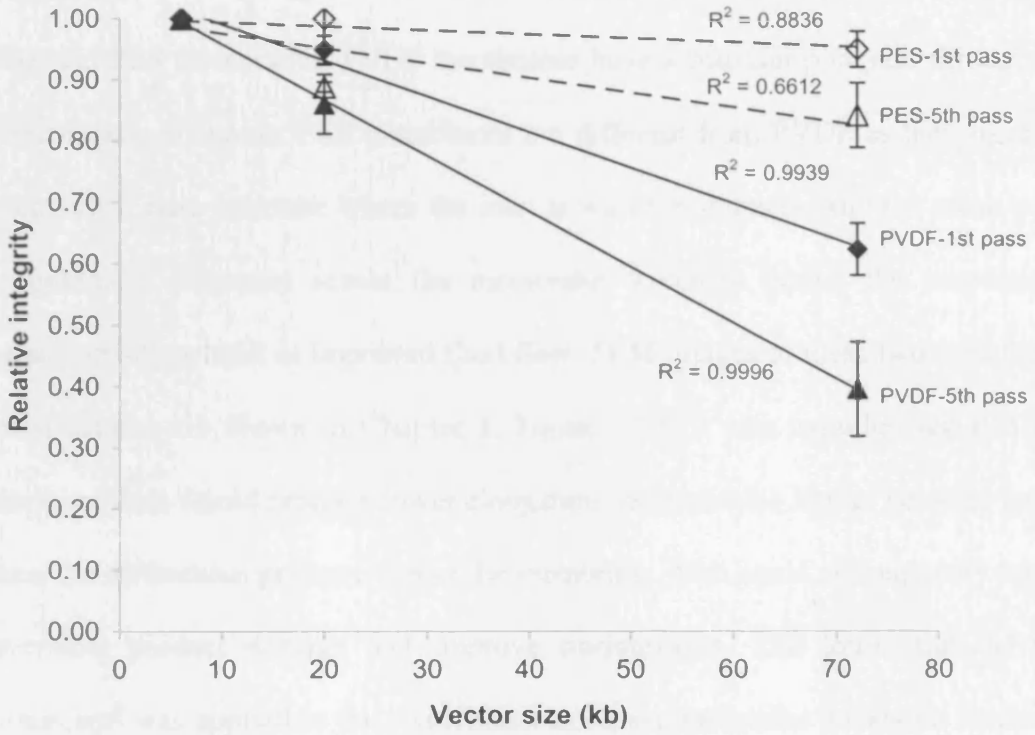

Figure 4.9: The effect of membrane type on relative integrity. Solutions containing gWIZ, pQR150 and p5180 were filtered through 0.22 μm PVDF (——) and 0.2 μm PES (- - - - -) membranes at a flux of 2.3 mL/min.cm^2 and were subjected to five consecutive filtrations, first pass (◆, ◇) and fifth pass (▲,△). The feed concentration was 30 μg/mL and analysis was carried out by the modified PicoGreen assay. The results shown are average of two sets of data, error bars indicate standard deviation and lines are linear regressions.

Next, solutions containing the 72 kb vector were filtered using combinations of PVDF and PES membranes. PVDF membranes have a constant pore size throughout the membrane thickness. PES membranes are different from PVDF as they have an asymmetrical pore structure where the inlet is wider in diameter and the mean pore size gradually decreases across the membrane thickness giving the membranes greater porosity as well as improved fluid flow. SEM images of these two membrane pore structures are shown in Chapter 1, Figure 1.13. It was hypothesised that the wider pore inlet would produce lower elongation shear and the higher porosity could reduce the differential pressure across the membrane. This could subsequently lower irreversible product damage and improve transmission. The lower flux of 0.1 $mL/min.cm^2$ was applied in this experiment to ensure molecular backbone breakage was not associated to elongational forces imposed by high fluxes.

The results (Table 4.3) showed higher DNA transmission and lower molecular degradation when PES membranes were applied. These results suggest that pore geometry is an important aspect to be considered when filtering large circular DNA vectors. Possibly the improved fluid flow of asymmetrical pore membranes is a critical factor for enhancing transmission and retaining integrity. This is in agreement with Larson et al. (2006) where extension of linear dsDNA molecules was influenced by the elongational shear rate of different microfunnel geometries. Aside from testing different membranes, improving the performance of filtration through buffer modifications will be discussed in the next section.

Table 4.3: Filtration of the 72 kb vector at a flux of 0.1 mL/min.cm^2 using combinations of PVDF and PES membranes.

Filtration process	DNA transmission per filtration pass (%)	Cumulative DNA retained (%)	Relative DNA integrity	Total product loss (%)
Feed	–	–	1.00	–
First pass: PVDF membrane	70	30	0.75	47
Second pass: PDVF membrane	87	43	0.65	60
Second pass: PES membrane	94	37	0.75	50
Feed	–	–	1.00	–
First pass: PES membrane	90	10	0.99	10
Second pass: PES membrane	92	18	0.86	28
Second pass: PVDF membrane	81	29	0.59	57

4.5 Effect of Formulation

4.5.1 Addition of NaCl

DNA molecules in close proximity can be highly rigid due to intermolecular electrostatic repulsions. As seen in earlier observations, a high percentage of circular DNA was retained by the membrane filter. Intermolecular electrostatic repulsion could be inhibiting the plasmids from deforming quickly and aligning in the liquid flow direction and therefore causing the retention observed in the earlier experiments. Filterability can be enhanced by improving the flexibility of these molecules through reducing molecular repulsion to facilitate deformation and minimise entanglements of the backbone strands. To test the hypothesis that filterability of large constructs could be improved through reduction of molecular repulsion, the effect of increased counterions in the formulation buffer was examined.

The addition of mono- or divalent counterions has been shown to neutralise the repulsion of the phosphate anions on the DNA backbone to promote structural stabilisation (Bloomfield, 1996; Lengsfeld et al., 2001; Marzilli et al., 1980). Since it is common to have NaCl at a concentration from 100 to 200 mM in DNA vaccine formulations (Volkin et al., 2002; Volkin et al., 2004), plasmid DNA solutions in 150 mM NaCl were prepared. The two larger DNA vectors – p5180 (72 kb) and p5176 (116 kb) were used in these filtration experiments. PVDF membrane filters of 0.22 μm pore size were used and the filtrations were performed at a constant flux of 2.3 $mL/min.cm^2$.

As shown in Figure 4.10, in the presence of 150 mM NaCl, the transmission increased by 47 and 11% for the 72 and 116 kb vectors respectively. These results are in agreement to Higuchi et al. (1997) who also reported higher transmission of circular DNA molecules in the presence of NaCl. Since the addition of NaCl improved the filtration performance, cationic polymers which could condense the DNA structures have the possibility of further reducing losses.

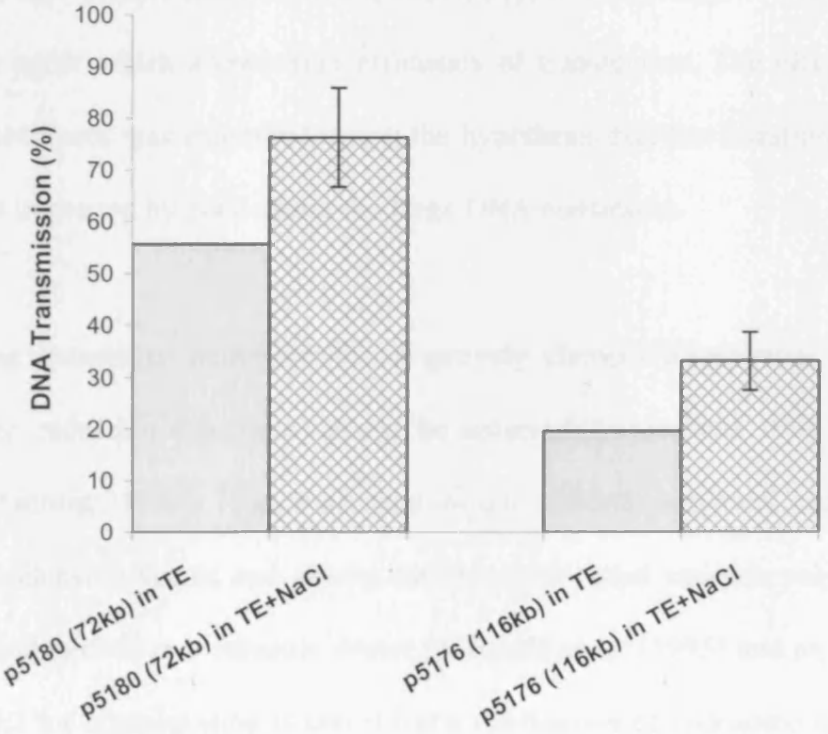

Figure 4.10: Effect of formulating buffer on product transmission. Solutions of p5180 (72 kb) and p5176 (116 kb) prepared in TE buffer plus 150 mM NaCl were filtered through 0.22 μm pore size PVDF membranes at a flux of 2.3 mL/min.cm^2. The feed concentration was 30 μg/mL.

4.5.2 Complexation with Condensing Agents

In this study, the sterile filtration of the DNA complexed with transfection agents was investigated. The complexes tested were polyethylenimine-DNA (PEI/DNA) and lipofectin-integrin binding peptide-DNA (LID). These formulations were selected because of the low-cost and availability of polyethylenimine (PEI) which is highly amenable for complexation to plasmid DNA in large scale processes and in contrast, LID complexes is an example of a sophisticated targeted and defined gene delivery agent which allows high efficiency of transfection. The effect of filtering DNA complexes was examined to test the hypothesis that the filtration performance could be improved by condensing the large DNA constructs.

By using cations to neutralise the negatively charged phosphates on the DNA backbone, reduction in particle size can be achieved (Bloomfield, 1991 Dunlap et al., 1997; Manning, 1980). High molecular weight cationic polymers can be effective DNA condensing agents and among the frequently used cationic polymers is PEI. PEI was identified as a versatile vector by Bousif et al. (1995) and an advantage of using PEI for complexation is that it has a mechanism of endosome disruption that does not need endosome-lytic agents for transfection (Garlick et al., 2005; Merlin et al., 2002). Since then, a number of researchers have worked on optimising the transfection efficiency of PEI/DNA complexes by looking into parameters such as polymer concentration (Lambert et al., 1996), molecular weight (Godbey et al, 1999a), N/P ratios (Boletta et al., 1997), branch or linear polymer (Dunlap et al., 1997) and packing efficiency (Godbey et al, 1999b).

For gene therapy applications, a difficulty of efficient transfection lies in the recognition of desired cells. However, through the incorporation of targeting elements that binds effectively to cell integrins (which are cell surface glycoproteins), transfection efficiency are enhanced (Hart et al., 1995). The use of integrin-targeting peptides has shown effective delivery of genes to restricted range of cells expressing the target integrin (Hart et al., 1995, Harbottle et al., 1998; White et al., 2003). In this method, the cationic lipid used was lipofectin which composed of DOTMA and the co-lipid DOPE while the peptide consisted of a lysine-chain. The individual components in LID complexes are combined through electrostatic interactions and the DNA is expected to be encapsulated within the particle (Sarkar et al., 2004).

Formulations using BAC p5180 (72 kb) were prepared with the help of colleagues – Andrew Wu (PEI/DNA complexes) and Supti Sarkar (LID particles). Before performing the filtrations, size of the formulated samples was measured using the Malvern Zetasizer. All size measurements were conducted at 25°C and taken over a period of 50–60 minutes to check for aggregation. Tendency to aggregation of the LID particles has been previously observed in NaCl, PBS and HEPES buffers, and hence ultra pure sterile filtered water was used in this formulation (Sarkar, S., Department of Biochemical Engineering, UCL, personal communication; Sarkar et al., 2003; Sarkar, 2005). Then, the DNA complexes were filtered at a flux of 0.2 mL/min.cm^2. The particle sizes of filtered samples were analysed again to examine any changes in size and additionally to determine product transmission. DNA concentrations were confirmed using UV spectrophotometry in which A_{260} readings was taken before and after filtration. The data showed that there was no free DNA in

both formulations. Sarkar, S. (2005) reported that no greater observed compaction on increasing N/P charge ratio from +4 to +10 was observed and the average size of particles decreased with the increasing plasmid size. Therefore, the N/P charge ratio applied was +10.

Laser particle size analysis of PEI/DNA and LID complexes indicated average diameters of 140 ± 14 and 221 ± 22 nm respectively (Figures 4.11 and 4.12). Aggregation of particles for both formulations was not detected over the observation period. The average size of the LID particles containing the 72 kb BAC analysed with the Zetasizer was larger than published results observed through atomic force microscopy (AFM) by White et al. (2003). The difference could be due to the drying of samples on mica surfaces in preparation for AFM. Dried particles may have contributed to smaller diameters.

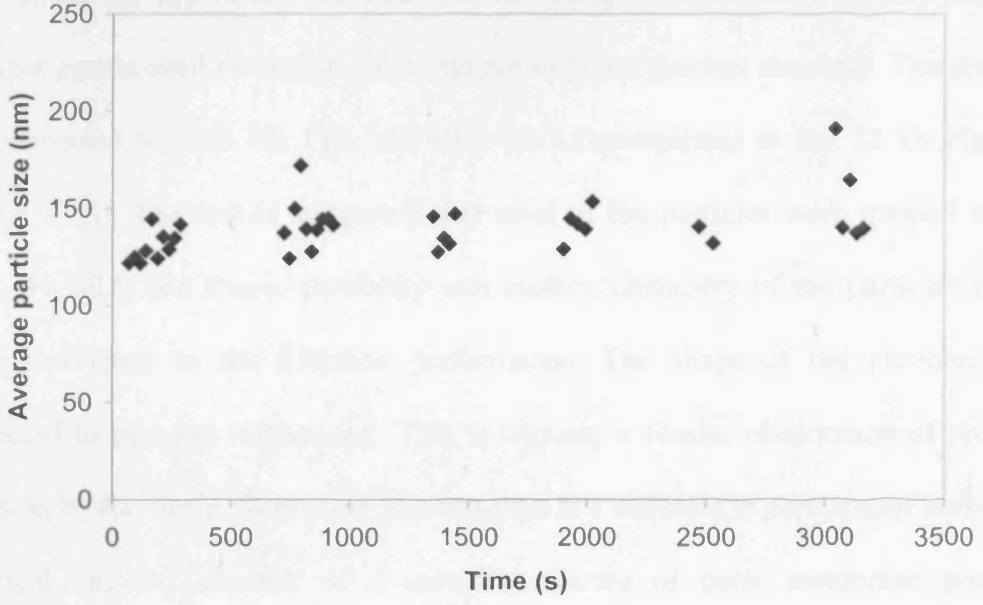

Figure 4.11: The particle size measurement of the PEI/DNA complexes over a 60 minute period. Average particle diameter was determined to be around 140 ± 14 nm.

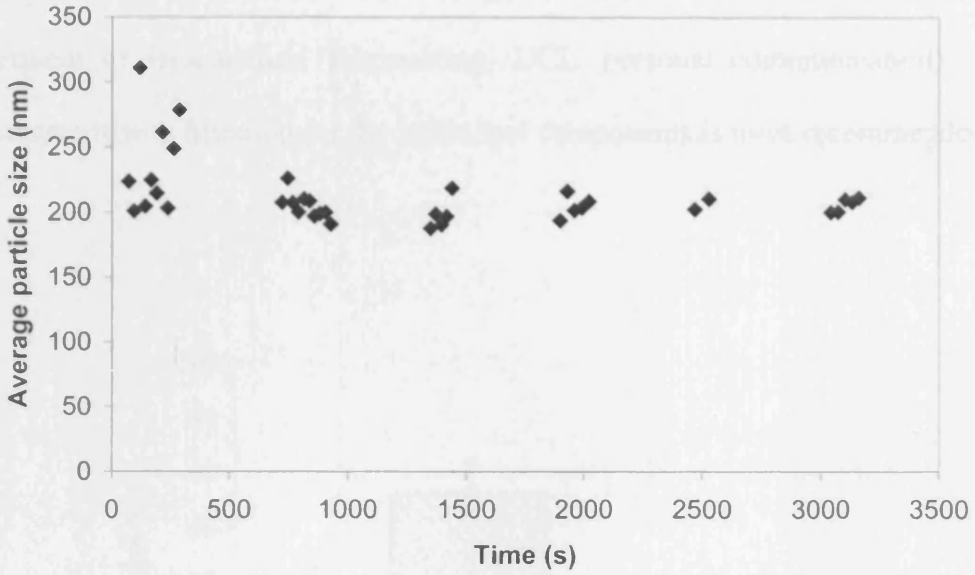

Figure 4.12: The particle size measurement of the LID complexes over a 60 minute period. Average particle diameter was determined to be 221 ± 22 nm.

After filtration, the results showed that the complexation with PEI and LI, two different agents used for transfection, did not improve product recovery. The product loss increased to 79% for PEI and 99% for LI complexed to the 72 kb plasmid (Figure 4.13). The results suggested that most of the particles were trapped in the pores. Possibly the shape, flexibility and surface chemistry of the particles had a strong influence in the filtration performance. The shape of the particles was suspected to be most influencing. This is because a similar observation of product retention by the sterile filters was also reported in a different experiment of involving spherical vesicles consists of a complex mixture of outer membrane proteins (Mukhopadhyay, T., Department of Biochemical Engineering, UCL, personal communication). Furthermore, when the individual polymer components were filtered separately, significant loss was not observed (Bos et al, 2000; Sarkar,

Department of Biochemical Engineering, UCL, personal communication; Wu, Department of Biochemical Engineering, UCL, personal communication). Thus, separate sterilising filtration for the individual components is most recommended.

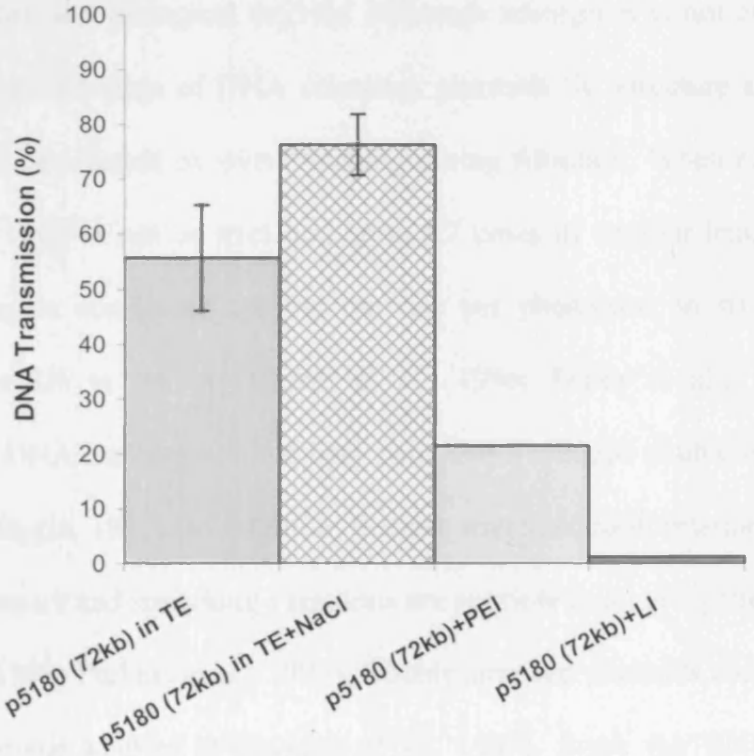

Figure 4.13: Effect of formulating buffer on product transmission. Solutions of p5180 (72 kb) in the presence of 150 mM NaCl, complexed with PEI and LI filtered through 0.22 μm pore size PVDF membranes at a flux of 0.2 mL/min.cm^2. The feed concentration was 30 μg/mL. For formulations in TE and NaCl, results shown are the average of two experiments, error bars indicate standard deviation.

4.6 Stability of DNA Vectors after Filtration

SC plasmids are an important component of gene based drugs. A study conducted by Tumanova et al. (2005) have shown that differences in purification methods can produce subtle variations in plasmid tertiary structure which subsequently influenced plasmid stability and biological activity. Although adsorption is not expected to be prevailing in the filtration of DNA solutions, plasmids SC structure and molecular stability could be affected by overstretching during filtration. When external forces are applied, a dsDNA can be stretched up to 1.7 times its contour length and above that, stretching is non-linear causing the rise per phosphate on its backbone to increase from 3.4 to 5.8 Å (Cluzel et al., 1996; Smith et al., 1996). These overstretched DNA has highly tilted base pairs and a reduced double helix diameter (Marko and Siggia, 1997). In addition, distinct stretched conformation shapes with differing dynamics and stretching variations are possible in an elongational flow (Hu and Perkins, 1999; Perkins et al., 1997). Double stranded plasmids nicked have also known to become knotted (Middaugh et al., 1997). Since the filtration process engages molecular deformation involving various stretching conformations, the stability of filtered DNA vectors was investigated to ensure that they were of the same quality as prior to filtration.

The DNA stability was assessed by measurement of the percent of SC plasmid after heat exposure at 60°C. It was hypothesized that DNA molecules with unstable conformations are expected to show less thermal stability. The use of accelerated stability studies by incubation at 50–60°C for the evaluation of degradation of plasmid DNA has been described by Evans et al. (1999) for the study of free radical

oxidation and depurination in pharmaceutical formulations and by Tumanova et al. (2005) for assessing the thermal stability of plasmids purified by various chromatographic techniques. Heat induced degradation can lead to irreversible inactivation due to depurination, deamination of cytosine residues, destruction of deoxyribose residues or hydrolytic cleavage of pyrimidine-glycosyl bonds (Lindahl and Nyberg, 1972). In this experiment, plasmid pQR150 (20 kb) was filtered at a flux of 2.3 mL/min.cm^2 using PVDF and PES membranes. Plasmids which have permeated the membranes were then chemically degraded by incubation in a water bath at 60°C for 2, 4 and 24 hours to examine if there were differences in stability.

Based on the gel densitometry scanning analysis (Figure 4.14), substantial differences between the non-filtered control samples and the filtered samples were not observed. There was also no considerable difference between samples filtered with either the PVDF or the PES membranes. The result confirms that the SC DNA molecules elongated during membrane permeation were able to revert back to their original topology when the stretching forces were relaxed in agreement with observations of linear dsDNA stretching by Strick et al. (1996).

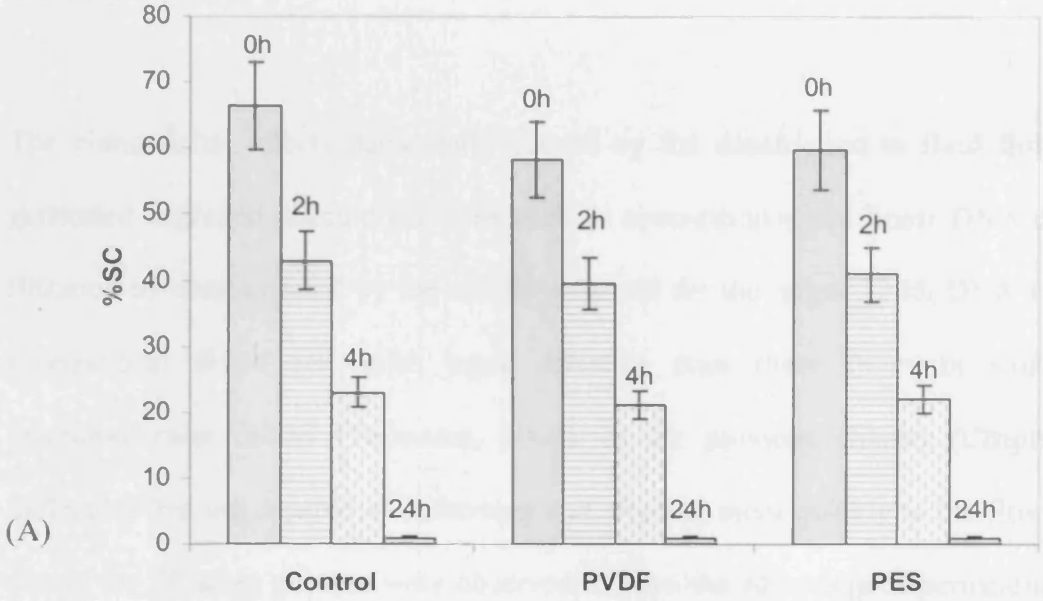

(A)

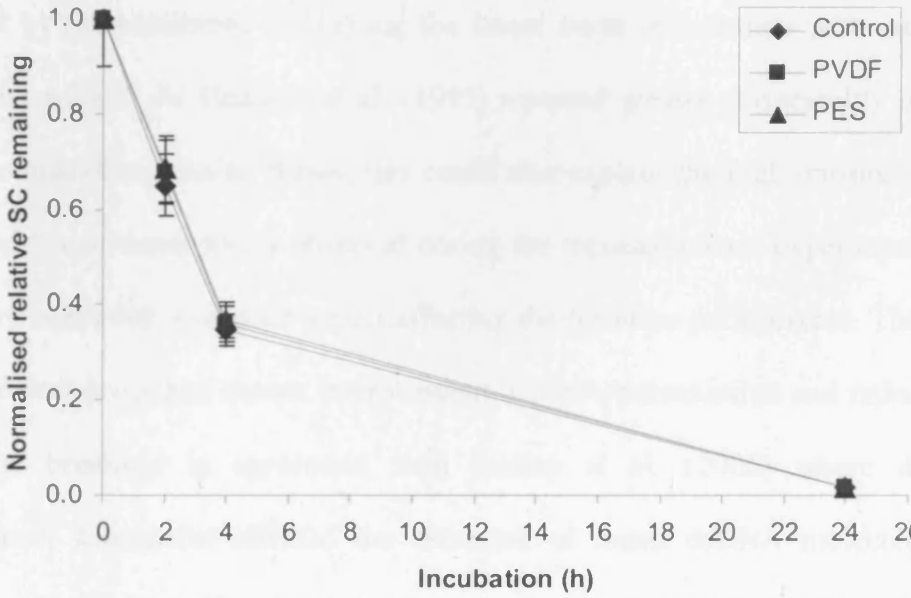

(B)

Figure 4.14: Stability of plasmid pQR150 (20 kb). All samples were subjected to degradation at 60°C for 0, 2, 4 and 24 hours. Analysis performed using gel densitometry scanning. (A) Percentage of SC pQR150 (20 kb) plasmid in non-filtered feed control and filtered samples through 0.22 μm PVDF membrane and 0.2 μm PES membrane. (B) Normalised data from (A) showing relative SC plasmid in non-filtered control (◆) and samples filtered with PVDF (■) and PES (▲).

4.7 Conclusion

The elongational effects particularly caused by the constriction to fluid flow had generated degraded plasmid isoforms such as open-circular and linear DNA during filtration as demonstrated by the results observed for the larger 72 kb DNA vector. Elongational flows are much more effective than shear flows in stretching macromolecular chains (Termonia, 2000). In the previous chapter (Chapter 3), molecules that are capable of deforming and aligning more quickly in the flow field during the filtration process were observed to have the advantage of permeating the membrane and those that do not elongate sufficiently in the flow direction were retained by the membrane explaining the linear trend of retention with increasing molecular weight. As Hirasaki et al. (1995) reported greater permeability of linear DNA compared to circular forms, this could also explain the high transmissions of degraded linear vector forms observed during the repeated passes experiments. Pore geometry is another important aspect affecting the filtration performance. The use of asymmetrical pores had shown improvement in DNA transmission and reduction of backbone breakage in agreement with Larson et al. (2006) where different microfunnel geometries affected the extension of linear dsDNA molecules. The addition of 150mM NaCl enhanced to some extent the filterability of 72 and 116 kb vectors. The added counterions had reduced molecular repulsion to facilitate deformation. By contrast, complexation with PEI or LI did not improve product recovery. The shape of the particles was suspected to have a strong influence in the filtration performance. The stability of naked plasmid DNA was not affected after filtration.

The pressure driven syringe system applied here had the advantage of using very low volume for high-throughput testing. Effects of different operating condition, membrane type, chemical environments, complexation agents and so forth can be determined rapidly. This is very beneficial as a process can be designed early in the drug development stage and regulatory requirements can be met without requiring large quantities of samples.

Chapter 5 – Constant Pressure Microfiltration

5.1 Introduction

In microfiltration or ultrafiltration, the fouling phenomenon can be due to adsorption or particle deposition which can take place inside the pores and/or on the outer layer of the membrane (Roorda and van der Graaf, 2000). The build up of retained materials which clogs the membrane can increase resistance to filtration and cause the permeate flux to decline over time. DNA molecules and other particles in the solution brought to the membrane surface by the permeate flow can be retained by the membrane during a dead-end filtration operation. Since plasmids with 5–30 kb have molecular weights $\geq$ 500–1000 times greater than typical therapeutic proteins (Table 3.1; Maa et al., 1998), it is important to assess the effects of increasing DNA concentration and plasmid size on the performance of the membrane filter.

In an earlier chapter (Chapter 3), confocal microscopy images (Figures 3.5 and 3.6) showed surface views of PicoGreen-stained membrane filters applied in the filtration of solutions containing the 20 and 72 kb DNA vectors. These images clearly indicated deposition of DNA vectors on the membrane surface and within the pore structures. Chapters 3 and 4 reported transmission and degradation of DNA vectors in which experiments were conducted using a constant filtration flux setup. The

constant filtration flux experiments are useful for obtaining information on product properties and require only ≤ 1 mL of sample. Constant transmembrane pressure experiments can provide information on membrane capacity using ≤ 10 mL of samples and facilitate the scale-up of a membrane filtration process. Details of the filtration setup can be found in Chapter 2, section 2.1.2. PVDF membranes with 0.22 μm pore size were used in the experiments to investigate the effects of DNA concentration, plasmid size and operating pressure.

Darcy's Law has been the basis for different derivation of filtration laws and equations (Roorda and van der Graaf, 2000). Widely applied membrane fouling models include pore blockage, gradual pore constriction, cake filtration and intermediate pore blockage (Bowen et al., 1995; Hermia, 1982; Laska et al., 2005). The gradual pore constriction model is a simple approach to determine the capacity of a membrane filter and to size normal flow filters where cumulative filtrate volume is measured through a small test membrane filter until the flow rate drops to about 10% of its initial value. Application of the linearised form allows shorter filtration times to be used in order that data can be extrapolated to longer filtration times (Badmington et al., 1995; Honig and Schwartz, 1997):

$$\frac{t}{V} = \frac{1}{Q_0} + \left(\frac{1}{V_{\max}}\right) t \qquad [5.1]$$

where V is the total filtrate volume collected over time t and Q_0 is the initial volumetric filtrate flow rate and V_{max} is the maximum fluid volume that can be filtered before the membrane is completely plugged. V_{max} is evaluated directly from the flux decay data as the reciprocal of the slope on a plot of t/V as a function of t.

The membrane filter system capacity can be calculated using the expression for flow rate as a function of time:

$$\frac{Q}{Q_0} = \left(1 + \frac{Q_0 t}{V_{\max}}\right)^{-2} \qquad [5.2]$$

to give

$$V_{capacity} = V_{\max}\left(1 - \sqrt{\frac{Q_{\min}}{Q_0}}\right) \qquad [5.3]$$

where Q_{min} is the minimum specified flow rate.

This is a very useful method because by utilising the V_{max} and membrane capacity information obtained from a small laboratory scale device (membrane area = 1 cm^2), the performance for large scale processing modules can be estimated. However, it is important to note that although the V_{max} method is used extensively for filter sizing, membrane fouling is based on the assumption of uniform constriction of cylindrical pores. If the system demonstrates complexity in the fouling mechanism, this model may not be adequate and then other models should be explored. For instance, a common problem reported for the sterile filtration of a therapeutic protein is membrane fouling due to unspecific adsorption (Dosmar, 2004; Maa et al., 1998). An alternative mathematical model was developed by Ho and Zydney (2000) for the filtrate flux which accounts for initial fouling due to pore blockage and subsequent fouling due to the growth of a cake or deposit over these initially blocked regions.

Therefore, assessment of the applicability of the gradual pore constriction model with its linearised form was necessary prior to adopting for use throughout the study.

5.2 Effect of DNA Concentration

The purpose of this study was to evaluate the effect of increasing DNA concentration on the performance of the membrane filter and also very importantly, to evaluate the applicability of the gradual pore constriction model to this filtration system. Filtrations of plasmids gWIZ (6 kb) and pQR150 (20 kb) were performed using the 0.22 μm pore size PDVF membrane filters with a filtration area of 1 cm^2. DNA solutions for the feed stream were adjusted to 15, 30 and 100 μg/mL. Filtration pressure was kept constant at 30 ± 1 kPa throughout the filtration period.

Prior to performing the filtrations, the viscosity of increasing DNA concentration was examined. The viscosity of DNA in solution should increase with concentration (Cooper et al., 2003). Highly viscous DNA solution could detrimentally affect the membrane filtration operation. To build a viscosity profile, purified DNA solution containing plasmid pQR150 (20 kb) was diluted serially from 950 to 30 μg/mL and solution viscosity measurements were recorded using a cone/plate viscometer at room temperature. The viscosity increased with the increasing concentration and the increment reached a plateau around the region of 3 mPa.s (Figure 5.1). A comparison to the values reported by Cooper et al. (2003) is shown in Figure 5.1 (B).

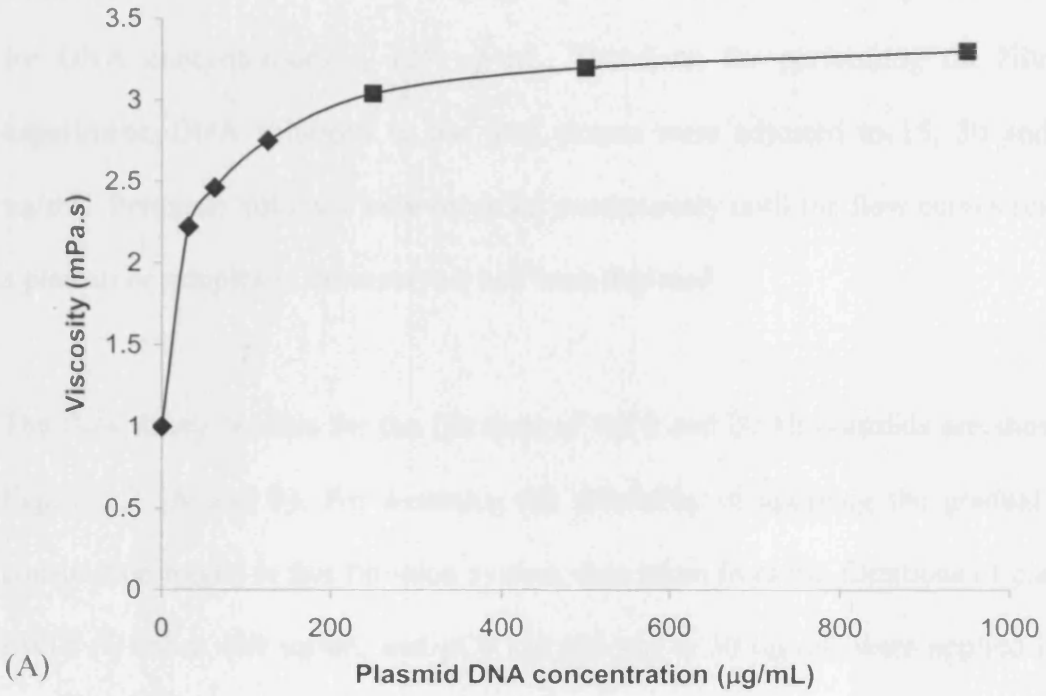

(A)

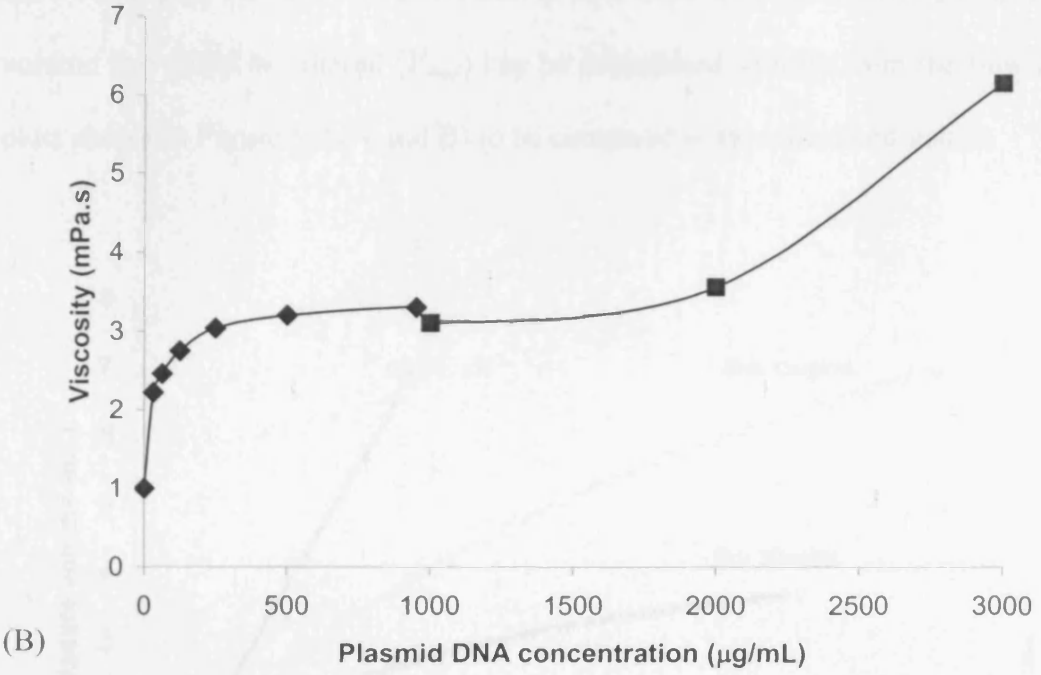

(B)

Figure 5.1: (A) Viscosity data of plasmid DNA solutions between concentrations of 30 to 950 μg/ml. Plasmid pQR150 (20kb) was used. (B) Experimental data (◆) combined with viscosity of DNA solutions obtained from data presented by Copper et al (2003) (▪).

Based on the observations above, considerable differences in viscosity were observed for DNA concentrations ≤ 125 μg/mL. Therefore, for performing the filtration experiment, DNA solutions in the feed stream were adjusted to 15, 30 and 100 μg/mL. Permeate volumes were recorded continuously until the flow curves reached a plateau or samples in the reservoir had been depleted.

The flow decay profiles for the filtration of the 6 and 20 kb plasmids are shown in Figure 5.2 (A and B). For assessing the suitability of applying the gradual pore constriction model in this filtration system, data taken from the filtrations of plasmid gWIZ (6 kb) at 100 μg/mL and pQR150 (20 kb) at 30 μg/mL were applied in the linear plot of filtration time per permeate volume versus time (up to 4 minutes) as shown in Figure 5.2 (C). These two sets of data were selected because the maximum volume that could be filtered (V_{max}) can be determined directly from the flow decay plots shown in Figure 5.2 (A and B) to be compared to the calculated values.

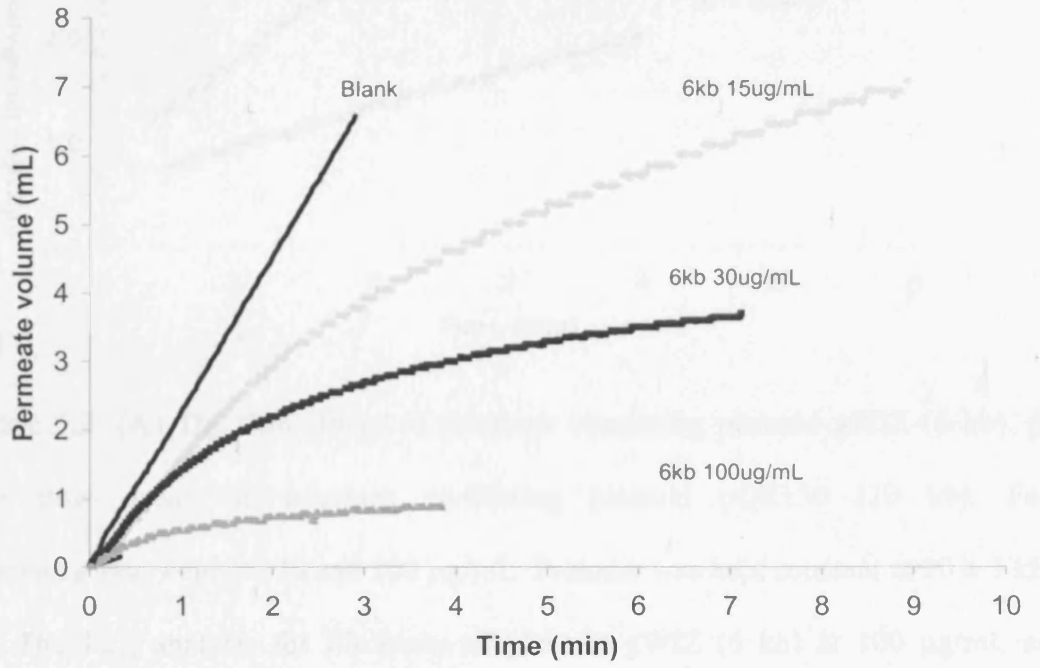

(A)

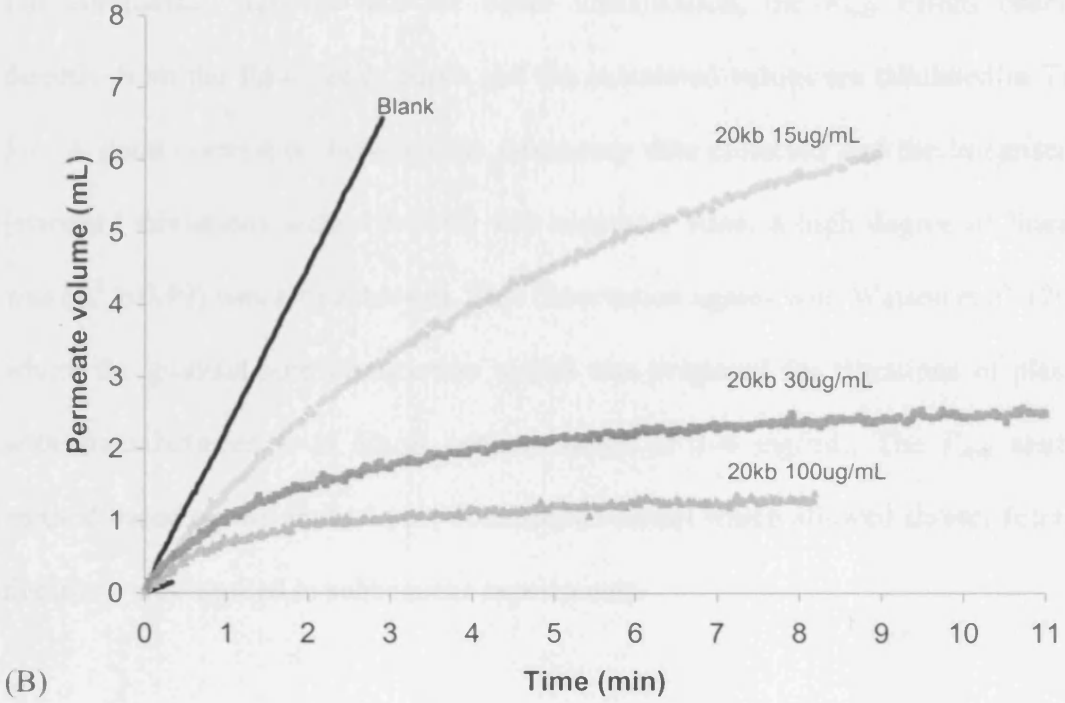

(B)

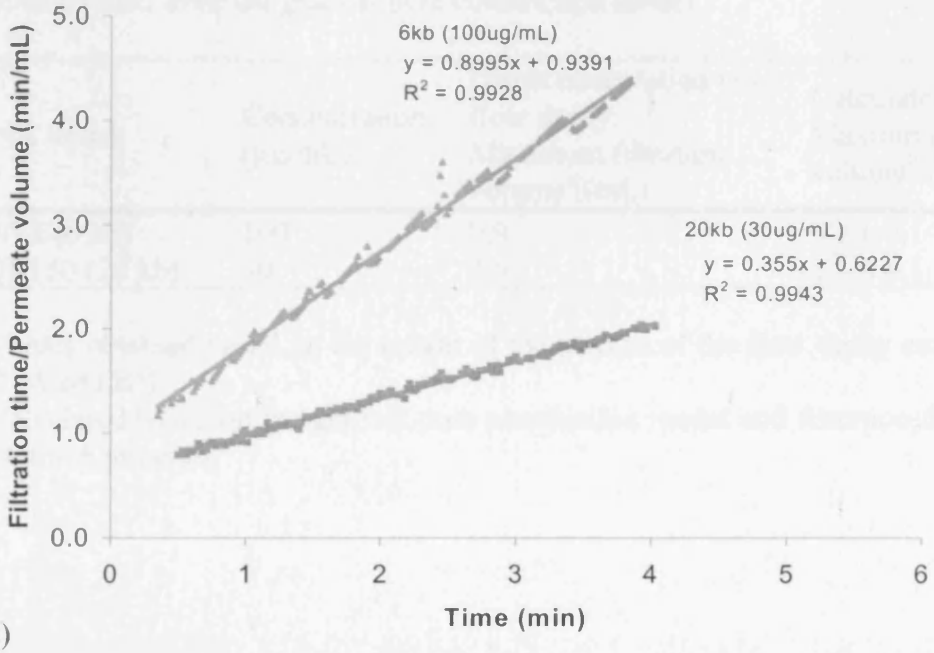

(C)

Figure 5.2: (A) The flow decay of solutions containing plasmid gWIZ (6 kb). (B) The flow decay of solutions containing plasmid pQR150 (20 kb). Feed concentrations were 15, 30 and 100 μg/mL. Pressure was kept constant at 30 ± 1 kPa. (C) The V_{max} analysis for filtrations of plasmid gWIZ (6 kb) at 100 μg/mL and pQR150 (20 kb) at 30 μg/mL.

For comparison puposes and for better visualisation, the V_{max} values observed directly from the flow decay curve and the calculated values are tabulated in Table 5.1. A good correlation between the laboratory data collected and the linearised fit (standard deviations were 10–15%) was obtained. Also, a high degree of linearity was ($R^2 \geq 0.99$) was also achieved. This observation agrees with Watson et al. (2006) where the gradual pore constriction model was proposed for filtrations of plasmid with sizes between 6–11 kb at concentrations of 2–4 mg/mL. The V_{max} analysis method based on the gradual pore constriction model which allowed shorter filtration durations was applied in subsequent experiments.

Table 5.1: Comparison of V_{max} values obtained directly from flow decay observations and calculated from the gradual pore constriction model.

DNA vector	Concentration (μg/mL)	Direct observation via flow decay: Maximum filtration volume[a] (mL)	Calculated V_{max}: Maximum filtration volume[b] (mL)
gWIZ (6 kb)	100	0.9	1.1 ± 0.1
pQR150 (20 kb)	30	2.5	2.8 ± 0.1

[a] Values obtained based on the height of the plateau of the flow decay curve (Figure 5.2 (A and B)).
[b] Calculated based on the gradual pore constriction model and filtration durations of 1, 4 and 6 minutes.

Next, for the evaluation of increasing DNA concentration on the performance of the membrane filter, the values for initial volumetric flow rate, Q_o, and V_{max} were calculated. Figure 5.3 shows the plot for initial flux (equivalent to Q_o per filtration membrane area) with respect to increasing DNA concentration. The results showed a decrease in filtration flux as feed concentration increases for the 6 and 20 kb

plasmids tested. This is not unexpected since an increase in solution viscosity from 2.2 to 2.6 mPa.s was observed for DNA concentrations ranging from 30 to 100 μg/mL (refer to Figure 5.1). The V_{max} per membrane area decreased as concentration increases suggesting a faster rate of fouling as DNA concentration increases (Figure 5.4).

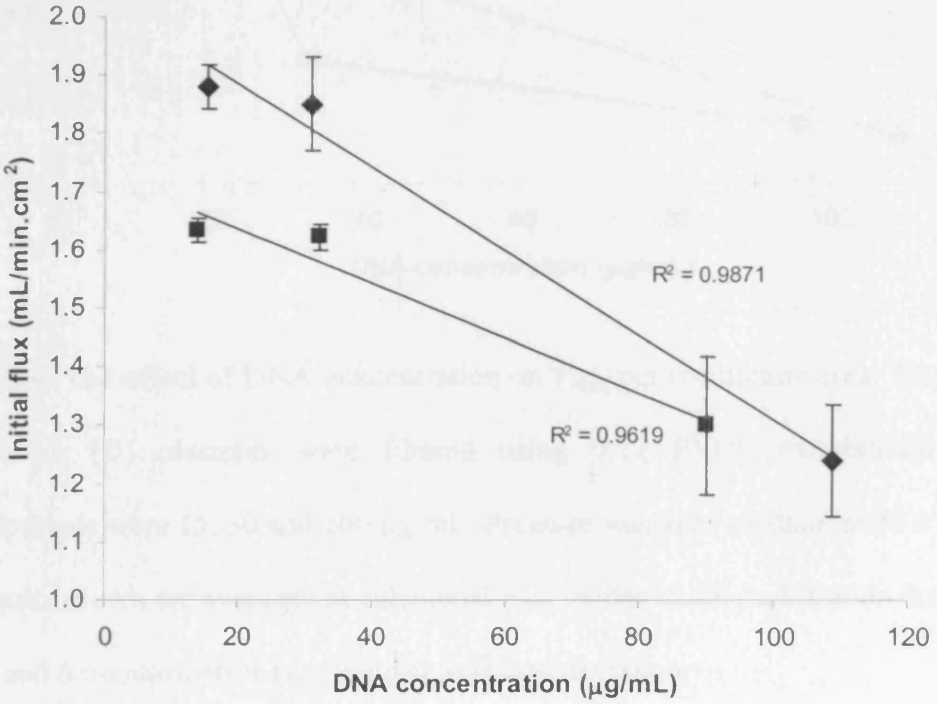

Figure 5.3: The effect of DNA concentration on initial filtration flux. The 6 (◆) and 20 kb (■) plasmids were filtered using 0.22 PVDF membranes. Feed concentrations were 15, 30 and 100 μg/mL. Pressure was kept constant at 30 ± 1 kPa. The results shown are averages of calculated initial flux values based on filtration durations of 1, 4 and 6 minutes, error bars indicate standard deviation and lines are linear regressions.

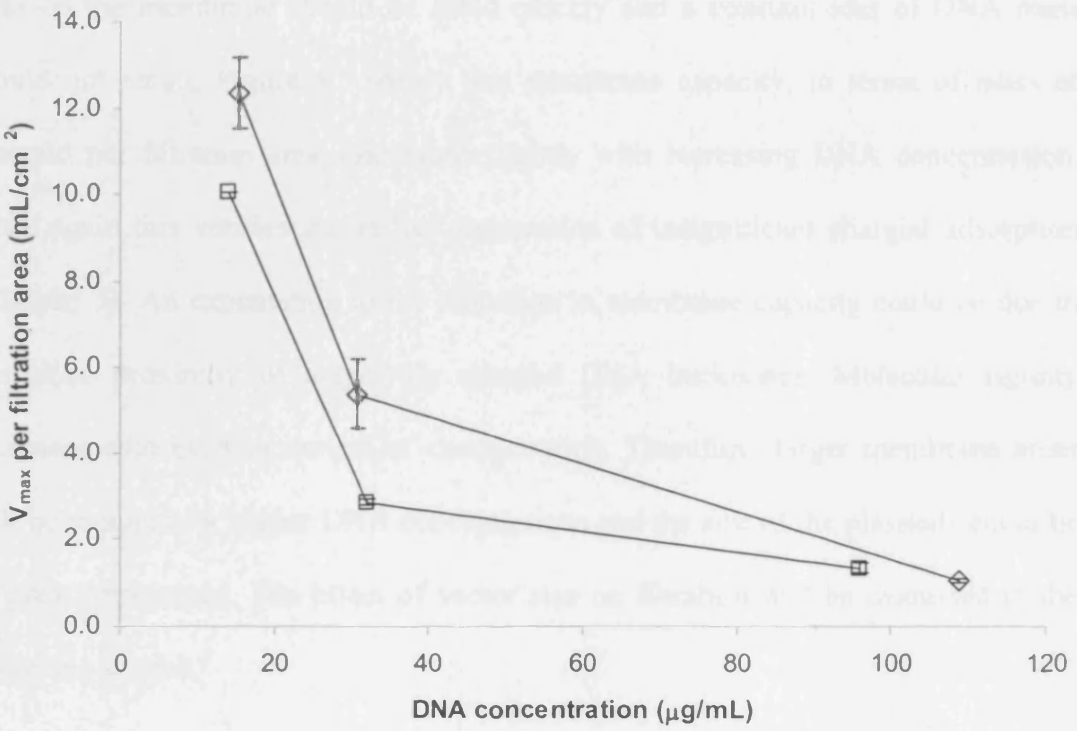

Figure 5.4: The effect of DNA concentration on V_{max} per membrane area. The 6 (◇) and 20 kb (□) plasmids were filtered using 0.22 PVDF membranes. Feed concentrations were 15, 30 and 100 μg/mL. Pressure was kept constant at 30 ± 1 kPa. The results shown are averages of calculated V_{max} values based on filtration durations of 1, 4 and 6 minutes, error bars indicate standard deviation.

A number of reports have stressed the seriousness of adsorption of biomaterials which causes significant yield loss and suggested unspecific adsorption testing needs to be a priority (e.g. Jonitz et al., 2004; Maa et al., 1998). (This phenomenon was not significant in earlier observations – Chapter 3 due to the shorter experiment times used). However, since this study entailed longer filtration durations, the data was re-examined to validate earlier interpretations. If unspecific adsorption was playing a role in hindering the filtration performance, membrane capacity could be expected to rise with an increase in concentration because the specific amount of charged binding

sites on the membrane should be filled quickly and a constant loss of DNA mass would not result. Figure 5.5 shows that membrane capacity, in terms of mass of plasmid per filtration area, decreased slightly with increasing DNA concentration. Once again this verifies the earlier observation of insignificant charged adsorption (Chapter 3). An explanation to the reduction in membrane capacity could be due to the close proximity of negatively charged DNA backbones. Molecular rigidity increases with each increment of concentration. Therefore, larger membrane areas will be required for higher DNA concentrations and the size of the plasmids could be of great importance. The effect of vector size on filtration will be discussed in the following section.

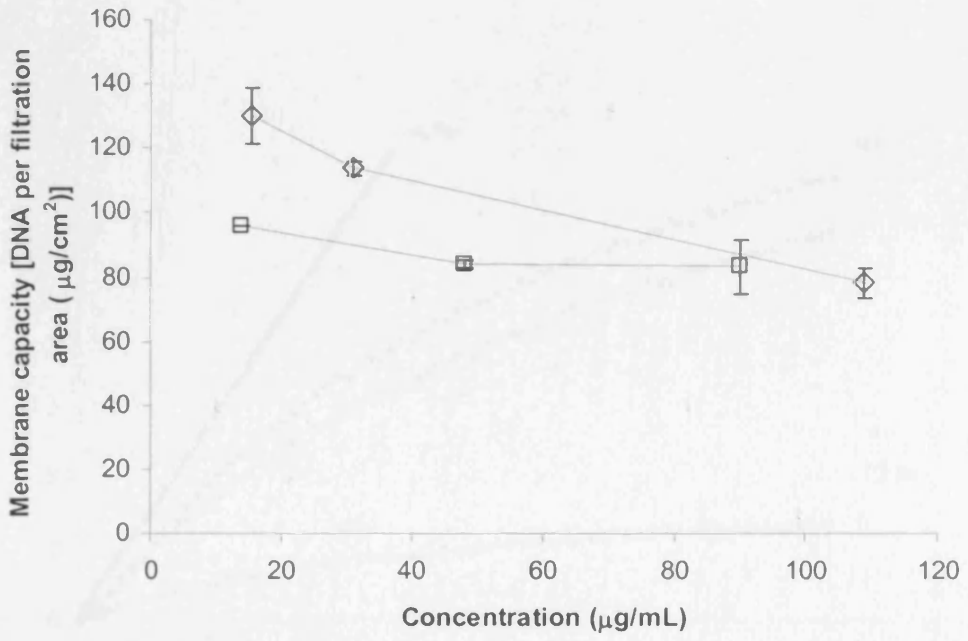

Figure 5.5: The effect of DNA concentration on membrane capacity. The 6 (◇) and 20 kb (□) plasmids were filtered using 0.22 PVDF membranes and filtration performed at 30 kPa. The results shown are averages of calculated V_{max} values based on filtration durations of 1, 4 and 6 minutes, error bars indicate standard deviation.

5.3 Effect of Vector Size

The effect of increasing DNA vector size on the performance of the membrane filter was investigated. Solutions of purified gWIZ (6 kb), pQR150 (20 kb) and p5180 (72 kb) DNA vectors were filtered using 0.22 μm pores size PVDF membranes (filtration area = 1 cm^2) at a constant pressure of 30 ± 1 kPa. Based on the flow decay profiles of the earlier experiment using various DNA concentrations (section 5.2), DNA solutions were adjusted to a concentration of 15 ± 2 μg/mL. Filtrations were allowed to run up to 7 minutes during which filtrate volume was recorded every 0.1s. The flow decay data collected is shown in Figure 5.6.

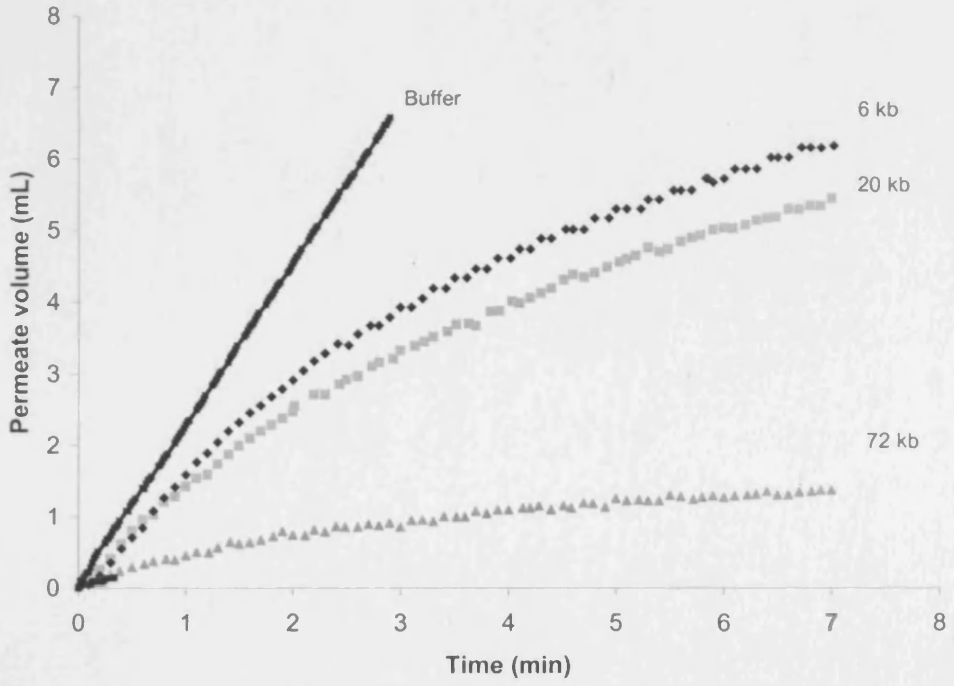

Figure 5.6: The flow decay of solutions containing gWIZ (6 kb), pQR150 (20 kb) and p5180 (72 kb). Feed concentration was 15 ± 2 μg/mL. Filtrations were performed at 30 ± 1 kPa.

The collected data was analysed using the V_{max} analysis method based on the gradual pore constriction model and Table 5.2 shows the V_{max} and Q_o values calculated for the 6, 20 and 72 kb vectors. These values were then applied in the plots shown in Figures 5.7 and 5.8. The results showed a decrease in initial permeate flux as well as V_{max} per membrane area for the increasing vector size tested. The decrease in flux was likely to be due to the increase in viscosity with molecular size and the decreasing V_{max} values show that membrane fouling increased with increasing molecular weight.

Table 5.2: V_{max} and Q_o calculated for filtration of the 6, 20 and 72 kb DNA vectors.

DNA vector	V_{max} (mL)	Q_o (mL/min)
gWIZ (6 kb)	11	2.0
pQR150 (20 kb)	10	1.6
p5180 (72 kb)	2	0.6

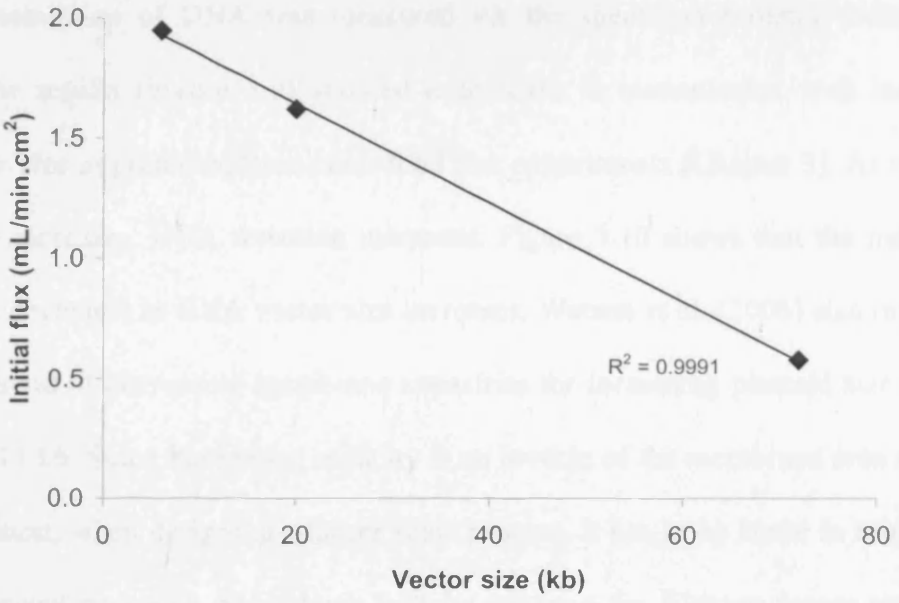

Figure 5.7: The effect of vector size on initial flux. Solutions of gWIZ (6 kb), pQR150 (20 kb) and p5180 (72 kb) filtered at 30 ± 1 kPa. Feed concentration was 15 ± 2 μg/mL.

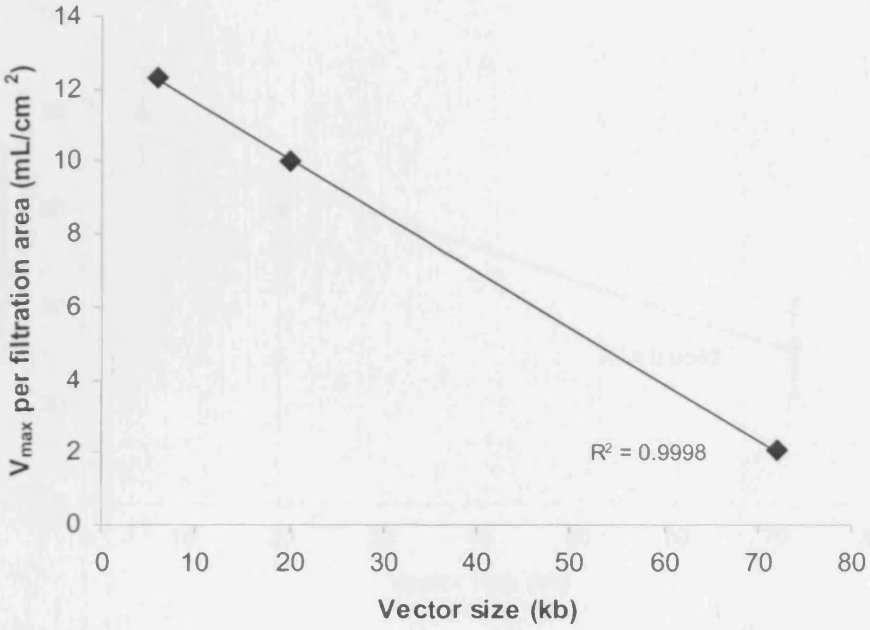

Figure 5.8: The effect of vector size on V_{max}. Solutions of gWIZ (6 kb), pQR150 (20 kb) and p5180 (72 kb) filtered at 30 ± 1 kPa. Feed concentration was 15 ± 2 μg/mL.

The transmission of DNA was measured via the spectrophotometry technique at A_{260}. The results (Figure 5.9) showed a decrease in transmission with increasing molecule size as predicted from controlled flux experiments (Chapter 3). As radius of gyration increases, DNA retention increases. Figure 5.10 shows that the membrane capacity decreases as DNA vector size increases. Watson et al. (2006) also reported a similar trend of decreasing membrane capacities for increasing plasmid size ranging from 5–11 kb. Since membrane capacity is an inverse of the membrane area required for filtration, when designing a larger scale process, it has to be borne in mind that a greater membrane area per volume will be required for filtering larger size DNA vectors of the same concentration.

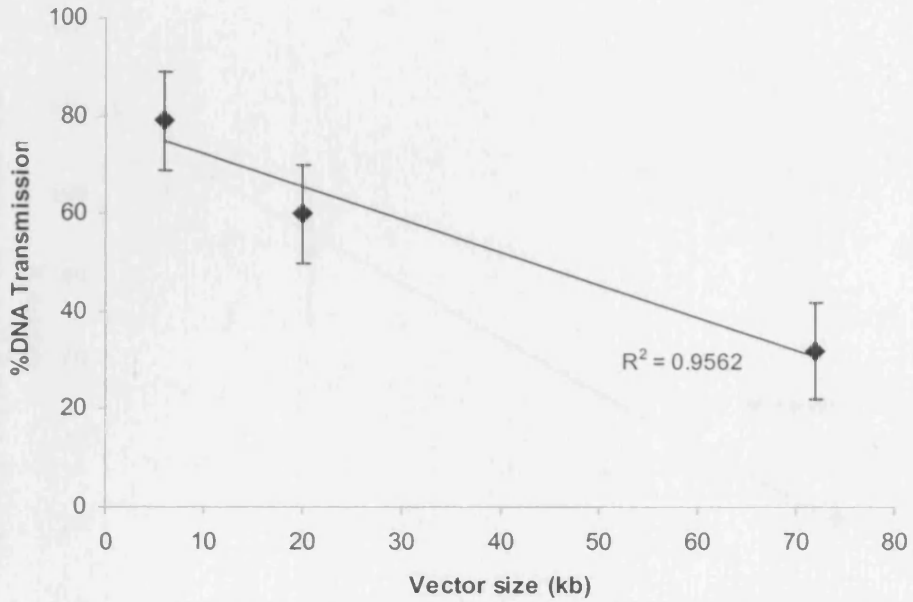

Figure 5.9: Transmission of gWIZ (6 kb), pQR150 (20 kb) and p5180 (72 kb) filtered at 30 ± 1 kPa. Feed concentration was 15 ± 2 μg/mL. The results shown are based on an average of two sets of spectrophotometry measurements, error bars indicate standard deviation and lines are linear regressions.

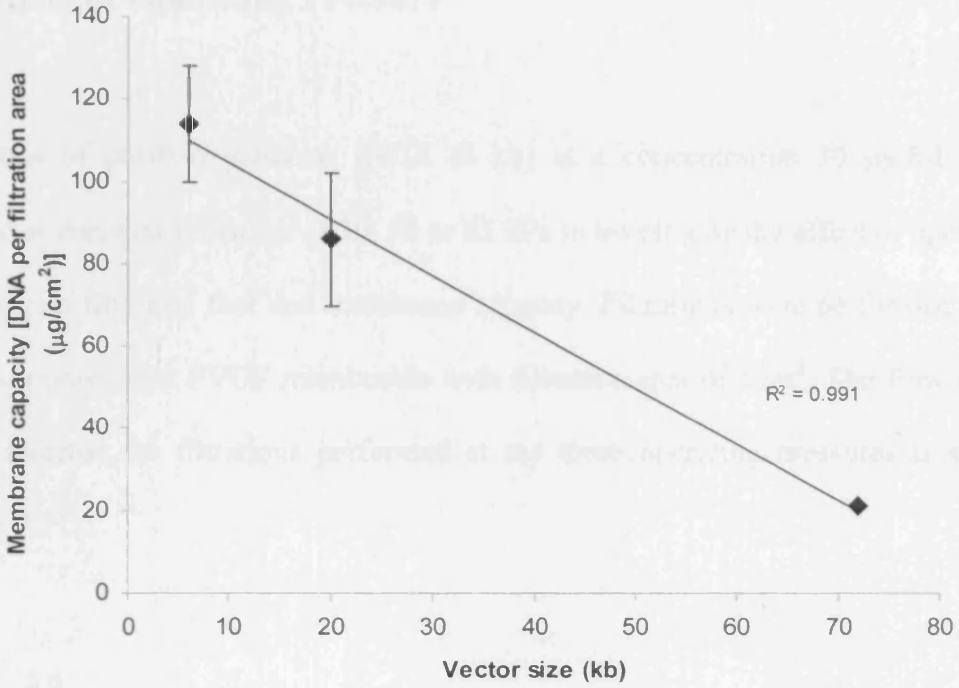

Figure 5.10: The effect of vector size on membrane capacity. Filtrations were performed at 30 ± 1 kPa. Feed concentrations were 15 ± 2 µg/mL. The results shown are based on an average of two sets of spectrophotometry measurements, error bars indicate standard deviation and lines are linear regressions.

5.4 Effect of Operating Pressure

Solutions of purified plasmids gWIZ (6 kb) at a concentration 30 μg/mL were filtered at constant pressures of 30, 50 or 65 kPa to investigate the effect of operating pressure on filtration flux and membrane capacity. Filtrations were performed using 0.22 μm pores size PVDF membranes with filtration area of 1cm^2. The flow decay data collected for filtrations performed at the three operating pressures is shown Figure 5.11.

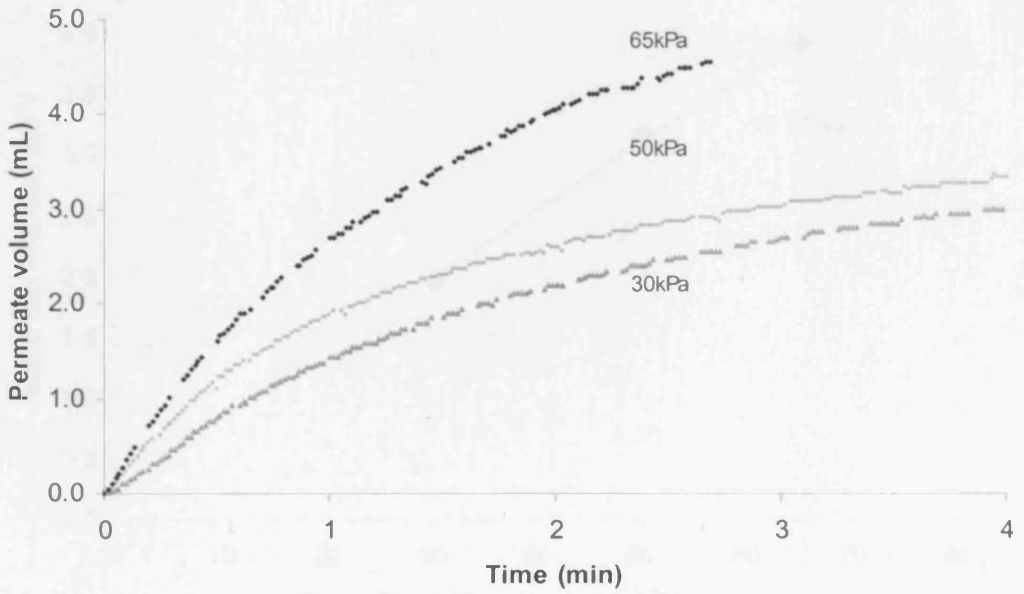

Figure 5.11: The flow decay of solutions containing plasmid gWIZ (6 kb). Feed concentration was 30 ± 2 μg/mL. Filtrations were performed at 30, 50 and 65 kPa.

As expected, the initial filtration flux increased proportionally with operating pressure (Figure 5.12). Figure 5.13 shows V_{max} per membrane area decreases as operating pressure increases indicating that less volume can be filtered at higher pressures due to greater fouling rates. The DNA transmission results determined via spectrophotometry at A_{260} (Figure 5.14) confirmed that a greater percentage of plasmid was retained by the membrane at higher operating pressures. The capacity of the membrane was also observed to decrease slightly with operating pressure (Figure 5.15) suggesting pressure could be a factor affecting the filtration performance.

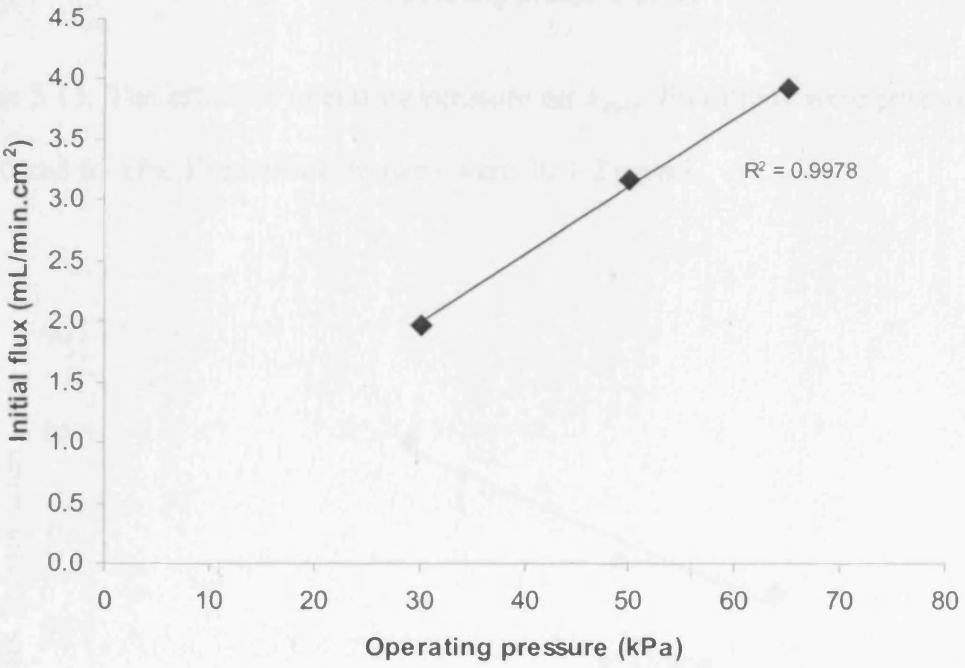

Figure 5.12: The effect of operating pressure on initial filtration flux. Filtrations were performed at 30, 50 and 65 kPa. Feed concentrations were 30 ± 2 μg/mL.

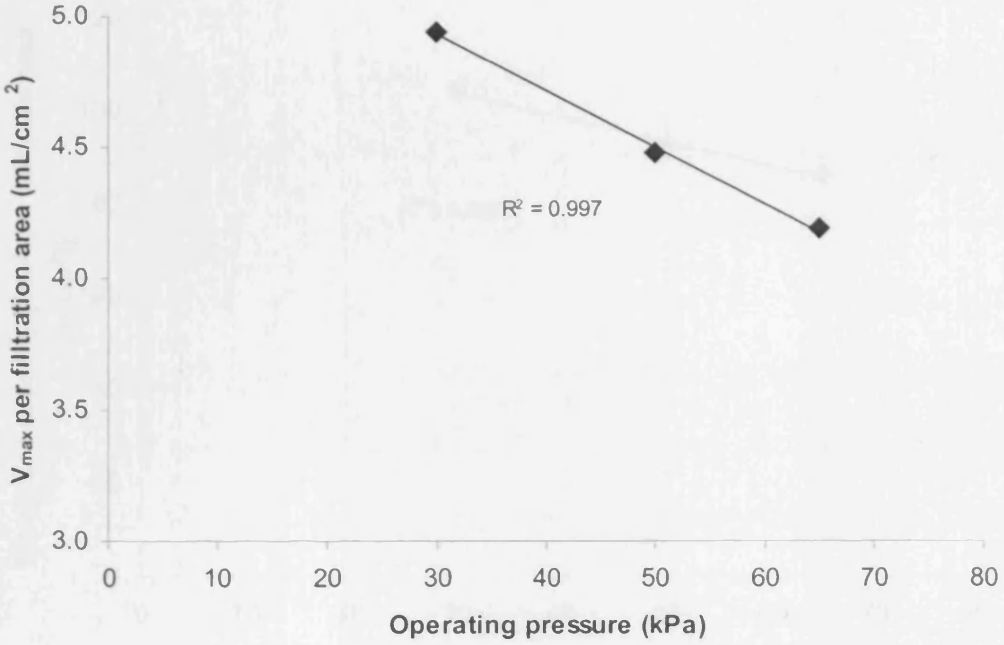

Figure 5.13: The effect of operating pressure on V_{max}. Filtrations were performed at 30. 50 and 65 kPa. Feed concentrations were 30 ± 2 µg/mL.

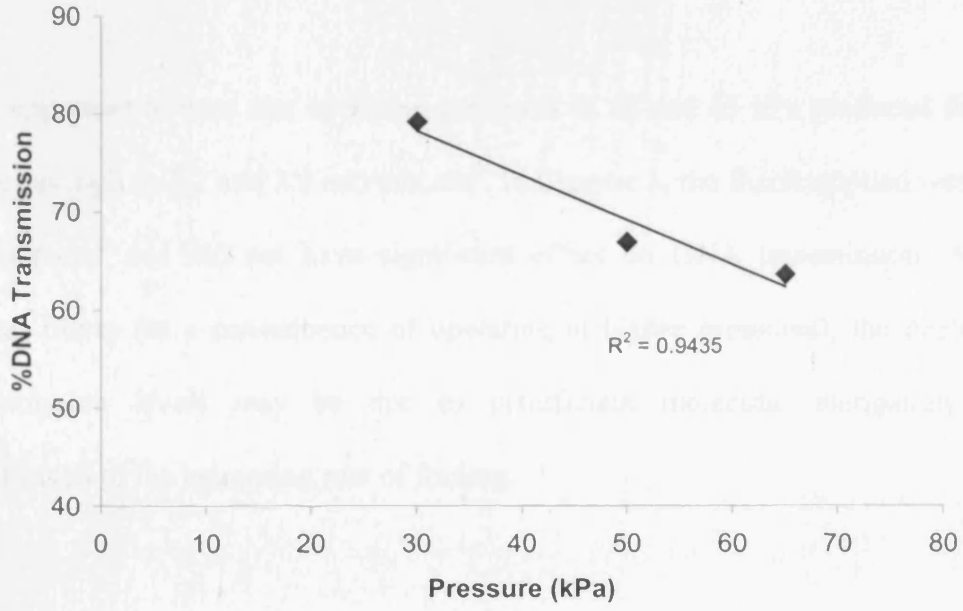

Figure 5.14: The effect of operating pressure on DNA transmission. Filtrations were performed at 30, 50 and 65 kPa. Feed concentrations were 30 ± 2 µg/mL.

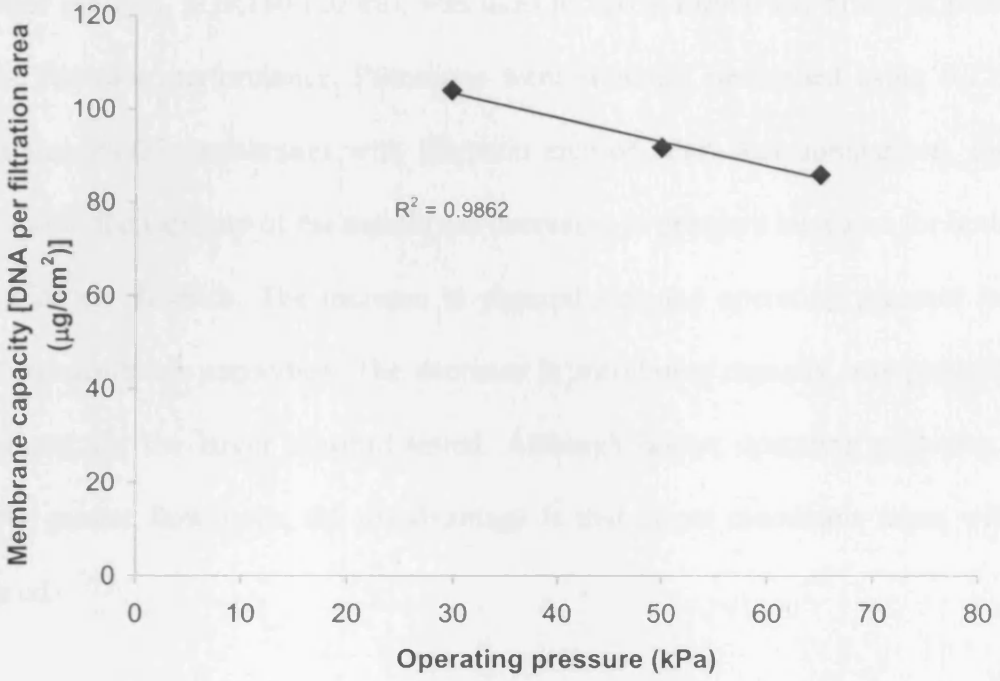

Figure 5.15: The effect of operating pressure on membrane capacity. Filtrations were performed at 30, 50 and 65 kPa. Feed concentrations were 30 ± 2 µg/mL.

It is important to note that operating pressures of 50 and 65 kPa produced filtration fluxes as high as 3.2 and 3.9 mL/min.cm^2. In Chapter 3, the fluxes applied were ≤ 2.3 mL/min.cm^2 and did not have significant effect on DNA transmission. At even higher fluxes (as a consequence of operating at higher pressures), the decrease of transmission levels may be due to insufficient molecular elongation which contributed to the increasing rate of fouling.

A larger plasmid, pQR150 (20 kb), was used to verify further the effect of pressure on the filtration performance. Filtrations were similarly performed using 0.22 μm pores size PVDF membranes with filtration area of $1cm^2$. For comparison, Figure 5.16 shows the capacity of the membrane decreases as pressure increases for both the 6 and 20 kb plasmids. The increase in plasmid size and operating pressure led to reduced membrane capacities. The decrease in membrane capacity was particularly significant for the larger plasmid tested. Although higher operating pressures can deliver greater flow rates, the disadvantage is that larger membrane areas will be required.

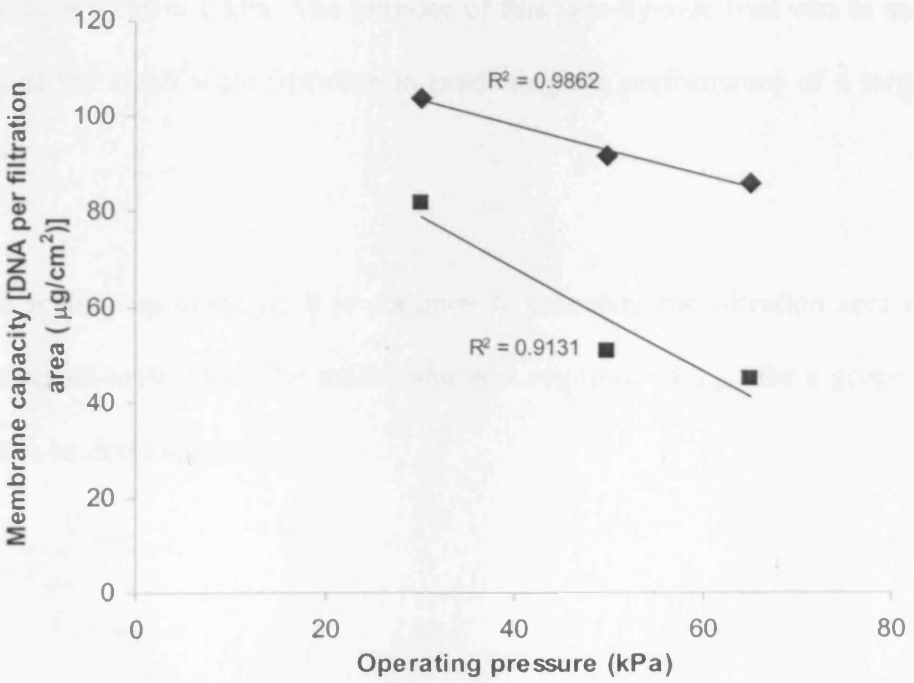

Figure 5.16: The effect of operating pressure on membrane capacity. Filtrations were performed at 30, 50 and 65 kPa. Feed concentrations containing plasmids gWIZ (6 kb) and pQR150 (20 kb) were adjusted to 30 ± 2 μg/mL.

5.5 Larger Scale Filtration

Some of the important process parameters for filtration scale-up are transmembrane pressure, filtration area, concentration and linear velocity or flux rate. In this experiment, two separate filtrations were performed using similar PVDF membrane filter but of different sizes – 13 and 25 mm diameters, corresponding to filtration areas of 1 and 4 cm^2 respectively. Since large quantities of purified plasmid solutions were not easily obtainable, there was a limitation to the scale of filtration that could be performed. Both filtrations were performed using solutions containing the 20 kb plasmid (pQR150) which were adjusted to 100 ± 2 µg/mL and were operated at the same pressure of 30 ± 1 kPa. The purpose of this side-by-side trial was to assess the accuracy of the small scale filtration in predicting the performance of a larger scale operation.

During a scaling up exercise, it is common to calculate the filtration area required based on small scale data. The membrane area required (A_{Large}) for a given volume (V_{Large}) can be determined by:

$$A_{Large} = \frac{V_{Large}}{\left(\frac{V_{max}}{A}\right)_{Small\ scale}} \qquad [5.4]$$

In this case, since a specific membrane of a larger size (4 cm^2) was used, the volume which could be filtered was calculated instead. From the experimental data, V_{max} per filtration area for the small scale filter (diameter = 13 mm and filtration area = 1 cm^2) was 1.4 mL/cm^2. It is essential to keep the biomaterial per filtration area constant when scaling up (Dosman, 2004). Therefore, the maximum volume that could be

filtered by the 25 mm diameter membrane (filtration area = 4 cm^2) using a solution of similar content was calculated to be 5.4 mL. For conducting the larger scale filtration, 10 mL of the 20 kb plasmid solution (100 ± 2 μg/mL) was used in the feed stream to ensure sufficient volume height on the top side of the membrane within the system. Permeate mass and volume was recorded continuously.

The flow decay profile is shown in Figure 5.17. When the small and large scale performances were compared, the difference in V_{max} per filtration area for the two different filtration scales was approximately 7% (Figure 5.18) and the difference in membrane capacities was approximately 6% (Figure 5.19). These are good indications that the small scale membrane (filtration area = 1 cm^2) can be used to predict the performance of a larger scale filtration (filtration area = 4 cm^2).

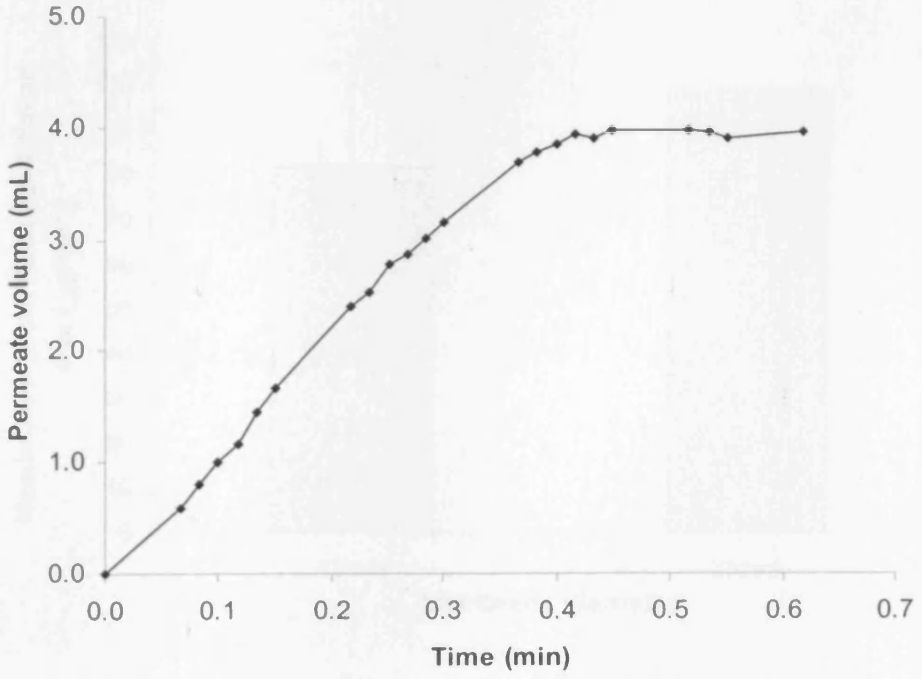

Figure 5.17: The flow decay of solutions containing plasmid pQR150 (20 kb). Feed concentration was 100 ± 2 μg/mL. Filtration was performed using a 25 mm diameter (filtration area of 4cm^2) PVDF membrane at 30 ± 1 kPa.

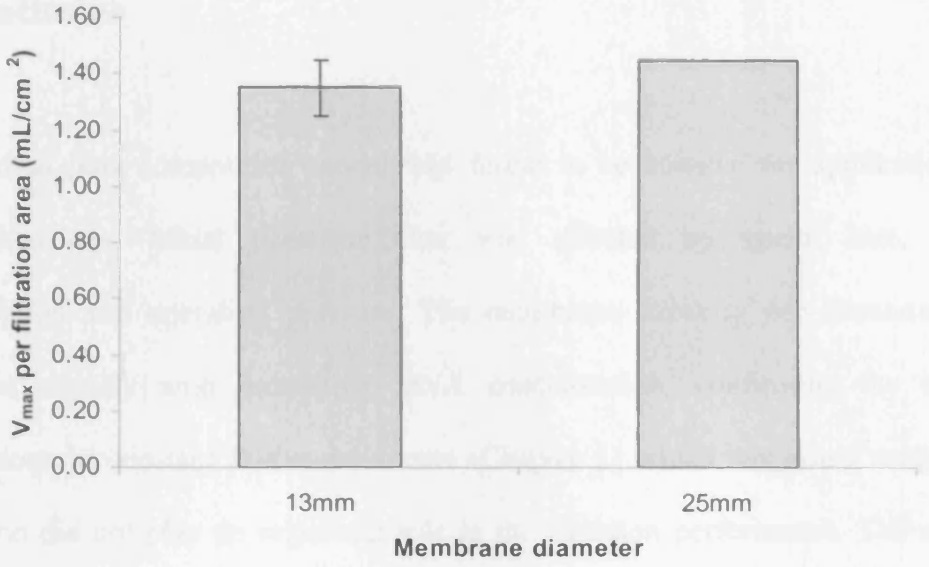

Figure 5.18: V_{max} comparison of 13 and 25 mm diameter membranes (filtration areas of around 1 and 4 cm^2 respectively). Filtrations were performed at 30 ± 1 kPa. Feed concentrations were adjusted to 100 ± 2 µg/mL. Error bar indicate standard deviation from two sets of data.

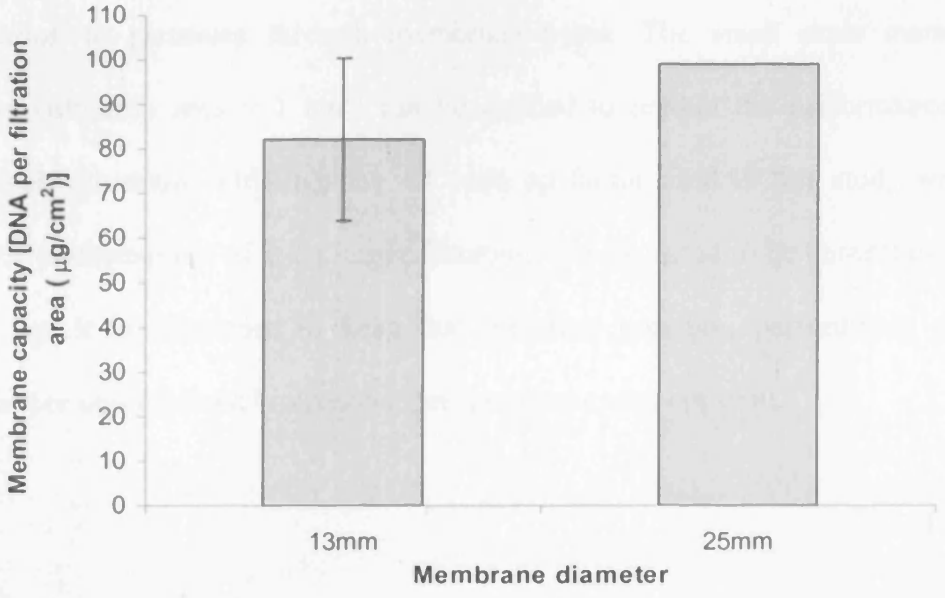

Figure 5.19: Membrane capacity comparison of 13 and 25 mm diameter membranes (filtration areas of 1 and 4 cm^2 respectively). Filtrations were performed at 30 ± 1 kPa. Feed concentrations were adjusted to 100 ± 2 µg/mL. Error bar indicate standard deviation from two sets of data.

5.6 Conclusion

The gradual pore constriction model was found to be suitable for application on DNA filtrations. Initial permeate flux was affected by vector size, DNA concentration and operating pressure. The membrane capacity per filtration area decreased slightly with increasing DNA concentration, confirming the earlier observations in constant flux experiments (Chapter 3) which suggested unspecific adsorption did not play an important role in the filtration performance. The results showed that membrane capacity and transmission decreased significantly with increasing vector size as predicted from controlled flux experiments (Chapter 3). The increase in operating pressure also led to reduced membrane capacities and the decline in capacity was observed to be more significant for the larger plasmid tested indicating that larger DNA vectors would require a longer time to facilitate their deformation to permeate through membrane pores. The small scale membrane filtration (filtration area = 1 cm^2) can be applied to predict the performance of a larger scale filtration. Although the 4× scale up factor used in this study was not huge, the performances of even larger filtrations are expected to be comparable. For scaling up, it is important to keep the operating pressure, performance of the filtration per unit area and biomaterial per membrane area constant.

Chapter 6 – Conclusion

6.1 Overall Conclusion

Normal-flow membrane filtrations of solutions containing purified plasmid DNA and bacterial artificial chromosomes were conducted using small scale filtration set-ups. The main aims were achieved through the investigations of various parameters affecting the product yield and quality, and the membrane filter's performance. The use of a pressure driven syringe system for conducting constant flux experiments had successfully enabled rapid acquisition of transmission and degradation data using very small sample volumes ($\leq$ 1 mL). While information useful to facilitate the scale-up of a membrane filtration process was attained with the use of a positive pressure filtration system which permitted constant pressure operations.

The performance of the membrane filtration operation was found to be significantly affected by the circular vectors' molecular size. The percentage of DNA transmission assessed spectrophotometrically varied from 98-13% for vector sizes ranging from 6-116 kb. Although DNA molecules tested in this study had radii of gyration larger than the membrane pore diameter of 0.22 μm, the high recovery rates particular for the smaller constructs tested indicated deformation at the molecular level had facilitated the passing of these constructs through the membrane pores. The linear

trend of retention with increasing molecular weight suggested molecules capable of deforming and aligning more quickly in the flow field during the filtration process had the advantage of permeation through the membrane pores. The retained molecules could be observed using confocal microscopy techniques.

Elongational effects caused by the constriction to fluid flow generated degraded open-circular and linear plasmid isoforms particularly for larger DNA constructs during the sterile filtration operation. Based on observations of the experiments performed at different fluxes, DNA concentrations and quantification of genomic DNA, adsorption of DNA molecules did not play an important role in contributing to the loss of product and linear DNA permeated the membrane more readily than circular vectors. This could also explain high transmissions of the degraded linear vector forms observed during the repeated passes experiments.

It was observed for DNA vectors $\geq$ 20 kb:

- The level of backbone breakage increased with molecular weight, flux and number of filtration passes.
- Greater DNA loss occurred during the first pass of filtration based on consecutive filtration experiments.
- The use of polyethersulfone (PES) membranes with asymmetrical pores improved DNA transmission and decreased DNA damage.
- The addition of 150 mM NaCl in the formulation buffer improved filtration transmission by 47% and 11% for the 72 and 116 kb vectors respectively.
- Complexation with PEI and a lipid integrin binding peptide did not improve product transmission.

The linearised form of the gradual pore constriction model (V_{max} analysis) was found to be applicable for DNA filtration. The performance of membrane filters was analysed. It was observed in constant pressure filtrations that:

- Initial permeate flux was affected by vector size, DNA concentration and operating pressure.
- Membrane capacity (DNA per filtration area) decreased slightly with increasing DNA concentration.
- Membrane capacity decreased with increasing DNA vector size.
- Membrane capacity decreased with increasing operating pressure.
- Small scale membrane filtration can be use to predict the performance of a larger scale filtration.

6.2 Recommendations

The following are some issues which require further investigations:

- Membrane types and properties –
  - ➢ The use of more membranes types should be explored for process optimisation. In this study, the use of commonly available PVDF and PES membranes led to differences in product transmission and degradation. These differences show that the material construction, and pore size distribution and tortuousity can be important factors affecting product loss.
- Formulations –
  - ➢ The addition of 150 mM NaCl to the formulating buffer led to remarkable improvements in transmissions and reduction in damage. Different molarity of NaCl to give a broad range of ionic strengths can be tested further for optimisation of salt concentration. The use of different salt types can also be explored.
  - ➢ In contrast to the addition of simple salts like NaCl, the use of more effective cationic agent, PEI, did not improve the filtration performance. Simple salts provide counterions for neutralisation of charges on the DNA backbone without condensation while the molecular compaction takes place in the presence of the condensing agents. Perhaps a range of surface charge of the charged particles should be investigated further. Other condensing agents such as poly-L-lysine, spermidine, or alcohols can be tested as well.

- Windows of operation –
  - This is powerful tool for visualisation of a process performance and should be employed for selecting the best process parameters for optimisation. More data points can be collected to develop this approach.
- Other materials – Filtration of proteins, polysaccharides or viruses can be investigated using the same filtration setups.
- Biological activity of the filtered DNA vectors – Transfection experiments can be conducted to test the biological activity of the filtered DNA vectors. Transient transfection studies using the gWIZ (6 kb) plasmid that had been filtered through 0.22 μm pore size PVDF membranes were performed successfully recently by a colleague at UCL (Wu, A., Department of Biochemical Engineering, UCL, personal communication). Therefore, other filtered DNA vectors (i.e. BAC p5179 (33 kb), p5180 (72 kb) and p5176 (116 kb)) can be tested as well.

Chapter 7 – Pilot Scale Plasmid DNA Processing Studies

7.1 Introduction

The World Health Organisation (2006) reported that the H5N1 avian flu virus strain first infected humans in 1997 and since then, 249 human cases have been confirmed with 146 deaths in a number of countries in the Asian and African continents. The long standing fear has been the possibility of a rapid mutation of the viral strain into a lethal form easily transmissible between humans and becomes as contagious as normal influenza (Wold Health Organisation, 2006). In case of a pandemic, the disease can only be contained effectively through prompt action (Ferguson et al., 2005; Longini et al., 2005).

Traditional virus-based flu vaccines are typically produced by injecting modified flu virus into fertilised chicken eggs and when large-scale production is required in urgent situations, the manufacture of such vaccines is slow (PowderMed, 2005). Due to the uncertainty of timing of a pandemic, current vaccine production facilities are not likely to be able to meet the worldwide demands (Hoare et al., 2005). DNA vaccine is an alternative which has already attracted global interest. For DNA vaccinations, a gene that codes for a protein or proteins equivalent to components of the virus is introduced into the body to produce the intended vaccine antigen to

induce an immune response, therefore nucleic acid vaccines can be applied as preventative vaccines for infectious diseases (Durland and Eastman, 1998). The company, PowderMed, had recently received approval from the UK Medicines and Healthcare Products Regulatory Agency (MHRA) to run the Phase I clinical trials using DNA vaccines which protect against the annual and pandemic avian influenza (PowderMed press release, September 2006). Here at the UCL Innovative Manufacturing Research Centre (IMRC), Department of Biochemical Engineering a number of studies have been conducted to address the issues faced in the large scale production of a DNA vaccine since it is possible to produce on many industrial sites using existing biopharmaceutical and antibiotics plants and requiring shorter time frames (Hoare et al., 2005).

In my core PhD research project (discussed in Chapters 1-6), investigations were centred on the sterilising filtration procedure which is among the last in the sequence of downstream processing unit operations. It was concluded that the performance of the membrane sterile filtration operation was significantly affected by the size of circular DNA vectors. Degraded OC and linear plasmid isoforms were generated following filtrations at high fluxes particularly for the larger DNA constructs. Many operations prior to the membrane sterilisation step such as cell harvest and resuspension, lysate clarification via centrifugation and passage through pumps could also potentially generate large quantities of degraded plasmid isoforms. Together with irreversible damage cascaded from earlier stages of processing, the overall yield and quality of the product would be greatly affected.

This chapter reports the studies which I had conducted in collaboration with doctoral and postdoctoral researchers alongside the second year undergraduates and MSc students in the department. The first study involved assessment of the effect of bacterial cell harvest via centrifugation and cell handling in the initial stages of plasmid DNA processing. It was hypothesised that in cells subjected to high stresses sufficient to cause lysis, alongside unfavourable handling conditions, the yield of plasmid DNA would be affected by release of product to the supernatant waste stream. For this investigation, *E. coli* cells containing either the 6 or 20 kb plasmid grown in 75-450 L bioreactors were harvested using either a disk-stack centrifuge or a solid-bowl centrifuge and subsequently used fresh or subjected to a freeze/thaw cycle. The next study was to evaluate the impact of passing *E. coli* clarified lysate containing a 20 kb plasmid through a centrifugal pump, a mono pump and a disk-stack centrifuge feed zone. These equipments are known to cause damage to fragile biomaterials due to elongational shear rate. Therefore, the extent of molecular backbone breakage caused by these processes was examined.

7.2 Effects of cell harvesting and cell storage methods on supercoiled plasmid DNA yield

7.2.1 Introduction

In a typical plasmid DNA production process, bacterial cells are harvested at late log or stationary phase, then the recovered cells are either resuspended immediately in an appropriate buffer for preparation of a chemical lysis procedure or stored frozen for subsequent processing (Durland and Eastman, 1998; Ferreira et al., 2000; Levy et al., 2000a). Continuous centrifugation is a common option for harvesting large culture volumes. Previous studies have shown that *E. coli* cells harvested with an intermittent-discharge, continuous flow disk-stack centrifuge are subjected to stresses that are sufficiently high to cause lysis (Gray et al., 1972; Higgins et al., 1978).

For this study, with the help of colleagues from the IMRC (Andrew Booth, Gerard Chan and Nick Willoughby), *E. coli* cells were grown in a complex medium in 75-450 L scale bioreactors and harvested using either a continuous-feed, intermittent solids-discharge, disk-stack centrifuge or a continuous-feed, batch-discharge, solid-bowl centrifuge. The main purpose was to examine the influence of cell harvest equipment on the early recovery stages of plasmid DNA. Post-harvest, the recovered cells were either resuspended in buffer and chemically lysed immediately or stored frozen for subsequent processing. A process flowsheet with details of sampling points is shown in Figure 7.1.

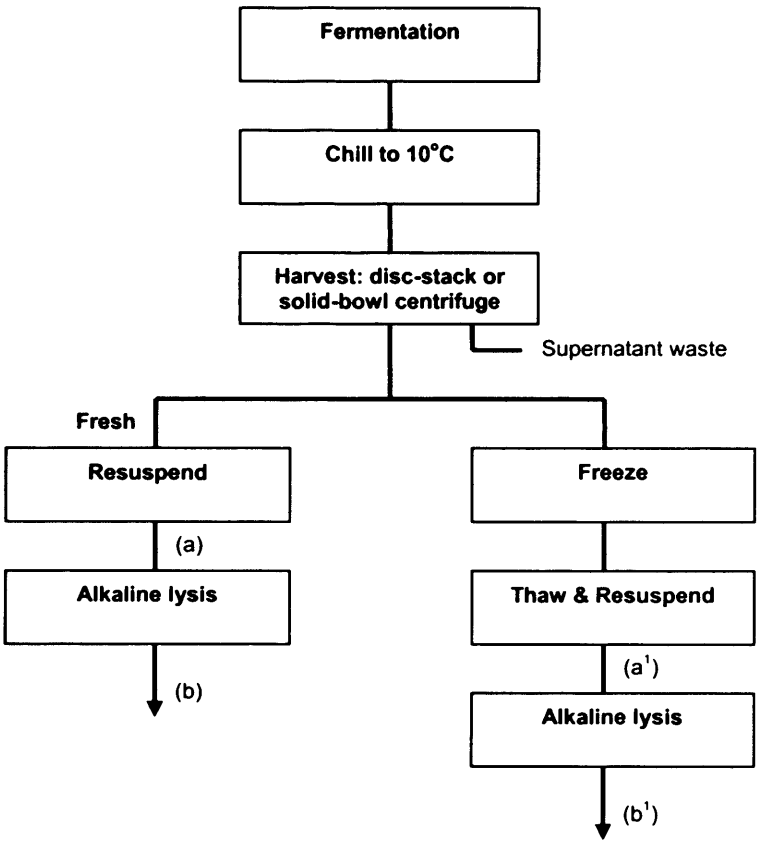

Figure 7.1: Process flowsheet options for *E. coli* cell recovery and handling. Sampling points for analysis are indicated in terms of method used.

Notes:

a and a^{1}: The cell suspension (OD_{600}= 50-60) was microcentrifuged, the supernatant was decanted and analysed. Released nucleic acids were analysed by PicoGreen and agarose gel electrophoresis.

b and b^{1}: Plasmid DNA was subjected to isopropanol precipitation or minichromatographic purification. The purified material was analysed by spectrophotometry, agarose gel electrophoresis and qPCR.

7.2.2 Materials and Methods

Fermentation

Plasmid gWIZ™, 6 kb (Aldevron, ND, USA), transformed and propagated in *E. coli* DH1 and plasmid pQR150, 20 kb (Jackson et al., 1995) transformed and propagated in *E. coli* DH5α (Gibco-Life Technologies, Gaithersburg, MD, USA) were used. Storage and shake flask culture conditions used are described elsewhere (Levy et al., 2000; Rock et al., 2003). Terrific broth (12 g L^{-1} Bacto-tryptone, 24 g/L yeast extract, 4 mL/L glycerol, 0.017 M KH_2PO_4, 0.072 M K_2HPO_4), at either 1 or 2 fold concentration was used. Cultures contained kanamycin at 50 μg/mL. All chemicals and media components were provided by Sigma-Aldrich (Poole, Dorset, UK) unless otherwise stated. Overnight 2 L shake flask cultures (working volume 500 mL) were used to inoculate a Series 2000 LH 75 L bioreactor (Inceltech, Pangbourne, Berks, UK) at a starting optical density at 600 nm (OD_{600}) of 0.5 and working volume of 45 L. The antifoam polypropyleneglycol (PPG) was added at a concentration of 0.36 mL/L. Bioreactor conditions were 37°C, 500 rpm agitation, 22.5 L/min airflow rate. The pH was maintained at 7.0 ± 0.1 and control was achieved through the automatic addition of 1 M sulphuric acid and 1 M NaOH when necessary. After 13 hours of growth the culture was either harvested or used to inoculate 300 L of Terrific broth to a starting OD_{600} of 0.5. The culture was grown within a 450 L total volume Chemap bioreactor (Chemap AG, Maenndorf, Switzerland) for 11 hours to a final OD_{600} of 20-24. Initial bioreactor conditions were 37°C, 200 rpm agitation, 180 L/min airflow rate. Foaming and pH were controlled as for the 75 L fermentation. At the end of the fermentation the culture was cooled to 10°C and harvested immediately.

Culture harvest

The culture was harvested using two pilot scale continuous centrifuges and a laboratory batch centrifuge. During the harvest of DH5α pQR150 cells, the CSA-1 (Westphalia Separator, Oelde, Germany) disk-stack centrifuge, outer disc radius 0.053 m, inner disc radius 0.021 m, 43 disks per stack, was operated at flow rates of 30, 50 and 60 L/h and discharged at 9800 rpm. During the recovery of DH1 gWIZ cells, the CSA-1 disk-stack centrifuge was operated at a flow rate of 90 L/h and discharged at 6800 rpm. The CARR (Carr Separations, Franklin, MA, USA) P6 Powerfuge solid-bowl centrifuge, inner weir radius 0.076 m, inner bowl radius 0.051 m, inner length of bowl 0.127 m was operated at 60 L/h. The equivalent settling areas for the disk-stack and solid-bowl centrifuges are approximately 640 and 1000 m^2 respectively (these values include a calibration factor to allow for non-ideal flow in either machine). The Beckman (Beckman Instruments, Palo Alto, CA, USA) J2-MI batch centrifuge, using the JA-10 rotor (inner radius 0.04 m, outer radius 0.075 m) was operated at 6000 rpm for 30 minutes. Harvested cells were stored initially at -20°C and then at -70°C. In some experiments fresh cells (kept on ice for no more than 2 hours after harvesting) were used.

Cell alkaline lysis and DNA purification

Cell pastes were resuspended with gentle shaking in TE buffer (50 mM Tris-Cl, 100 mM EDTA, pH 8.0) at OD_{600} of 50 or 65. Cells were lysed in the absence or presence of RNaseA using a modified alkaline lysis protocol as described in Levy et al. (2000). For some experiments, clarified lysates were isopropanol precipitated, washed with ethanol, resuspended in TE buffer containing 100 μg/mL RNaseA and incubated for 1 hour at 37°C. For plasmid yield analysis, serial dilutions of lysate (prepared with TE buffer containing RNaseA) were loaded into at least three different minichromatographic QIAprep® Spin columns (Qiagen Ltd, West Sussex, UK). Values reported are those that fell within a linear range of response and are the average of 2 or 3 independent purifications. DNA concentrations were determined by UV spectrophotometry at 260 nm (A_{260}). For analysis of nucleic acids released during cell resuspension, cell suspensions were briefly microcentrifuged and the supernatant recovered. The supernatant was precipitated using isopropanol in the presence of 0.2 M NaCl. The precipitated DNA was washed with 70 %v/v ethanol and treated to remove contaminating RNA where required.

Agarose gel electrophoresis

Please refer to Chapter 2 (Section 2.2.4).

PicoGreen assay for released nucleic acids

Samples of supernatant from centrifuged cells were tested for nucleic acid content using the standard PicoGreen assay (Molecular Probes, Leiden, The Netherlands). A series of preliminary experiments indicated a linear response for supernatant dilutions in the range of 1 in 1000 and 1 in 5000. After dilution, 50 μL of diluted samples were placed on a microplate and 50 μL PicoGreen (1 in 400 working concentration) was added and mixed. After 5 minutes, the fluorescence was recorded using a Packard Fluorocount Microplate Fluorometer (Packard Instrument Company, Meriden, CT, USA) at an excitation wavelength of 480 nm and emission of 520 nm. The samples were corrected for background fluorescence using blanks of TE buffer and PicoGreen.

Fluorescence response with spiked DNA indicated that 1 in 1000 dilution could give good discernible differences between 500, 125 and 31 ng DNA mL^{-1}. Under such conditions, a calibration curve using supernatants from a homogenised cell suspension (100% lysed cells) indicated that fluorescence enhancement was linearly related to the percentage of lysed cells up to 15%, beyond this value a plateau was reached (Figure 7.2). The percentage of lysed cells expected in the context of continuous centrifugation with the machines used in the present study is in the range of 1-15% (Chan and Hoare, personal communication).

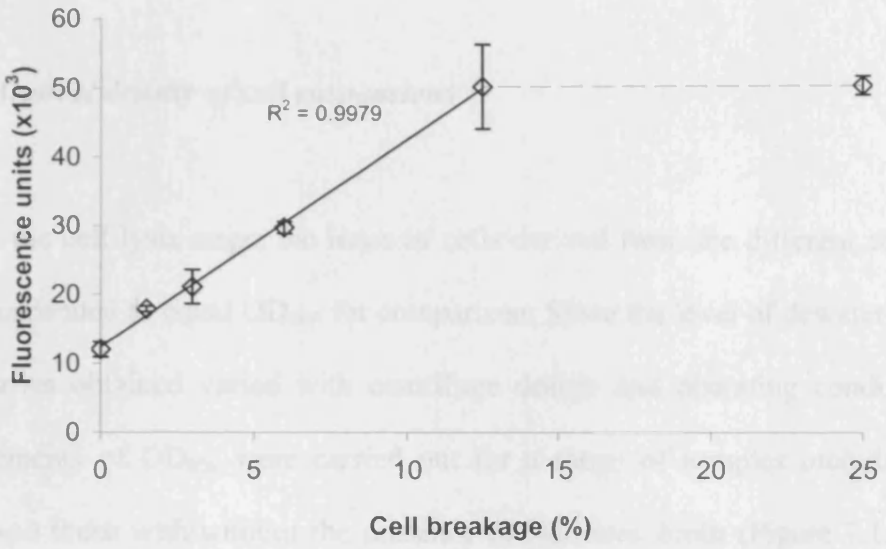

Figure 7.2: Calibration curve using supernatants from a homogenised *E. coli* cell suspension. Analysed using the standard PicoGreen assay, dilution of supernatant from a homogenised cell suspension was 1/5000, results shown are averages, and error bars represent standard deviations.

qPCR assay

Please refer to Chapter 2 (Section 2.2.6).

7.2.3 Results and Discussions

7.2.3.1 Optical density of cell suspensions

Prior to the cell lysis stage, the mass of cells derived from the different centrifuges was resuspended to equal OD_{600} for comparison. Since the level of dewatering of the cell slurries obtained varied with centrifuge design and operating conditions, the measurements of OD_{600} were carried out for a range of samples including fresh, frozen and those with/without the presence of entrained broth (Figure 7.1, points a and a^1). This step was conducted to determine if the level of dewatering, and particularly entrained broth, could affect comparison. As seen in Figure 7.3, a good correlation ($R^2 = 0.98$) between OD_{600} of cell suspensions from the solid-bowl and the disk-stack centrifuges and cell mass was obtained. No significant contribution of the entrained broth to optical density measurements was observed.

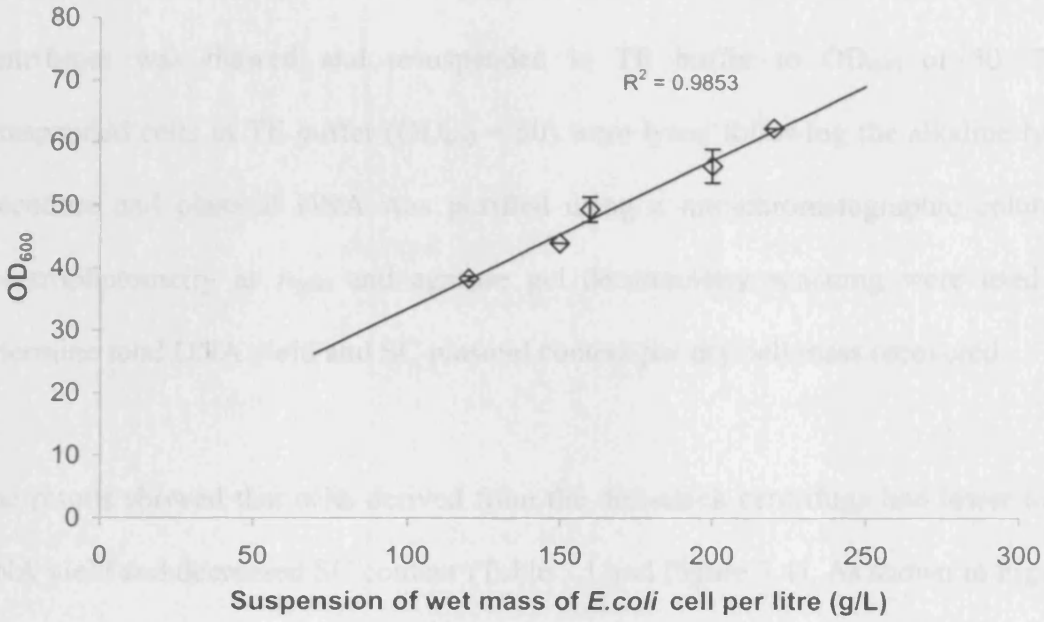

Figure 7.3: Optical density measurements of *E. coli* cell suspended in TE buffer. Cells were either harvested from the solid-bowl or the disk-stack centrifuges. Results shown are average of measurements based on 2-4 independent resuspensions, and error bars represent standard deviations.

7.2.3.2 Analysis of plasmid DNA extracted from frozen cells

E. coli DH5α cells containing pQR150 plasmid (20 kb) were grown in a 450 L bioreactor with 2×TB medium until an $OD_{600} \approx 20$, the entire culture was then rapidly cooled to 10°C. The culture was totally recovered using two different pilot scale continuous centrifuges – a solid-bowl and a disk-stack. The operating conditions chosen were based on the equivalent settling area. The equivalent settling areas for the disk stack and tubular bowl centrifuges are approximately 640 and 1000 m^2 respectively. The cell paste obtained was stored frozen (initially at -20°C, then at

-70°C) in small batches. For the experiments, cell biomass derived from the two centrifuges was thawed and resuspended in TE buffer to OD_{600} of 50. The resuspended cells in TE buffer (OD_{600} = 50) were lysed following the alkaline lysis procedure and plasmid DNA was purified using a minichromatographic column. Spectrophotometry at A_{260} and agarose gel densitometry scanning were used to determine total DNA yield and SC plasmid content per dry cell mass recovered.

The results showed that cells derived from the disk-stack centrifuge had lower total DNA yield and decreased SC content (Table 7.1 and Figure 7.4). As shown in Figure 7.4 even after chromatographic purification which removes a proportion of degraded plasmid forms and chromosomal DNA – the material derived from the disk-stack centrifuge had increased levels of contaminant DNA species such as linear plasmid and low molecular weight DNA fragments.

Table 7.1: Plasmid pQR150 (20 kb) yield from cells recovered by large-scale centrifugation and subsequently processed after a freeze/thaw cycle (analysis point b[1], Figure 7.1).

Centrifuge model	DNA yield per dry cell weight[α] (µg/mg)	%SC[β]	Approx. SC yield per dry cell weight (µg/mg)
Solid-bowl[χ]	6.4 ± 0.4	71	4.5
Disk-stack[δ]	5.4± 0.3	40	2.2

Notes:

[α] Estimation based on 1 OD_{600} = 0.5 g/L dry cell weight (Moat and Foster, 1995), samples were analysed in duplicates or triplicates, results shown are averages ± standard deviations.
[β] Analysis was by agarose gel densitometry scan.
[χ] The solid-bowl centrifuge was operated at 60 L/h.
[δ] The disk-stack centrifuge was operated at 50 L/h and solids were discharged at 9800 rpm.

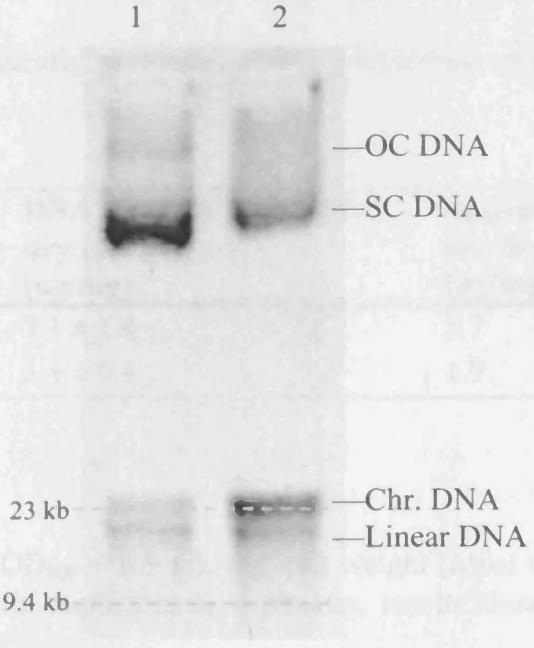

Figure 7.4: Effect of continuous centrifugation on supercoiled plasmid pQR150 (20 kb) yield. Agarose gel electrophoresis of purified pQR150 samples derived from an equal mass of cells harvested using a solid-bowl centrifuge operated at 60 L/h (lane 1) and a disk-stack centrifuge operated at 50 L/h (lane 2). Lanes 1 and 2 were loaded with an equal mass of total DNA (250 ng).

Next, the recovery of a different plasmid was tested to see if a decreased SC yield would be evident as observed in the earlier experiment using the disk-stack centrifuge. *E. coli* cells containing gWIZ (6 kb) were grown at 450 L scale with 2xTB medium, the entire culture was then rapidly cooled down to 10°C prior to harvesting by continuous centrifugation. Plasmid DNA analysis indicated a similar trend as that observed for the larger plasmid. Cells harvested with the solid-bowl centrifuge showed higher total DNA yield and SC content than those processed with the disk-stack centrifuge (Table 7.2 and Figure 7.5). It is evident from Figure 7.5, that the decrease in SC yield can be attributed to conversion of the plasmid to open circular (OC) and linear forms.

Table 7.2: Plasmid gWIZ (6 kb) yield from cells recovered by large-scale centrifugation and subsequently processed after a freeze/thaw cycle (analysis point b[1], Figure 7.1).

Centrifuge model	**DNA yield per dry cell weight[α] (µg/mg)**	**%SC[β]**	**Approx. SC yield per dry cell weight (µg/mg)**
Solid-bowl[χ]	7.1 ± 1.4	80	5.7
Disk-stack[δ]	3.4 ± 0.4	55	1.9

Notes:

[α] Estimation based on 1 OD_{600} = 0.5 g/L dry cell weight (Moat and Foster, 1995), samples were analysed in duplicates or triplicates, results shown are averages ± standard deviations.

[β] Analysis was by agarose gel densitometry scan.

[χ] The solid-bowl centrifuge was operated at 60 L/h.

[δ] The disk-stack centrifuge was operated at 90 L/h and solids were discharged at 6800 rpm.

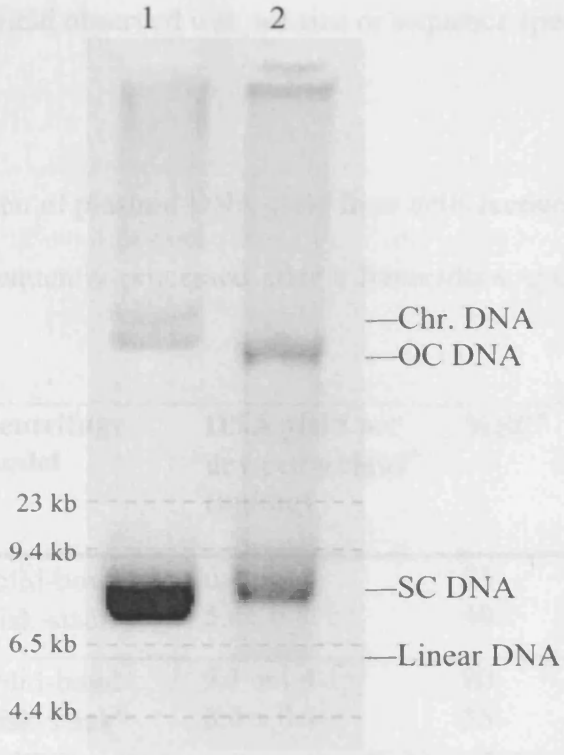

Figure 7.5: Effect of continuous centrifugation on supercoiled plasmid gWIZ (6 kb) yield. Agarose gel electrophoresis of purified pQR150 samples derived from an equal mass of cells harvested using a solid-bowl centrifuge operated at 60 L/h (lane 1) and a disk-stack centrifuge operated at 90 L/h (lane 2). Lanes 1 and 2 were loaded with an equal mass of total DNA (200 ng).

Taken together (Table 7.3), results obtained with the 20 and 6 kb plasmids indicated that the decrease in SC yield observed was not size or sequence specific.

Table 7.3: For comparison of plasmid DNA yield from cells recovered by large-scale centrifugation and subsequently processed after a freeze/thaw cycle (analysis point b[1], Figure 7.1).

Cells[α]	**Plasmid**	**Centrifuge model**	**DNA yield per dry cell weight**[β] **(μg/mg)**	**%SC**[χ]	**Approx. SC yield per dry cell weight (μg/mg)**
E. coli DH5α	pQR150 (20 kb)	Solid-bowl[δ]	6.4 ± 0.4	71	4.5
		Disk-stack[ε]	5.4± 0.3	40	2.2
E. coli DH1	gWIZ (6 kb)	Solid-bowl[δ]	7.1 ± 1.4	80	5.7
		Disk-stack[ϕ]	3.4 ± 0.4	55	1.9

Notes:

[α] Cells were grown in a 450 L bioreactor with 2xTB medium.
[β] Estimation based on 1 OD_{600} = 0.5 g/L dry cell weight (Moat and Foster, 1995), samples were analysed in duplicates or triplicates, results shown are averages ± standard deviation.
[χ] Analysis was by agarose gel densitometry scan.
[δ] The solid-bowl centrifuge was operated at 60 L/h.
[ε] The disk-stack centrifuge was operated at 50 L/h and solids were discharged at 9800 rpm.
[ϕ] The disk-stack centrifuge was operated at 90 L/h and solids were discharged at 6800 rpm.

7.2.3.3 Analysis of plasmid DNA extracted from fresh cells

It is often more convenient to freeze cell biomass before proceeding with downstream operations to cater for the time lag between equipment availability and also to use smaller batches. Hence, a series of experiments were conducted to compare SC yields from fresh and frozen/thawed cells derived from the solid-bowl and the disk-stack centrifuges respectively. *E. coli* cells containing pQR150 (20 kb) were grown at 75 L scale with a 1×TB culture medium, the entire culture was rapidly cooled down to 10°C prior to harvesting by continuous centrifugation. The material derived from each centrifuge was kept at 4°C and plasmid DNA extracted within 2 hours; the rest of the material was kept frozen until further use.

Results obtained indicated that the freeze/thaw cycle led to losses in SC DNA yield ranging between 10-21% for material derived from both centrifuges tested (Table 7.4). In all cases material derived from the disk-stack centrifuge had lower SC yield. Fresh cells derived from the disk-stack centrifuge had 28-40% lower SC yield than those derived from the solid-bowl machine (Table 7.4). For the frozen cells, SC yields were 36% lower for material derived from the disk-stack centrifuge compared to material processed through the solid-bowl centrifuge.

Table 7.4: Plasmid yield from cells recovered by large-scale centrifugation and subsequently processed fresh (no storage) or after a freeze/thaw cycle (analysis point b or b[1], Figure 7.1).

Cell harvest equipment	**Storage condition of recovered cells**[α]	**DNA yield per dry cell weight**[β] **(µg/mg)**	**%SC**[χ]	**Approx. SC yield per dry cell weight (µg/mg)**
Batch (JA-10)	Fresh	5.1	69	2.9
Solid-bowl 60 L h	Fresh	5.8 ± 0.2	71	3.3
Disk-stack[δ] 30 L/h	Fresh	4.6 ± 0.2	67	2.4
Disk-stack[δ] 60 L/h	Fresh	3.6 ± 0.1	69	2.0
Solid-bowl 60 L/h	Frozen	4.8 ± 0.2	70	2.8
Disk-stack[δ] 30 L/h	Frozen	3.8 ± 0.2	63	1.9
Disk-stack[δ] 60 L/h	Frozen	3.5 ± 0.4	55	1.8

Notes:

[α] *E. coli* DH5α pQR150 (20 kb) were grown in a 75 L bioreactor with 1xTB culture medium.

[β] Estimation based on 1 OD_{600} = 0.5 g/L dry cell weight (Moat and Foster, 1995), samples were analysed in triplicates, results shown are averages ± standard deviation.

[χ] Analysis was by agarose gel densitometry scan.

[δ] Solids were discharged at 9800 rpm.

Notably, the magnitude of the difference between centrifuges seemed to be less pronounced than the one reported in Table 7.3 for frozen material. It is important to note that variations in experimental parameters such as bioreactor scale, culture medium could be probably contributing to differences in magnitude observed. Further detailed studies, would be required to determine the exact contribution of each parameter to the magnitude of the effect observed.

7.2.3.4 Effect of cell resuspension holding time

After the harvest stage, the recovered cells are usually resuspended in an appropriate buffer before proceeding to the lysis stage. In a small scale laboratory environment, the resuspension step can be done quickly within 5-15 minutes. But at a larger scale, achieving a homogeneous suspension with a large mass of cells would entail longer times. Consequently, the effect of holding time during cell resuspension becomes a relevant consideration.

A series of laboratory based experiments were designed to assess the effect of holding time at the resuspension stage. Frozen cells harvested with the solid-bowl centrifuge operated at 60 L/h were thawed, resuspended in TE buffer to OD_{600} of 65 and kept at a constant temperature of 13°C for time periods of 2, 4 and 6 hours. At the respective time intervals, cells were lysed chemically and plasmid DNA was purified (analysis point b[1], Figure 7.1). Meanwhile, a small aliquot of each of the cell suspensions was briefly centrifuged using a laboratory microcentrifuge and the supernatant was subjected to DNA analysis using the standard PicoGreen assay (analysis point a[1], Figure 7.1).

As shown in Figure 7.6 and Table 7.5, total DNA release into the supernatant increased with increasing holding time. Concurrently, Figure 7.7 shows a significant decrease in total DNA and SC yield associated with an increase in released nucleic acids into the resuspension buffer. Purified plasmid samples were subjected to qPCR to determine the level of chromosomal contamination. Results obtained indicated that

the chromosomal contamination still remaining in the purified samples increased with incubation time (Table 7.5).

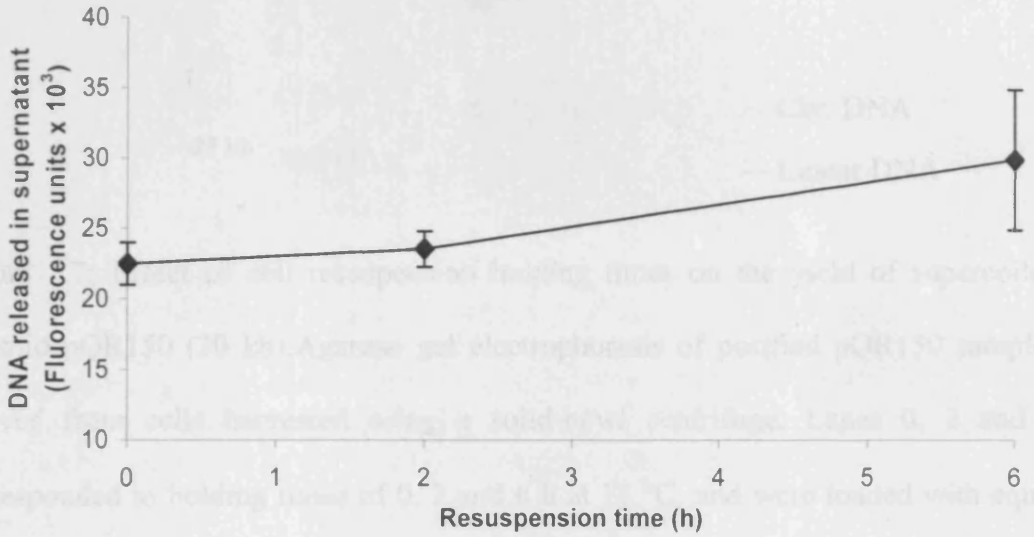

Figure 7.6: Effect of cell resuspension holding temperature. *E. coli* cells harvested using a solid-bowl centrifuge were stored frozen which was subsequently thawed and resuspended at 13 °C for 0, 2 and 6 h. Cells were centrifuged briefly and supernatants analysed in triplicates using PicoGreen, dilution of supernatant was 1/5000 (analysis point a[1], Figure 7.1), results shown are averages, error bars represent standard deviations.

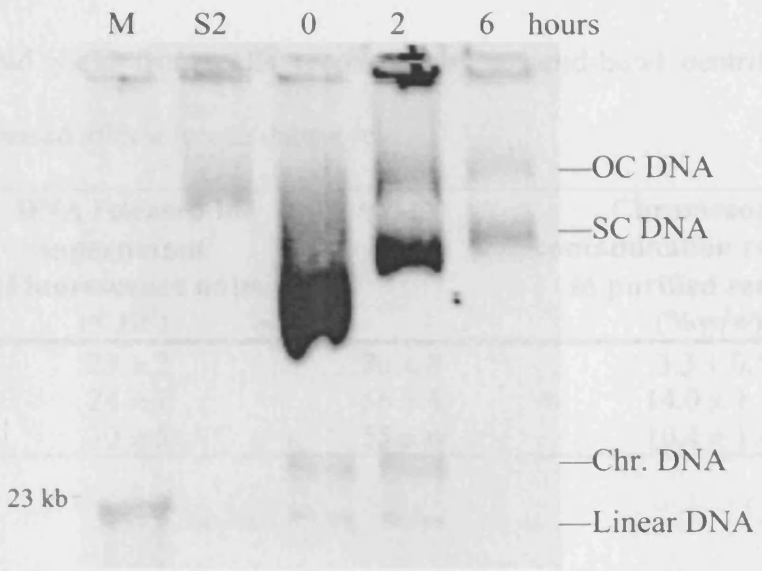

Figure 7.7: Effect of cell resuspension holding times on the yield of supercoiled plasmid pQR150 (20 kb).Agarose gel electrophoresis of purified pQR150 samples derived from cells harvested using a solid-bowl centrifuge. Lanes 0, 2 and 6 corresponded to holding times of 0, 2 and 6 h at 13 °C, and were loaded with equal volume of purified DNA solution to enhance visualisation of decreased total yield. Abbreviations: M, λ Hind III molecular weight marker; S2, control sample chemically degraded at 60°C for 48 hours.

Table 7.5: Plasmid yield from cells recovered by a solid-bowl centrifuge and subsequently processed after a freeze/thaw cycle.

Resuspension time (h)[α]	**DNA released in supernatant**[β] **(Fluorescence units × 10^3)**	**%SC**[χ]	**Chromosomal contamination remaining in purified samples**[δ] **(%w/w)**
0 (Control)	23 ± 2	80 ± 8	3.3 ± 0.1
2	24 ± 1	56 ± 6	14.0 ± 1.2
6	30 ± 5	55 ± 6	10.4 ± 1.4

Notes:

[α] Cells were resuspended at 13°C for 0-6 h.
[β] Analysis by PicoGreen assay, supernatant was diluted 1/5000 (analysis point a[1], Figure 1).
[χ] Analysis by agarose gel densitometry scan (analysis point b[1], Figure 7.1).
[δ] Analysis by qPCR (analysis point b[1], Figure 7.1). Experiments were conducted in triplicate, results shown are averages ± standard deviation.

In a separate experiment performed by a colleague in the department, Cassandra Rock, the effect of temperature during holding of the cell suspension was evaluated. Cells were similarly resuspended to OD_{600} = 65 in TE buffer and incubated at 4, 13 and 25°C for increasing periods of time. The results showed a remarkable 45% greater in fluorescence signal at 25°C compared to the 4 and 13°C samples after 2 hours of incubation.

The DNA degradation observed in the holding time experiment alongside the observations at various holding temperatures of cell resuspension suggest continued enzymatic activity at the cell resuspension stage despite the presence of EDTA in the TE buffer. A number of genetically engineered *E. coli* strains has recently been developed to aid processing (Cooke et al., 2003; Cooke et al., 2001; Ward et al., 2000) perhaps a specifically engineered strain that can prevent SC plasmid and

chromosomal DNA nicking during cell recovery stages could provide means for a more robust and consistent process.

7.2.4 Conclusion

Overall, the results showed that stress on cells during centrifugation, storage and resuspension can strongly affect the product yield and the level of chromosomal contamination of the product stream. Materials derived from the disk-stack centrifuge had increased levels of contaminant DNA species such as linear plasmid and low molecular weight chromosomal DNA fragments compared to those obtained from the solid-bowl centrifuge. The freezing of cells led to further product loss. The amount of released nucleic acids at the resuspension stage was observed to be proportional to the level of chromosomal contamination of purified samples and inversely proportional to the total product yield. Increasing holding time during the resuspension stage reduced SC yield.

A large amount of degraded DNA can be generated during the cell recovery and handling procedures and it was found that the degraded DNA forms could not be effectively removed during the alkaline lysis step or with the minichromatographic columns used in this study. This would affect not only the quality of the product but also the final sterilisation process as Watson et al. (2006) reported that larger membrane areas would be required for filtering plasmid samples that contained higher percentage of the degraded OC form. Moreover, in my previous observations (Chapter 3), linear DNA forms permeate membrane pores more readily compared to

circular forms and there are no other steps to remove these unwanted species. Therefore, more studies will need to be carried out to define critical process parameters and hence device appropriate optimisation strategies.

7.3 Effect of Centrifugal pump, mono pump and disk-stack centrifuge feed zone on clarified lysates containing a 20 kb plasmid

7.3.1 Introduction

The effect of shear stress from various pumps and valves has been reported on enzymes (Virkar et al., 1981), microalgae species (Jaouen et al., 1999; Vandanjon et al., 1999) and human albumin (Gomme et al., 2006). While damage of fragile biological materials in the feed zone of centrifuges has been described by Boychyn et al. (2001) and Hutchinson et al. (2006). Since plasmid DNA molecules are susceptible to irreversible damage by fluid stresses during primary recovery and purification processes (e.g. Carlson et al., 1995; Chamsart et al., 2001; Levy et al., 1999; Tsai et al., 1999), it is important to examine the influence of pumps and clarifying equipment used after the cell lysis step. In this work, the extent of irreversible plasmid damage after either passing through a pump and a disk stack centrifuge feed zone was investigated. Two different pumps – centrifugal and mono, were tested and the equipments were operated with the help of postdoctoral researchers Andrew Booth and Ria Boushaba.

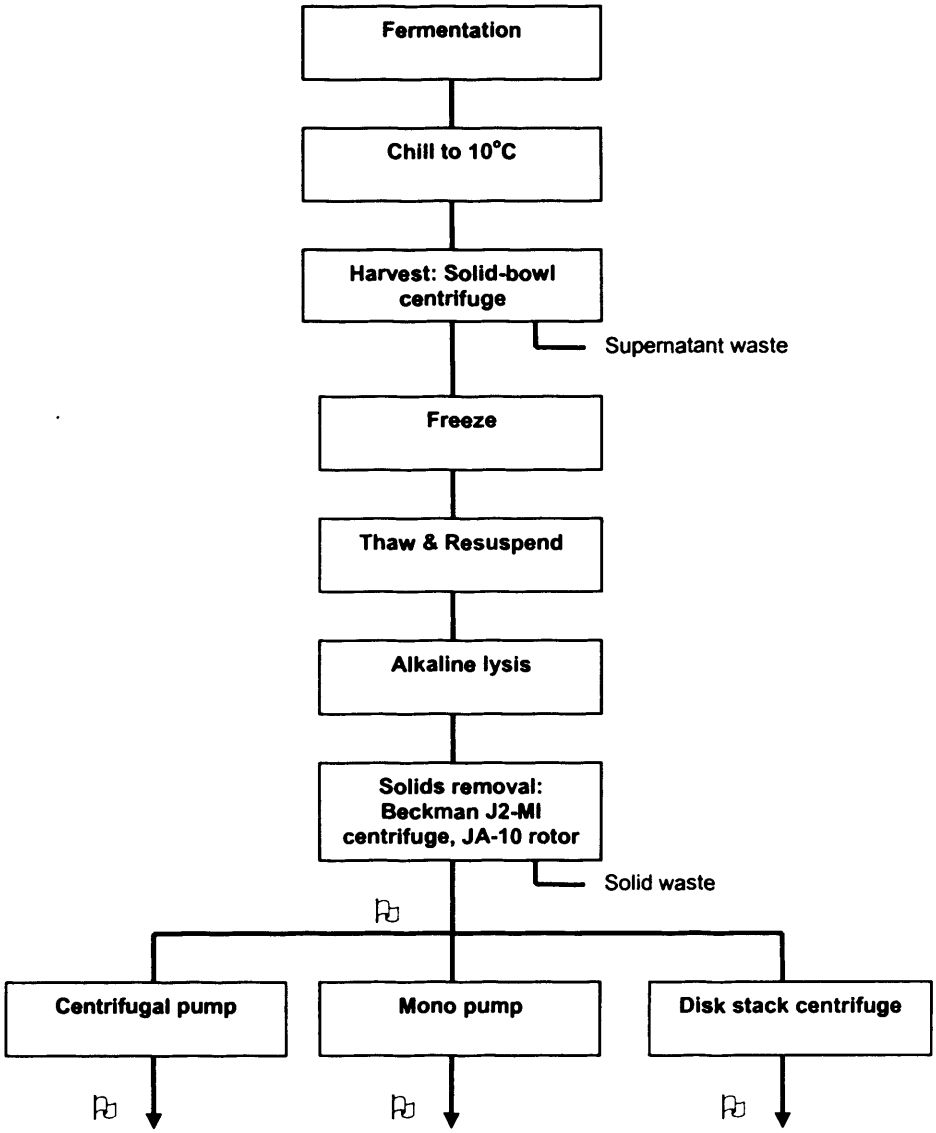

Figure 7.8: Process flowsheet for clarified lysate. Sampling points for analysis are indicated (⚑).

Note:

⚑ : Plasmid DNA was subjected to isopropanol precipitation and gel electrophoresis.

7.3.2 Methods and Materials

Fermentation

E. coli DH5 α (Gibco-Life Technologies, Gaithersburg, MD, USA) containing plasmid pQR150 (20 kb) were grown in a complex medium in a 450 L scale bioreactor and harvested using a continuous-feed, batch-discharge, solid-bowl centrifuge. Details of cells fermentation, harvest and storage are as described in section 7.2.2.

Alkaline lysis

A modified alkaline lysis procedure was used in this study. *E. coli* cells (120 g/L) were thawed and resuspended in 1 L of TE buffer. Cell lysis was achieved by the addition of 1 L of 200 mM NaOH, containing 1%w/v SDS. After an incubation of 10 min while being stirred at a mixing speed of 275 rpm, the lysate solution was neutralised using 1 L of potassium acetate solution (3 M, pH 5.5). The neutralised lysate was then chilled on ice for 10 minutes. The Beckman (Beckman Instruments, Palo Alto, CA, USA) J2-MI batch centrifuge, using the JA-10 rotor operated at 13,000 rpm for 30 minutes was used for clarifying the lysate prior to feeding into the individual unit operations.

Pump operations

The total working volume was set as 3 L for the operation of both the centrifugal pump (Stuart Turner Ltd, Oxfordshire, UK) and mono pump (Mono Pumps Ltd, Manchester, UK). Clarified lysate solutions were contained in tanks and gently stirred to achieve good mixing. A centrifugal pump coupled (with a valve) was connected to the tank and the lysate solution was cycled through the pump head for one hour. The centrifugal pump with a rotor diameter of 52 mm was operated at a fixed rotating speed of 4000 rpm. To minimize the detrimental effect of the valve, the valve was fully opened. The flow rate was measured to 5.7 L/min and the pressure drop across the centrifugal pump head was set to be around 0.9 bar. Similarly, a mono pump (without any valve) was connected to the tank containing the lysate and was operated at the same flow rate.

Centrifuge operation

Pilot scale centrifugation experiments were performed on a continuous flow CSA-1 disk-stack centrifuge (Westfalia, Germany). The disc stack centrifuge consisted of 43 conical discs that were separated by spacer ribs resulting in a disc gap width of 0.5 mm. A 10 L sample of *E. coli* lysate was fed to the rotating bowl by a central pipe from the top and accelerated to the pre-determined rotating speed of the bowl. The flow rates used were 50, 70 and 120 L/h. Separation of solid particles from the liquid phase was achieved in the narrow-flow channels of the disc stack. The solid particulates were deposited at the underside of the upper disc and discharged after the run was complete. The clarified liquid phase travelled to the top of the bowl and was

discharged continuously via a nozzle near the top centre of the centrifuge bowl. Lysate samples (6 mL) were collected at the end of each run for subsequent DNA analysis.

Alcohol precipitation and agarose gel electrophoresis

Please refer to Chapter 2.

7.3.3 Results and Discussions

7.3.3.1 Centrifugal and Mono Pumps

Lysate samples containing plasmid pQR150 (20 kb) were continuously pumped through the centrifugal pump and the Mono pump heads for periods up to 60 minutes. Samples were collected after the first pass, then at 1, 3, 5, 10, 20, 40 and 60 minutes respectively. Based on the simulations generated by the CFX software (kindly performed by Hu Zhang), the maximum elongational strain rates for the six blades inside the centrifugal pump varied from 3.1×10^4 s^{-1} to 2.8×10^4 s^{-1} and was found to be maximum at the edge of the blades whereas for the mono pump, elongational strain rate was calculated to be 3.8×10^4 s^{-1}.

The results showed increasing plasmid degradation as the lysate samples continuously pass through the centrifugal and the mono pump heads (Figures 7.9 and

7.10). The SC, OC, linear DNA and other minor bands corresponding to fragments, chromosomal or single stranded DNA were analysed via densitometry scanning and results are as shown in Figure 7.10. Each band was expressed as a percentage of the total intensity of the respective lanes and the relative integrity refers to the ratio of %SC after processing with respect to the %SC in the feed stream.

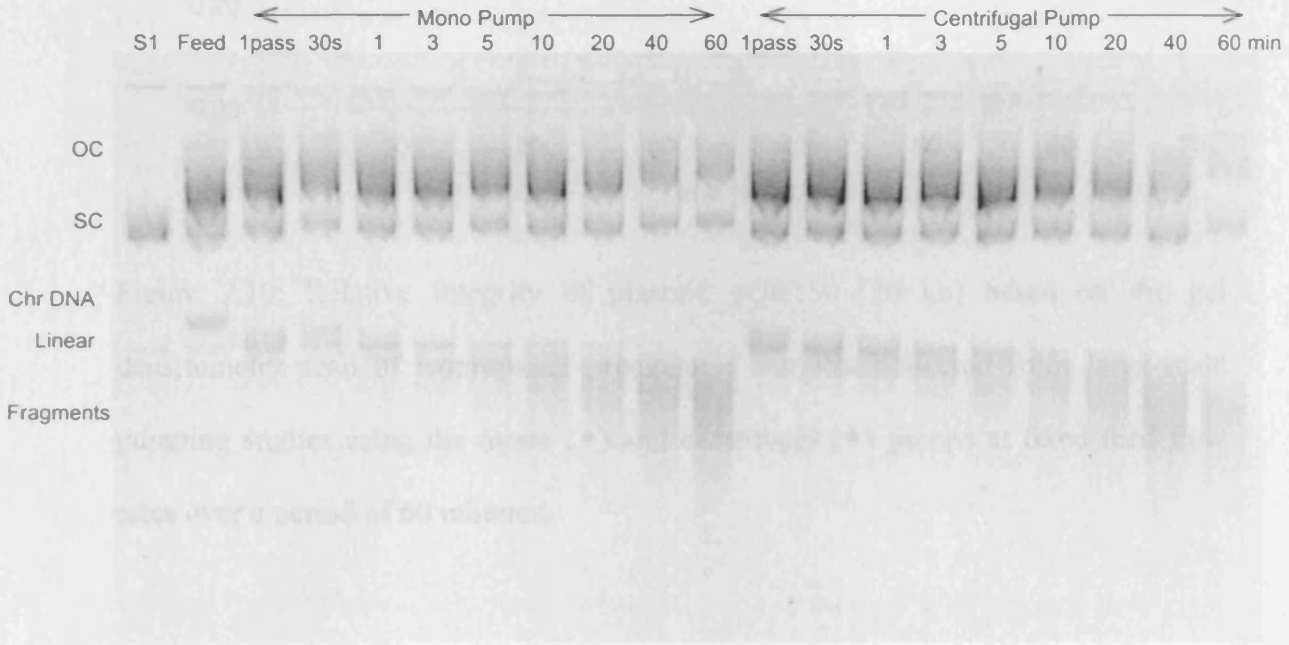

Figure 7.9: Agarose gel electrophoresis of isopropanol precipitated plasmid pQR150 (20 kb) samples collected from large-scale pumping studies using the Mono and Centrifugal pumps at fixed feed flow rates over a period of 60 minutes. Control sample S1 corresponds to purified plasmid pQR150 (20 kb) and S2 is S1 degraded at 60°C for 48 hours. Abbreviations: OC – open circular; SC – supercoiled.

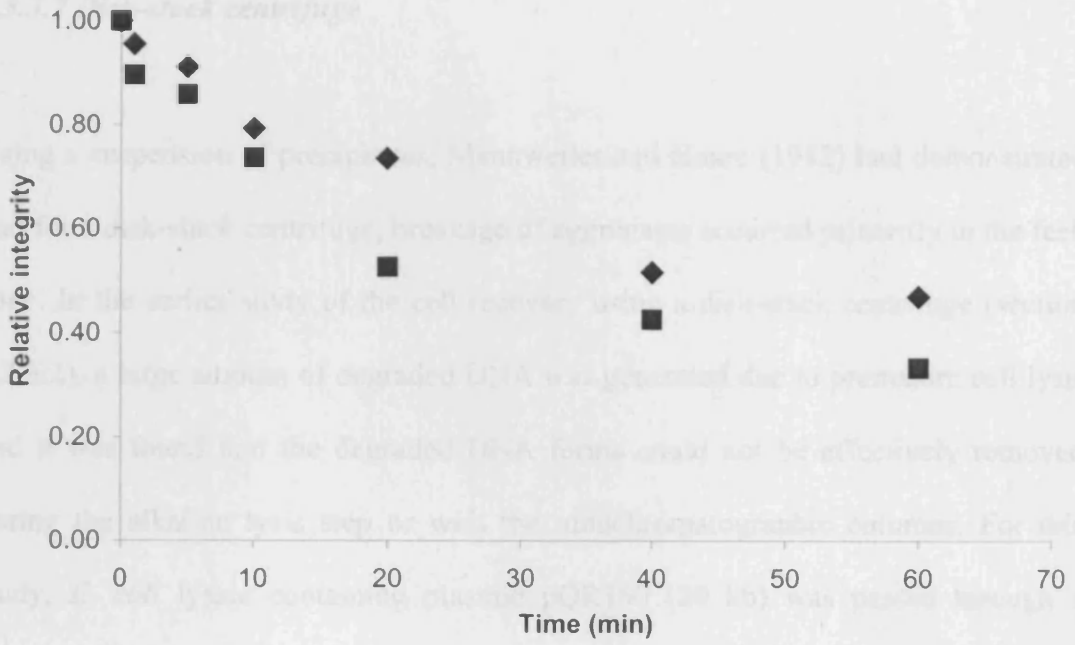

Figure 7.10: Relative integrity of plasmid pQR150 (20 kb) based on the gel densitometry scan of isopropanol precipitated samples collected from large-scale pumping studies using the mono (◆) and centrifugal (■) pumps at fixed feed flow rates over a period of 60 minutes.

As shown in Figure 7.10, the plasmid degradation process was gradual and increasing with time. The difference in product damage after passing through the two pumps was not significant particularly when processing times were ≤ 10 minutes. After processing for one hour, the 20 kb plasmid relative integrity was 33% and 47% for the centrifugal and mono pumps respectively; slightly higher percentage of backbone breakage observed from the centrifugal pump.

7.3.3.2 Disk-stack centrifuge

Using a suspension of precipitates, Mannweiler and Hoare (1982) had demonstrated that for a disk-stack centrifuge, breakage of aggregates occurred primarily in the feed zone. In the earlier study of the cell recovery using a disk-stack centrifuge (section 7.2.3.2), a large amount of degraded DNA was generated due to premature cell lysis and it was found that the degraded DNA forms could not be effectively removed during the alkaline lysis step or with the minichromatographic columns. For this study, *E. coli* lysate containing plasmid pQR150 (20 kb) was passed through a continuous flow, disk-stack centrifuge feed zone to evaluate the extent of plasmid backbone breakage as degraded DNA here can potentially affect the purification process further downstream. The lysate samples were fed through the centrifuge feed zone at flow rates of 50, 70 and 120 L/h.

An aliquot of the plasmid samples fed through the centrifuge at the various flow rates were collected and then alcohol precipitated to concentrate the plasmids for gel electrophoresis analysis. Figure 7.11 shows the gel image of the isopropanol precipitated samples and it is evident that the SC content had decreased after passing through the disk-stack centrifuge feed zone. Based on the gel densitometry scan analysis, degradation of plasmid was found to be 28-31% after passing through the centrifuge feed zone region but damage was not significantly dependent on the flow rates applied (Table 7.6).

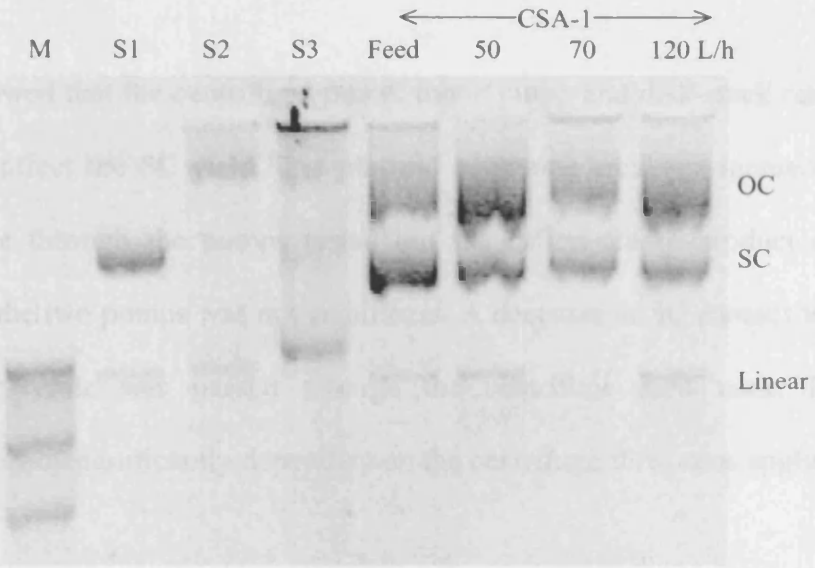

Figure 7.11: Agarose gel electrophoresis isopropanol precipitated plasmid pQR150 (20 kb) samples after passing through the centrifuge feed zone at flow rates of 50, 70 and 120 L/h. Control sample S1 corresponds to purified plasmid pQR150 (20 kb), S2 is S1 degraded at 60°C for 48 hours and S3 is single stranded S1 obtained by performing the alkaline lysis step in the presence of excessive NaOH. Abbreviations: M – λ HindIII molecular size marker; OC – open circular; SC – supercoiled.

Table 7.6: Relative integrity of plasmid pQR150 (20 kb) after passing through the disk-stack centrifuge feed zone.

Sample	SC (%)	Relative integrity of SC DNA
Feed	50 ± 2	1.00
50L/h	35 ± 2	0.72 ± 0.05
70L/h	34 ± 2	0.71 ± 0.05
120L/h	33 ± 2	0.69 ± 0.07

7.3.4 Conclusion

The results showed that the centrifugal pump, mono pump and disk-stack centrifuge feed zone can affect the SC yield. The plasmid backbone breakage increased with processing time through the pumps tested but the difference in product damage resulting from the two pumps was not significant. A decrease in SC content was also observed after lysate was passed through the centrifuge feed zone. Plasmid degradation was not significantly dependent on the centrifuge flow rates applied.

These observations clearly indicated susceptibility of the 20 kb plasmids in a lysate environment to shear damage in a large-scale manufacturing process environment. Therefore, during the design of a process for the recovery of plasmids, it is essential to characterise the hydrodynamic environment which is associated to a particular unit operation or within the ancillary equipment. Since obtaining pilot scale trial data from a pump, a centrifuge or other unit operations requires a large amount of materials, scale down mimics which can generate equivalent elongational strain rates have been designed at the IMRC. It will be useful to compare the results obtained in this study to small scale studies to verify the accuracy of plasmid degradation predictions.

Chapter 8 – References

American Society of Mechanical Engineers (ASME) (2001). Measurement of fluid flow using small bore precision orifice meters.

Annex 6, Good manufacturing practices for sterile pharmaceutical products, WHO Technical Report Series, 902 (2002).

Aucamp JP, Cosme AM, Lye GJ, Dalby PA. (2005). High-throughput measurement of protein stability in microtiter plates. Biotechnology and Bioengineering, 89, 5, 599–607.

Badmington F, Honig E, Payne M, Wilkins R. (1995). Pharmaceutical Tech., 19, 64–76.

Baker RW. (2000). Membrane Technology and Applications, McGraw-Hill Companies Inc., USA.

Barton JK, Lippard SJ. (1980). Heavy metal interactions with nucleic acids. Nucleic Acid-Metal Ion Interactions, Wiley-Interscience Publications, John Wiley & Sons Inc.

Birnboim H, Doly J. (1979). A rapid alkaline extraction procedure for screening recombinant plasmid DNA. Nucleic Acids Res, 76, 1513–1523.

Blaber M. (2004). Quantification of Protein Concentration. Retrieved 14 June 2006. <http://wine1.sb.fsu.edu/BCH4053l/Lecture03/Lecture03.htm >

Bloomfield VA. (1991). Condensation of DNA by multivalent cations: Considerations on mechanism. Biopolymers, 31, 1471–1481.

Bloomfield VA. (1996). DNA condensation. Curr. Opin. Struct. Biol., 6, 334–341.

Boles TC, White JH, Cozzarelli NR. (1990). Structure of plectonemically supercoiled DNA, J. Mol. Biol., 213, 931–951.

Bos GW, Trullas-Jimeno A, Jiskoot W, Crommelin DJA, Hennink WE. (2000). Sterilization of poly(dimethylamino)ethyl methacrylate)-based gene transfer complexes. International Journal of Pharmaceutics, 211, 79–88.

Boussif O, Lezoualch F, Zanta MA, Mergny MD, Scherman D, Demeneix, Behr JP (1995). A versatile vector for gene and oligonucleotide transfer into cells in culture and *in vivo*: polyethylenimine. ProcNatl Acad Sci USA, 92, 7297–7301.

Bowman RD, Davidson N. (1972). Hydrodynamic shear breakage of DNA. Biopolymers, 11, 2601–2624.

Bowen WR, Gan Q. (1991). Properties of microfiltration membranes: Flux loss during constant pressure permeation of bovine serum albumin. Biotechnol Bioeng, 38, 688–696.

Boychyn M, Doyle W, Bulmer M, More J, Hoare M. (2000). Laboratory scaledown of protein purification processes involving fractional precipitation and centrifugal recovery. Biotechnol Bioeng, 69, 1–10.

Boychyn M, Yim SS, Ayazi Shamlou P. (2001). Characterization of flow intensity in continuous centrifuges for the development of laboratory mimics. Chem Eng Sci, 56, 4759–4770.

Brannen JP. (1970). On the role of DNA in wet heat sterilization of micro-organisms. J Theor Biol, 27, 425–432.

Bussey LB, Adamson, R, Atchley A. (1998). Methods for purifying nucleic acids. WO Patent 98/05673.

Bustamante C, Marko JF, Siggia ED, Smith, S. (1994). Entropic elasticity of λ-phage DNA. Science, 265, 1599–1600.

Butler VA. (1996). Points to consider on plasmid DNA vaccines for preventative infectious disease indications. Office of Vaccine Research and Review, Centre for Biologics Evaluation and Research, Food and Drug Administration.

Campeau P, Chapdelaine P, Seigneurin-Venin S, Massie B, Tremblay JP. (2001). Transfection of large plasmids in primary human myoblasts. Gene Ther, 8, 1387–1394.

Cardona M, Blosse P. (2005). Guidelines for selecting sterilizing grade membrane filters. CEP, 34-37. Retrieved 24 April 2006 <www.cepmagazine.org>

Chamsart S, Patel H, Hanak JAJ, Hitchcock AG, Nienow AW. (2001). The impact of fluid-dynamic-generated stresses on chDNA and pDNA stability during alkaline lysis for gene therapy products. Biotechnol Bioeng, 75, 387–392.

Chan G, Booth AJ, Mannweiler K, Hoare M. (2006). Ultra scale-down studies of the effect of flow and impact conditions during *E.coli* cell processing, Biotechnology and Bioengineering, (in press).

Cherng JY, Talsma H, Crommelin DJA, Hennink WE. (1999). Long Term Stability of Poly((2-dimethylamino)ethyl Methacrylate)-Based Gene Delivery Systems. Pharm Res, 16, 1417–1423.

Ciccolini LAS, Ayazi Shamlou P, Titchener-Hooker N, Ward JM, Dunnill P. (1998). Time course of SDS-alkaline lysis of recombinant bacterial cells for plasmid release. Biotechnol Bioeng, 60, 768–770.

Ciccolini LAS, Ayazi Shamlou P, Titchener-Hooker N. (2002). A mass balance study to assess the extent of contaminant removal achieved in the operations for the primary recovery of plasmid DNA from *E. coli* cells. Biotechnol Bioeng, 77, 796–805.

Clamme JP, Azoulay J, Mely Y. (2003). Monitoring of the formation and dissociation of polyethylenimine/DNA complexes by two photon fluorescence correlation spectroscopy. Biophysical Journal, 84, 1960–1968.

Cluzel P, Lebrun A, Heller C, Lavery R, Viovy J-L, Chatenay D, Caron F. (1996) Science, 271, 792–794.

Compton ST, Henning, KA, Chen M, Mansoura MK, Ashlock, MA. (1999). An improved method for routine preparation of intact artificial chromosome DNA (340–1000 kb) for transfection into human cells. Nucleic Acids Res, 27, 1762-1765.

Cooke, GD, Cranenburgh RM, Hanak JAJ, Dunnill P, Thatcher DR, Ward JM. (2001). Purification of essentially RNA free plasmid DNA using a modified *Escherichia coli* host strain expressing Ribonuclease A. J Biotech, 85, 297–304.

Cooke, GD, Cranenburgh RM, Hanak JAJ, Ward JM. (2003). A modified Eschericia coli protein production strain expressing staphylococcal nuclease, capable of auto-hydrolysing host nucleic acid. J Biotechnol, 101, 229–239.

Cooper, MJ, Kowalczyk, TH, Pasumarthy MK. (2003). Method of nucleic acid compaction. US Patent number: 6,506,890.

Darquet AM, Rangara R, Kreiss P (1999). Minicircle: an improved DNA molecule for *in vitro* and *in vivo* gene transfer. Gene Ther, 6, 209–18.

Doi M, Edwards SF. (1986). The theory of polymer dynamics, Oxford University Press.

Dosmar, M (2004). Modified regenerated cellulose ultrafilters. Bioprocessing, Genetic Engineering News, 24 (18), 46–47.

DNA-labels (2006). Retrieved 24 April 2006, from Wikimedia Commons database <http://commons.wikimedia.org/wiki/Image:DNA-labels.png>

Dunlap DD, Maggi AS, Marco R, Monaco L. (1997) Nanoscopic structure of DNA condensed for gene delivery. Nucleic Acids Res, 25, 3095–3101.

Dunleavy M. (n.d.) Polyethersulfone Membranes Facilitate Sterile Filtration Of Biological Materials. Millipore Corporation. Retrieved 24 April 2006, <http://www.biosciencetechnology.com/>.

Durland RH, Eastman, EM. (1998). Manufacturing and quality control of plasmid-based gene expression systems. Advanced Drug Delivery Rev, 30, 33–48.

Eon-Duval A, Gumbs K, Ellett C. (2003). Precipitation of RNA impurities with high salt in a plasmid DNA purification process: use of experimental design to determine reaction conditions. Biotechnol Bioeng 83, 544–553.

Eon-Duval A, MacDuff RH, Fisher CA, Harris MJ, Brook C. (2003). Removal of RNA impurities by tangential flow filtration in an RNase-free plasmid DNA purification process. Anal Biochem, 316, 66–73.

Evans RK, Xu Z, Bohannon KE, Wang B, Bruner MW, Volkin DB. (2000). Evaluation of degradation pathways for plasmid DNA in pharmaceutical formulations via accelerated stability studies. J Pharm Sci, 89, 976–87.

Gieck K, Reiner R. (1997). Engineering Formulas, 7th Edition, McGraw-Hill Professional.

Gray PP, Dunnill P, Lilly MD. (1972). The continuous-flow isolation of enzymes. Proc. IV IFS: Ferment Technol Today, 347–351.

Griffith M, Gietz RD. (2003). *Escherichia coli* endA deletion strain for use in two-hybrid shuttle vector selection. BioTechniques, 35, 272–278.

Ferrando M, Rozek A, Zator M, Lopez F, Guell C. (2005). An approach to membrane fouling characterization by confocal scanning laser microscopy. J Membrane Sci, 250, 283–293.

Ferreira, GNM, Monteiro, GA, Prazeres, DMF, Cabral, JMS. (2000). Downstream processing of plasmid DNA for gene therapy and DNA vaccine applications. Trends Biotechnol, 18, 380–388.

Francis AA, Regan JD. (1986) Detection and repair of UV-induced photosensitive lesion in the DNA of human cells. Mutat Res, 165, 151–157.

Felgner PL. (1997). Non-viral strategies for Gene Therapy. Scientific American, 276 (6), 102–106.

Gardlik R, Pálffy R, Hodosy J, Lukács J, Turňa J and Celec P. (2005). Vectors and delivery systems in gene therapy. Medical Science Monitor, 11, 4, 110–121.

Gehl J. (2003). Electroporation: theory and methods, perspectives for drug delivery, gene therapy and research. Acta Physiol Scand, 177, 437–47.

Gene Therapy, Human Genome Project Information. Retrieved 12 June 2006. <http://www.ornl.gov/sci/techresources/Human_Genome/medicine/genetherapy.shtml>

Gene Therapy Trials Worldwide (January 2006). Retrieved 24 April 2006. <http://www.wiley.co.uk/genmed/clinical/>

Godbey WT, Wu KK, Hirasaki GJ and Mikos AG. (1999) Improved packing of poly(ethylenimine)/DNA complexes increases transfection efficiency. Gene Therapy 6, 1380–1388.

Haber C, Skupsky J, Lee A, Lander R. (2004). Membrane chromatography of DNA: Conformation-induced capacity and selectivity. Biotechol Bioeng, 88, 26–34.

Hart SL, Harbottle RP, Cooper R, Miller A, Williamson R, Coutelle C. (1995). Gene delivery and expression mediated by an integrin binding peptide. Gene Ther, 11, 552–554.

Hart SL., Collins L, Gustaffson K, Fabre JW. (1997). Integrin-mediated transfection with peptides containing arginine-glycine-aspartic acid domains. Gene Ther, 4, 1225–1230.

Herman F. (1996). J Mol Med, 74, 213–221.

Hitchcock AG (2005). Purification of biological macromolecules. WO Patent 2005/035758.

Higgins JJ, Lewis DJ, Daly WH, Mosqueira FG, Dunill P, Lilly MD. (1978). Investigation on the unit operations involved in the continuous flow isolation of beta-galactosidase from *E. coli*. Biotechnol Bioeng, 159–182.

Hirasaki T, Sato T, Tsuboi T, Nakano H, Noda T, Kono A, Yamaguchi K, Imada K, Yamamoto N, Murakami H, Manabe S. (1995). Permeation mechanism of DNA molecules in solution through cuprammonium regenerated cellulose hollow fiber (BMM™). J Membrane Sci, 106, 123–129.

Higuchi A, Kato K, Hara M, Sato T, Ishikawa G, Nakano H, Satoh S, Manabe S. (1996). Rejection of single stranded and double stranded DNA by porous hollow fiber membranes. J Membrane Sci, 116, 191–197.

Higuchi A, Yoshimura T, Kato K, Hara M, Higuchi M, Minoura N., Hirasaki T, Sato T, Ishikawa G, Nakano H, Satoh S, Manabe S. (1997). Sieving study of chromatin and histone-DNA complex by porous hollow fiber membranes. J Membrane Sci, 126, 7–11.

Hoare M, Levy MS, Bracewell DG, Doig SD, Kong S, Titchener-Hooker N, Ward JM, Dunnill P. (2005). Bioprocess Engineering Issues That Would Be Faced in Producing a DNA Vaccine at up to 100 m^3 Fermentation Scale for an Influenza Pandemic. Biotech Progress, 21, 1577–1592.

Holmes D, Quigley M. (1981). A rapid boiling method for the preparation of bacterial plasmids. Anal. Biochem, 114, 1, 193–197.

Honig ES, Schwartz PD (1997). Filtr Sep, 34, 73–78.

Horn, N.A., Meek, J.A., Budahazi, G. and Marquet, M. (1995). Cancer gene therapy using plasmid DNA: purification of DNA for human clinical trials. Hum. Gene Ther., 6, 565–573.

Hunkeler, D., Nguyen, T.Q., Kausch, H.H. (1996). Polymer solutions under elongational flow: 1. Birefringence characterization of transient and stagnation point elongational flows. Polymer, 37 (19), 4257–4269.

Ish-Horowitz D, Burke JF. (1981). Rapid and efficient cosmid cloning. Nucleic Acid Res, 9, 2989–2998.

Jackson G, Sherestha S, Ward JM. (1995). Metabolic engineering of the toluene degradation pathway. J Cell Biochem, S21A CIA48.

Jackson NB, Liddell JM, Lye GJ. (2006). An automated microscale technique for the quantitive and parallel analysis of microfiltration operations. Journal of Membrane Science. 276, 31–34.

Jornitz, M., Meltzer, T.H., Soelkner, P.G. (2003). Modern Sterile Filtration – The Economics. Pharmaceutical Technology Europe. Retrieved 24 April 2006, from Pharmaceutical Technology Europe. <http://www.ptemag.com/pharmtecheurope/article/articleDetail.jsp?id=60282&pageID=1&sk=&date>.

Kahn DW, Butler MD, Cohen DL, Gordon M, Kahn JW, Winkler ME. (2000). Purification of plasmid DNA by tangential flow filtration. Biotechnol. Bioeng, 69, 101–106.

Kuriyama S, Mitoro A, Tsujinoue H (2000). Particle-mediated gene transfer into murine livers using a newly developed gene gun. Gene Ther, 7, 1132–1136.

Lander RJ, Winters MA, Meacle FJ, Buckland BC, Lee AL. (2002). Fractional precipitation of plasmid DNA from lysate by CTAB. Biotechnol Bioeng, 79, 776–784.

Lander RJ, Winters MA, Meacle FJ. (2001). Process for the scaleable purification of plasmid DNA. WO Patent 01/46215 A1.

Lis JT, Schleif R. (1975). Size fractionation of double-stranded DNA by precipitation with polyethylene glycol. Nucleic Acids Res, 2, 383–389.

Langowski J, Hammermann M, Klenin K, May R, T'oth K. (1999). Superhelical DNA studied by solution scattering and computer models. Genetica. 106, 49–55.

Larson RG, Perkins TT, Smith DE, Chu S. (1997). Hydrodynamics of a DNA molecule in a flow field. Phy Rev E., 55(2), 1794–1797.

Larson RG, Hu H. (1999). Brownian dynamics simulation of a DNA molecule in an extension flow field. J Rheol., 43(2), 267–304.

Larson JW, Yantz GR, Zhong Q, Charnas R, D'Antoni CM, Gallo MV, Gillis KA, Neely LA, Phillips KM, Wong GG, Gullans SR, Gilmanshin R. (2006). Single DNA molecule stretching in sudden mixed shear and elongational microflows. Lab Chip, 6, 1187–1199.

Lengsfeld, CS, Anchodoquy TJ. (2002). Minireview: Shear-induced degradation of plasmid DNA. J Pharm Sci, 91, 1581–1589.

[a]Levison PR, Badger SE, Dennis J, Hathi P, Davies MJ, Bruce IJ, Schimkat D. (1998). Recent developments of magnetic beads for use in nucleic acid purification. J Chromatogr A, 816, 107–111.

[b]Levison PR, Badger SE, Hathi P, Davies MJ, Bruce IJ, Grimm V. (1998). New approaches to the isolation of DNA by ion-exchange chromatography. J Chromatogr A, 827, 337–344.

Levy, M.S., Colins, I.J., Yim, S.S., Ward, J.M., Titchener-Hooker, N., Ayazi-Shamlou, P., Dunnill, P. (1999). Effect of shear on plasmid DNA in solution. Bioprocess Eng, 20, 7–13.

[a]Levy, M.S., O'Kennedy, R.D., Ayazi Shamlou, P. and Dunnill, P. (2000). Biochemical engineering approaches to the challenges of producing pure plasmid DNA. Trends Biotechnol, 18, 296–305.

[b]Levy, M.S., Lotfian, P., O' Kennedy, R., Lo-Yim, M.Y. and Ayazi Shamlou, P. (2000). Quantitation of supercoiled circular content in plasmid DNA solutions using a fluorescence based method. Nucleic Acids Res, 28, e57.

[c]Levy MS, Collins IJ, Tsai J, Ayazi-Shamlou P, Ward JM, Dunnill P. (2000). Removal of contaminant nucleic acids by nitrocellulose filtration during pharmaceutical-grade plasmid DNA processing. J Biotech, 76, 197–205.

Li S, Huang L. (2000). Nonviral gene therapy: promises and challenges. Gene Ther, **7**, 31–34.

Lindenbaum M, Perkins E, Csonka E, Fleming E, Garcia L, Greene A, Gung L, Hadlaczky G, Lee E, Leung J, MacDonald N, Maxwell A, Mills K, Monteith D, Perez CF, Shellard J, Stewart S, Stodola T, Vandenborre D, Vanderbyl S, Ledebur HC. (2004). A mammalian artificial chromosome engineering system (ACE System) applicable to biopharmaceutical protein production, transgenesis and gene-based cell therapy. Nucleic Acids Res, 32, 21, e172.

Lyubchenko Y, Shlyakhtenko LS. (1997). Visualization of supercoiled DNA with atomic force microscopy. Proc. Natl. Acad. Sci. USA, 94, 496–501.

Maa Y, Hsu CC. 1998. Investigation on fouling mechanisms for recombinant human growth hormone sterile filtration. J Pharm Sci, 87, 808–812.

Mandelkern, L. (1983). An introduction to macromolecules, 2nd Edition, Springer-Verlag New York Inc., USA.

Marko, J.F. (1998). DNA under high tension: Overstretching, undertwisting, and relaxation dynamics. Phys Rev E, 57, 2134–2149.

Marquet M, Horn NA, Meek JA. (1995). Process development for the manufacture of plasmid DNA vectors for use in gene therapy. Bio Pharm, 9, 26–37.

Marzilli, L.G. and Kistenmacher, T.J. (1980). Structural principles of metal ion-nucleotide and metal ion-nucleic acid interactions. Nucleic Acid-Metal Ion Interactions, Wiley-Interscience Publications, John Wiley & Sons Inc.

Micheletti M, Barrett T, Doig SD, Baganz F, Levy MS, Woodley JM, Lye GJ. (2006). Fluid mixing in shaken bioreactors: Implications for scale-up predictions from microlitre scale microbial and mammalian cell cultures. Chem Eng Sci, 61, 2939–2949.

Microporous Membrane Structures (n.d.) Retrieved 24 April 2006, from Millipore Corporation website <http://www.millipore.com>.

Middaugh CR., Evans RK, Montgomery DL, Casimiro DR. (1998). Analysis of plasmid DNA from a pharmaceutical perspective. J Pharm Sci, 87, 131–146.

Moat AG, Foster JW. (1995). Microbial Physiology, 3rd Edition, John Wiley & Sons, NJ, USA.

Molloy MJ, Hall VS, Bailey SI, Griffin KJ, Faulkner J, Uden M. (2004). Effective and robust plasmid topology analysis and the subsequent characterization of the plasmid isoforms thereby observed. Nucleic Acids Res, 32 (16), e129.

Mountain, A. (2000). Gene therapy: the first decade. Trends Biotechnol., 18, 119–128.

Necina R, Jancar J, Podgornik A, Barut M, Strancar A, Merhar M. (2003). Method and device for isolating and purifying a polynucleotide of interest on a manufacturing scale. WO Patent 03/051483.

O'Kennedy RD, Ward JM, Keshavarz-Moore E. (2003). Effects of fermentation strategy on characteristics of plasmid DNA production. Biotechnol. Appl. Biochem. 37, 83–90.

Perkins, T.T., Smith, D.E., Larson, R.G. and Chu, S. (1995). Stretching of a single tethered polymer in a uniform flow. Science, 268, 83–87.

Perkins, T.T., Smith, D.E., and Chu, S. (1994). Direct observation of tube-like motion of a single polymer chain. Science, 264, 819–822.

Perkins, T.T., Smith, D.E., and Chu, S. (1997). Single polymer dynamics in an elongation flow. Science, 276, 2016–2021.

Polyvinylidene difluoride (PVDF) membrane (n.d.). Retrieved 24 April 2006, from Millipore Corporation website <http://www.millipore.com>

PowderMed Press Release, September 2006. Unique flu vaccine trial to start in London – Opportunity to Trial New Vaccine That Could Help In the Fight Against Annual and Pandemic Flu. Retrieved 25 September 2006. <www.powdermed.com/media.htm>

Prather KJ, Sagar S, Murphy J, Chartrain M. (2003). Industrial scale production of plasmid DNA for vaccine and gene therapy: plasmid design, production and purification. Enzyme Microbial Technol, 33, 865–883.

Prazeres D, Schulep T, Cooney C. (1998). Preparative purification of supercoiled plasmid DNA using anion-exchange chromatography. J Chromatogr, 806, 31–45.

QIAGEN® Plasmid Purification Handbook for QIAGEN Plasmid Midi, Maxi, Maxi and Giga Kits (2000). QIAGEN Ltd, West Sussex, UK.

Qiu P, Ziegelhoffer P, Sun J (1996) Gene gun delivery of mRNA in situ results in efficient transgene expression and genetic immunization. Gene Ther, 3, 262–68.

Reynolds T, Boychyn M, Sanderson T, Bulmer M, More J, Hoare M. (2003). Scale-down of continuous filtration for rapid bioprocess design: Recovery and dewatering of protein precipitate suspensions. Biotechnol Bioeng, 83, 4, 454–464.

Reese, H.R. and Zimm, B.H. (1990). Fracture of polymer chains in extensional flow: Experiments with DNA, and a molecular dynamics simulation, J Chem Phys, 92, 4, 2650–2662.

Richards, E.G. (1980). An introduction to physical properties of large molecules in solution - IUPAB Biophysics Series. Cambridge University Press.

Rippe K, Mücke N, Langowski J. (1997). Superhelix dimensions of a 1868 base pair plasmid determined by scanning force microscopy in air and in aqueous solution, Nucleic Acids Res, 25, 9, 1736–1744.

Robinson H. (2000). DNA vaccines. Clin Microbiol Newslett, 22, 17–22.

Rock C, Ayazi Shamlou P, Levy MS. (2003). An automated microplate-based method for monitoring DNA strand breaks in plasmids and bacterial artificial chromosomes. Nucleic Acids Res, 31, 11, 1–6.

Sarkar S. (2005). Biophysical characterisation of plasmid formulation. Thesis. Department of Biochemical Engineering, University College London.

Sarkar S, Zhang H, Levy MS, Hart SL, Hailes HC, Tabor AB, Ayazi Shamlou P. (2003). Prediction of size distribution of lipid–peptide–DNA vector particles using Monte Carlo simulation techniques. Biotechnol Appl Biochem, 38, 95–102.

Schleef M, Voβ C, Schmidt T. (2002). DNA drugs – Production and quality assurance. Eng Life Sci, 6, 157–160.

Seeley, K.A. (n.d.) Filtration of Dilute Protein and DNA Solutions. Retrieved 24 April 2006, from Pall Corporation website <http://www.pall.com/laboratory_1219.asp>.

Shizuya H, Birren B, Kim U-J. (1992). Cloning and stable maintenance of 300-kb fragments of human DNA in *Escherichia coli* using an F-factor based vector. Proc Natl Acad Sci USA, 89, 8794–8797.

Smith, SB, Cui Y, Busmante C. (1996). Overstretching B-DNA: The elastic response of individual double-stranded and single-stranded DNA molecules. Science, 271, 795–799.

Stein CA, Cohen JS. (1988). Oligodeoxynucleotides as inhibitors of gene expression: a review. Cancer Res, 48, 2659–2668.

Strick TR, Allemand JF, Bensimon D, Croquette V. (1998). Behavior of supercoiled DNA. Biophys J, 74, 2016–2028.

Strick, T.R., Allemand, J.F., Bensimon, D., Bensimon, A. and Croquette, V. (1996). The elasticity of a single supercoiled DNA molecule. Science, 271, 1835–1837.

Stryer L. (1981). Biochemistry, 2nd ed., W.H. Freeman & Co.

Subramaniam M, Holpainen J, Paukku, Eriksson O, Huhtaniemi I, Kinnunen P (2000). Characterisation of three novel cationic lipids as liposomal complexes with plasmid DNA. Biochimica et Biophysica Acta 1468, 6–10.

Shubsda MF, Goodisma J, Dabrowiak JC. (1997). Quantitation of ethidium-stained closed circular DNA in agarose gels. J Biochem Biophys Methods, 34, 73–79.

Sutherland JC, Monteleone DC, Trunk JG, Bennett PV, Sutherland BM. (2001). Quantifying DNA damage by gel electrophoresis, electronic imaging and number-average length analysis. Electrophoresis, 22, 843–854.

Thatcher DR, Hitchcock A, Hanak JAJ, Varley DL. (2003). Method of plasmid DNA production and purification. US Patent 6,503,738.

Teraoka I. (2002). Polymer solutions: An introduction to physical properties, John Wiley & Sons, Inc., NY, USA.

Termonia Y. (2000). Coil-stretch transition in deformation flows. J Polymer Sci, 38, 2422–2428.

Tumanova I, Boyer J, Ausar SF, Burzynski J, Rosenrance D, White J, Scheidel J, Parkinson R, Maguire H, Middaugh R, Weiner D, Green A. (2005). Analytical and Biological Characterization of Supercoiled Plasmids Purified by Various Chromatographic Techniques. DNA and Cell Biology, 24 (12), 819–831.

Udeuehi AN, Stammberger U, Frese S, Schmid RA. (2001). Efficiency of non-viral gene delivery system which increase the size of lipoplexes prevent serum-associated inhibition of transfection. J Gene Med, 2, 32–30.

Urthaler J, Necina R, Ascher C, Wöhrer H. (2004). Methods and devices for producing biomolecules. WO Patent 2004/085643.

Urthaler J, Buchinger W, Necina R. (2005). Improved downstream process for the production of plasmid DNA for gene therapy. Acta Biochimica Polinica, 52, 3, 703–711.

US FDA 21 Code of Federal Regulations-Parts 210 and 211 (updated December 2005). Retrieved 24 April 2006, from US FDA CDER website <http: www.fda.gov/cder/dmpq/cgmpregs.htm>.

Vilalta A, Whitlow V, Martin T. (2002). Real-time PCR determination of Escherichia coli genomic DNA contamination in plasmid preparations. Anal. Biochem. 301, 151–153.

Voβ C, Schmidt T, Schleef M, Friehs K, Flaschel E. (2003). Production of supercoiled multimeric plasmid DNA for biopharmaceutical application. J Biotech. 105 (3), 205–213.

Volkin DB, Evans RK, Bruner M, Xu Z. (2002). DNA pharmaceutical formulations comprising citrate or triethanolamine and combinations thereof. US Patent 6,387,695.

Volkin DB, Evans RK, Bruner M. (2004). DNA vaccine formulations. US patent application number 20040138165.

Vologodskii, A., Levene, S.D., Klenin, K.V., Frank-Kamenetskii, M. and Cozzarelli, N.R. (1992). Conformational and thermodynamic properties of supercoiled DNA. J. Mol. Biol., 227, 1224–1243.

Wade-Martins R, Frampton J, James, MR. (1999). Long-term stability of large insert genomic DNA episomal shuttle vectors in human cells. Nucleic Acids Res, 27, 1674–1682.

Watson JD, Crick FHC. (1953). Molecular structure of nucleic acids: A structure for deoxyribose nucleic acid. Nature, 171, 737–738.

Watson MP, Winters MA, Sagar SL, Konz JO. (2006). Sterilizing filtration of plasmid DNA: Effects of plasmid concentration, molecular weight, and Conformation. Biotechnol. Prog, 22, 465 –470.

Walther W, Stein U. (2000). Viral vectors for gene transfer: a review of their use in the treatment of human diseases. Drugs, 60, 249–71.

Walther W, Stein U, Voss C, Schmidt T, Schleef M and Schlag PM. (2003). Stability analysis for long-term storage of naked DNA: impact on nonviral *in vivo* gene transfer. Anal Biochem, 318 (2), 230–235.

Welty JR, Wicks CE, Wilson RE. (1983). Fundamentals of Momentum, Heat, and Mass Transfer, 3rd Edition, John Wiley & Sons, Inc.

Wheeler CJ, Felger PL, Tsai Y, Marshall J. (1996) A novel cationic lipid greatly enhances plasmid DNA delivery and expression in mouse lung. Proc Nat Academy Sci USA, 93, 11454–11459.

White RE, Wade-Martins R, Hart S, Frampton J, Huey B, Desai-Mehta A, Cerosaletti M, Concannon P, James MR. (2003). Functional delivery of large genomic DNA to human cells with a peptide-lipid vector. J Gene Med, 5, 883–892.

Whorlow RW. (1992). Rheological Techniques, 2nd Edition. Ellis Horwood Ltd., UK.

Zeman LJ, Zydney AL. (1996). Microfiltration and ultrafiltration – Principles and Applications. Marcel Dekker Inc., NY, USA.

Zhdanov RI, Podobed OV, Vlassov VV. (2002). Cationic lipid-DNA complexeslipoplexes – for gene transfer and therapy. Bioelectrochemistry, 58, 53–64.

Zydney AL, Ho CC. (2002). Scale-up of microfiltration systems: fouling phenomena and analysis. Desalination, 146, 75–81.

Appendix A: List of Abbreviations

A	Membrane area
A_{260}	Absorbance at a wavelength of 260 nm
A_{280}	Absorbance at a wavelength of 280 nm
AFM	Atomic force microscopy
BAC	Bacterial artificial chromosome
cGMP	Current Good Manufacturing Practices
chrDNA	Chromosomal deoxyribonucleic acid
Cn	Concentration
DNA	Deoxyribonucleic acid
DOPE	Dioleoyl phosphatidylethanolamine
DOTMA	*N*-[1-(2,3-dioleyloxy)propyl]-*N*,*N*,*N*trimethylammonium chloride
E. coli	*Escherichia coli*
F	Fluorescence
HEPES	*N*-[2-hydroxyethyl]piperazine-N'-[2-ethanesulphonic acid]
IMRC	Innovative Manufacturing Research Centre
kb	Kilo base pairs
LB	Luria-Bertani medium
LID	Lipid-integrin binding peptide-deoxyribonucleic acid complex
M	Molecular weight marker
n.d.	No date
N/P	Molar ratio of nitrogen atoms to phosphate atoms
NaCl	Sodium chloride
OC	Open circular
PCR	Polymerase Chain Reaction
PEI	Polyethylenimine
PEI/DNA	Polyethylenimine-deoxyribonucleic acid complex
PES	Polyethersulfone
PTFE	Poly(tetrafluoroethylene)
PVDF	Polyvinylidene fluoride
qPCR	Quantitative Polymerase Chain Reaction
Q_{min}	Minimum specified flow rate
Q_0	Initial volumetric filtrate flow rate
RF	Relative fluorescence ratio
R_g	Radius of gyration
RNA	Ribonucleic acid
SC	Supercoiled circular
SEM	Scanning electron microscopy
t	Time
TE	Tris-EDTA
USD	Ultra scale-down
v/v	Volume per volume
V_{max}	Maximum fluid volume that can be filtered before a membrane is completely plugged
w/v	Weight per volume
WHO	World Health Organisation

Appendix B: Broth/Buffer Recipes

Luria-Bertani Broth

Tryptone	10.0 g
NaCl	10.0 g
Yeast extract	5.0 g

- Make up to 1 L with H_2O
- Autoclave

Terrific Broth

Tryptone	12.0 g
Yeast extract	24.0 g
Glycerol	4 mL
Phosphate buffer:	
KH_2PO_4	2.3 g
K_2HPO_4	12.6 g

- Make up to 1 L with H_2O
- Autoclave

1 M Tris-HCl, pH 8

Tris Base	121.1 g
H_2O	800 mL
HCl (concentrated)	42 mL

- Adjust to pH 8
- Adjust volume to 1 L with H_2O
- Autoclave

0.5 M EDTA, pH 8

$EDTA_2.H_2O$	186.1 g
H_2O	800 mL
NaOH pellets	20.0 g

- Add solid to approximately 300 mL H_2O
- Stir vigorously
- Adjust to 1 L with H_2O
- Adjust to pH 8
- Autoclave

TE Buffer, pH 8

1 M Tris-HCl, pH 8	10mL
0.5 M EDTA, pH 8	2 mL

- Adjust to 1 L with H_2O
- Autoclave